Non-Coherent Slot Synchronization Techniques for WCDMA Systems

Ahmed Hassan

A Thesis

in

The Department

of

Electrical & Computer Engineering

Presented in Partial Fulfillment of the Requirements
for the Degree of Master of Applied Science at
Concordia University
Montréal, Québec, Canada

July 2008

Your file Votre référence
ISBN: 978-0-494-42492-6
Our file Notre référence
ISBN: 978-0-494-42492-6

Abstract

Non-Coherent Slot Synchronization Techniques for WCDMA Systems

Ahmed Hassan

This Thesis investigates a host of new synchronization techniques for WCDMA. We assume the presence of more than one base station (BS) (multi-target) in the vicinity of the mobile station (MS), and consider the effects of multipath, Raleigh fading, and different carrier frequency offsets. Through the Thesis, we concentrate on the first stage of the three-stage cell search procedure which is slot synchronization. The slot synchronization stage has been always the most challenging stage since it deals with the largest amount of uncertainty in the cell search, and it determines the timing resolution to the other two stages. We also introduce the concept of using parallel code verification circuits to be added to the state of art pipelined techniques to yield better synchronization results. The received WCDMA synchronization codes are combined in different scenarios according to the proposed non-coherent synchronization technique. The results are compared with recent approaches of combining the WCDMA synchronization codes. The comparison reveals some improvements in the mean synchronization time for some of our rules herein. It also shows superiority of the new rules for different carrier frequency offsets especially at low signal to interference ratios.

Acknowledgements

Several people helped me to make this research a success. First of all, I owe a great debt of gratitude to my supervisor Professor Dr. Ahmed Elhakeem. I consider myself fortunate working under his guidance and receiving affluent knowledge towards this research and discovery. I really feel privileged for his attention to complete a successful research.

I would like to express my deepest gratitude to my parents, my brother Mohamed and his family Amel, Ahmed, and Amena for their affection and continuous inspiration throughout this research work. Without their help, it would not have been possible to complete this research work.

I am also grateful to my graduate colleagues at Concordia Research Laboratory. They influenced me a lot in this research.

Ahmed Hassan
June 11, 2008

Dedicated

To My Parents

Contents

List of Figures

Abbreviations

AICH	Acquisition Indication Channel
AWGN	Additive White Gaussian Noise
BCH	Broadcast Channel
CDMA	Code Division Multiple Access
CN	Core Network
CPICH	Common Pilot Channel
CS	Circuit-Switched
DS-CDMA	Direct-Sequence CDMA
DPCCH	Dedicated Physical Control Channel
DPDCH	Dedicated Physical Data Channel
EDGE	Enhanced Data Rates for GSM Evolution
FACH	Forward Access Channel
FDD	Frequency-Division Duplex
FDMA	Frequency Division Multiple Access
FM	Frequency Modulation
GIC	Group Identification Code
GMSK	Gaussian Minimum Shift Keying
GSM	Global System for Mobile communication
GPRS	General Packet Radio Service
GPS	Global Positioning System

HSCSD	High Speed Circuit Switched Data
IMT-2000	International Mobile Telecommunications-2000
IS-95	Interim Standard
ITU	International Telecommunication Union
MC	Multi-Carrier
ME	Mobile Equipment
MS	Mobile Stations
MSC	Mobile Switching Centre
OVSF	Orthogonal Variable Spreading Factor
P-CCPCH	Primary Common Control Physical Channel
PCH	Paging Channel
PICH	Page Indication Channel
PSC	Primary Synchronization Code
PRACH	Physical Random Access Channel
PS	Packet-Switched
PSK	Phase Shift Keying
QoS	Quality of Service
QPSK	Quadrature-PSK
RACH	Random Access Channel
RNC	Radio Network Controller
RNS	Radio Network Subsystems
RRM	Radio Resource Management
RS	Reed-Solomon

S-CCPCH	Secondary Common Control Physical Channel
SCH	Synchronization Channel
SF	Spreading Factor
SIR	Signal to Interference Ratio
SGNS	Serving GPRS Support Node
SNR	Signal-to-Noise Ratio
SSC	Secondary Synchronization Code
TDD	Time-Division Duplex
TDMA	Time Division Multiple Access
TD-SCDMA	Time Division Synchronous CDMA
TIA	Telecommunication Industry Association
UE	User Equipments
UMTS	Universal Mobile Telecommunication System
UTRA	UMTS Terrestrial Radio Access
UTRAN	UMTS Terrestrial Radio Access Network
USIM	UMTS Subscriber Identity Module
WCDMA	Wideband-Code Division Multiple Access
1 G	First Generation
2 G	Second Generation
3 G	Third Generation
3GPP	Third Generation Partnership Project

Chapter 1

Introduction

1.1. Motivation

Wireless communications for voice and data transmission are currently undergoing very rapid developments. Many of the emerging wireless systems incorporate considerable signal processing intelligence in order to provide advanced services such as multimedia transmission. The demanded traffic grows rapidly and the new capacity enhancements are required to satisfy the future needs. In order to make optimal use of available bandwidth and to provide maximal flexibility, many wireless systems operate as multiple-access systems, such that different users share the channel bandwidth on a random-access basis.

In this new decade, we experience a communication revolution, which may outgrow the revolution of the past decade. With this revolution, and with a fixed available spectrum, it is necessary to use the available spectrum more effectively. However, it is important for the communication system to resist interference, to operate with low-energy spectral

density, to provide multiple access capability with less external control, and to make it difficult for unauthorized receivers to demodulate the message.

Code Division Multiple Access (CDMA) is a generic term for multiple access scheme utilized by various wireless communication technologies. CDMA employs spread-spectrum technology to allow multiple users to share simultaneously a finite amount of radio spectrum. Data of different users is multiplexed over the same physical channel. CDMA permits different radios to share the same spectrum. The sharing of spectrum is essential to achieve high capacity by simultaneously allocating the available bandwidth among multiple users. The use of CDMA in wireless communications has grown considerably over the past decade especially in Mobile Networks. This is because CDMA is considered as a promising high spectral and power efficient technique (low fading margin) in multiple-access applications. In addition, it has well known merits in the field of secure communications. Each user is assigned a code which spreads the signal bandwidth in such a way that only the same code at the receiver side can despread it. CDMA has the property that the unwanted signals with different codes get spread, making them like noise to the receiver [1] [2].

Since the mid of 1990, the cellular communications industry has witnessed explosive growth in conjunction with the rapid development in the added multimedia services with high data rates. This motivated the use of CDMA as an efficient transmission technique for wideband services and high data rate applications. The third generation (3G) mobile systems have created new services such as mobile Internet browsing, e-mail, high-speed data transfer, video telephony, multimedia, video-on-demand, and audio-streaming. These data services had different Quality of Service (QoS) requirements and traffic

characteristics in terms of burstiness and required bandwidth. Currently two third generations of mobile communication systems are specified: Wideband-Code Division Multiple Access (WCDMA) known as Universal Mobile Telecommunication System (UMTS) and CDMA2000. Both WCDMA and CDMA2000 are based on CDMA technology to offer a way to accomplish the high data rates that support multimedia with high capacity. UMTS is the most important 3G cellular communication standard based on WCDMA as an air interface has already started to be deployed in many countries around the world providing multimedia capabilities and high capacity. However, CDMA2000 is deployed only in North America and South Korea to support the multimedia revolution.

1.2. Cellular Systems

First generation (1G) mobile communication systems started in the early to mid 1980's were based on analog Frequency Modulation (FM) technology. These 1G systems had a number of performance limitations which included low quality voice service, capacity limitation and inability to provide global roaming. All the 1G cellular systems employed Frequency Division Multiple Access (FDMA) where one channel was assigned to a certain user for the call duration.

The rapid growth in the number of subscribers and the incompatibility between different 1G systems were the main reason behind the evolution towards second generation (2G) cellular systems. The 2G systems take the advantage of compression and coding techniques associated with digital technology. All the 2G systems employ digital modulation schemes. Multiple access techniques like Time Division Multiple Access (TDMA) and CDMA are used in the second generation systems. The various 2G systems

included global system for mobile communication (GSM) and Interim Standard (IS-95). GSM systems are based on TDMA [3] [4]. TDMA is a channel access method for shared medium (usually radio) networks. It allows several users to share the same frequency channel by dividing the signal into different timeslots. The users transmit in rapid succession, one after the other, where each using his own timeslot. This allows multiple stations to share the same transmission medium (radio frequency channel) while using only the part of its bandwidth they require [5]. In North America, IS-95 was the first CDMA-based digital cellular standard pioneered by Qualcomm. The brand name for IS-95 is CDMA One. IS-95 uses CDMA as a multiple access scheme for digital radio to send voice, data and signaling data between mobile phone and cell sites to permit several radios to share the same frequencies. Unlike TDMA, a competing system used in the 2G GSM, all radios can be active all the time, because network capacity does not directly limit the number of active radios. Since larger number of phones can be served by smaller number of cell-site, the CDMA-based standards (IS-95) have a significant economic advantage over TDMA-based standards (GSM), or the oldest cellular standards (1G) that used FDMA [6]. However, different 2G technologies were not interoperable and not available across geographic areas. In addition, the low bit rate of 2G systems could not meet subscriber demands for multimedia services.

The 3G is the term used to describe the latest generation of mobile services, superseding 2G. The 3G networks provide advanced voice communications and high-speed data connectivity, including access to the Internet, mobile data applications and multimedia content. The International Telecommunication Union (ITU), working with industry standards bodies from around the world, has defined the technical requirements

and standards as well as the use of spectrum for 3G systems under the IMT-2000 (International Mobile Telecommunications-2000) program [7]. Based on these requirements, the ITU approved six radio interface modes for IMT-2000 standards. Three of the six approved standards (CDMA2000, Time Division Synchronous CDMA (TD-SCDMA), and WCDMA) are based on CDMA. However, CDMA2000 and WCDMA are considered as the two main standards. More technically, WCDMA and CDMA2000 are a wideband spread-spectrum mobile air interface that utilize the Direct-Sequence CDMA (DS-CDMA) method to achieve higher speeds and support more users [4] [8].

In the Spread Spectrum systems, the transmitted signal is spread over a broadened bandwidth. The job is done by multiplying the user's information bits with a pseudorandom bit stream running several times as fast. The bits in the pseudorandom bit stream are referred to as chips, so the stream is known as a chipping, or spreading code. It increases the bit-rate of the signal as well as the amount of bandwidth it occupies by a ratio known as the spreading factor (SF), namely, the ratio of the chip rate to the information data rate [1] [10].

Typical scenario occurs in Mobile networks, where there are multiple users or mobile stations (MSs) in a cell. Each user has a unique scrambling code used to differentiate between the different users within the same cell. The scrambling codes should be of low cross correlation properties with the each other. In a cellular system, the MS should correlate the received signal transmitted by the BS with its own scrambling code. Only the signal of that particular MS will be despread however all the other signals will remain spread. Fig. 1-1 shows a block diagram of a DS-CDMA transmitter and receiver. In brief, spreading is performed by multiplying the information data with a scrambling code

sequence of a bit rate higher than the information data rate. At the receiving side, the signal is multiplied with the exact synchronized scrambling code sequence to detect the transmitted data successfully [8] [9].

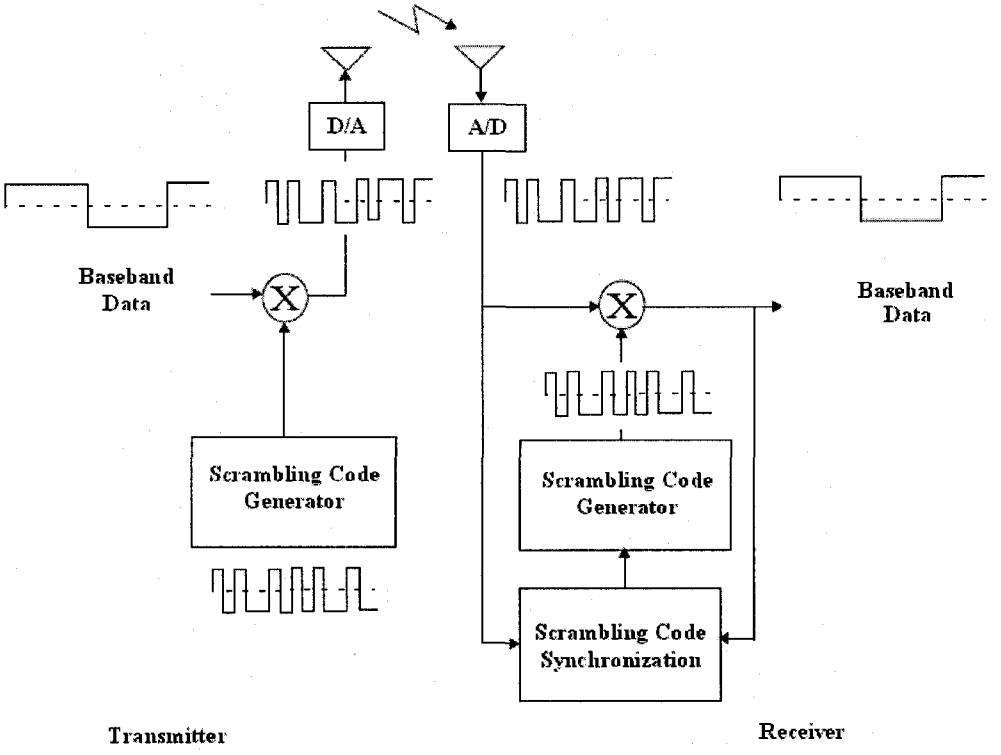

Figure 1-1: DS-CDMA Transmitter-Receiver Block Diagram

1.3. Difference between CDMA2000 & WCDMA

WCDMA also referred to as UMTS terrestrial radio access (UTRA), is the air interface standard used in UMTS networks. WCDMA is a Wideband DS-CDMA spread spectrum system. User information bits are spread over a wide bandwidth by a spreading code and

multiplied with a pseudo-random scrambling code. WCDMA has a flexible multi rate transmission scheme to support the transmission of different types of services with different data rates and QoS parameters. UMTS is being shaped and being standardized within the Third Generation Partnership Project (3GPP) [11]. The participants have come together for the specific task of specifying a 3G system based on an evolved GSM communication core network (CN) but opted for a totally new radio access technology in the form of a WCDMA. The WCDMA proposal offered two different modes of operation to distinguish by how they separate the two directions of communication. Frequency-division duplex (FDD) employs separate uplink and downlink frequency bands with a constant frequency offset between them. The other form, time-division duplex (TDD), puts the uplink and the downlink in the same band, and then time-shares transmissions in each direction. This mode may be useful for indoor applications or for operators with spectrum restrictions. The FDD version of UTRA is so well known that discussions about any of the other 3G radio interfaces are usually framed as comparisons with it [8][9][12].

Besides UTRA, one other technology in the new generation is based on CDMA-multi-carrier (MC) mode CDMA, usually called CDMA2000. This mode is intended to provide 3G services over mobile radio networks which include existing (2G) IS-95 know as CDMA-One. Concluding that, CDMA2000 is the evolution of IS-95 towards the 3G for enabling a variety of data intensive applications. The multi-carrier mode is very similar to the FDD form of WCDMA. The dissimilarities stem from the need to allow the IS-95 mode to work in the enhanced 3G network just as GSM handsets can be accommodated in the UTRA extension. Therefore, CDMA2000 proposal is based partly on IS-95 principles with respect to synchronous network operation, physical channels, and so on,

but it is a wideband version with three times the bandwidth of IS-95 [3] [4]. The CDMA2000 standard is being developed under the care of the Telecommunication Industry Association (TIA) of the US, and involved the participation of the international technical community through the 3GPP2 working group [4] [8] [13].

The main difference between WCDMA and CDMA2000 is that WCDMA supports asynchronous BSs that assign different scrambling codes to the cell sites. However CDMA2000 relies on synchronized BSs using the same scrambling code with different code shifts to enable the MS to acquire the scrambling code in relatively short time. The Global Positioning System (GPS) clock is used as an external time reference by all BSs to synchronize their operations. This allows the MS to use different phases of the same scrambling code to distinguish between adjacent BSs.

In contrast, in asynchronous WCDMA system, each BS has an independent time reference that the MS does not have any prior knowledge of it. Since there is no external time synchronization between different BSs, different phases of the same code cannot be used to distinguish adjacent BS as in CDMA2000. Thus, each BS can be identified using distinct scrambling codes. Consequently, cell search, referred to the process of achieving code, time and frequency synchronization of the MS with the BS and its scrambling code, takes longer time compared to a synchronous CDMA system (CDMA2000). Cell search is complicated in the presence of multiple unrelated signals that are either intended for other mobile systems within a cell or from other BSs.

Thus, it is very important to develop efficient algorithms and hardware implementations to reduce the synchronization time of the cell search for asynchronous CDMA systems (WCDMA) [8] [9].

1.4. Research Focus

This thesis investigates a host of new techniques for synchronization of BS pilot codes of the WCDMA systems, concretely for UTRA FDD mode as specified and standardized by the 3GPP. The study is mainly based on computer simulations taking many practical system aspects into account. The objective of this thesis is to identify different methods and techniques used by MS to quantify the initial cell search performance and to reduce the synchronization time taken by the MS to find, synchronize to and identify the BS to which it has the lowest path lose.

1.5. Thesis Organization

The thesis is divided into five main parts. Each covered in a single chapter. Chapter one includes general introduction to CDMA and Mobile Networks. Chapter two describes the evolution in the Mobile network services, WCDMA system and the synchronization channels in WCDMA cell search and introduces the three step cell search algorithm used in WCDMA for synchronization between the MS and the BS. Chapter three describes the related work and the state of art work and suggestions by the 3GPP working group of the different synchronization techniques used in the literature. Chapter four is dedicated to the contribution and the conclusion of the improved cell search techniques used to reduce the synchronization time for the MS to look for a target cell including simulation and considering practical aspects such as low signal to interference ratio (SIR), fading channel and multiple BS's. Chapter four includes also a comparison of different cell search algorithms and the new proposed techniques, plus a discussion. Finally,

conclusion, future work, and an overview of a future direction of this research are given in chapter five. Appendix contains parts of the MATLAB codes used for the two new proposed contributions. A large number of references are quoted throughout the thesis and are listed in the reference.

Chapter 2

WCDMA System

2.1. Background

The GSM system was initially developed to carry speech, as well as low speed data. The user data rate over the radio interface using a single physical channel, i.e. a single timeslot per TDMA frame, was initially 9.6 kbps. Two new services had been introduced as part of GSM phase 2 known by 2.5G which allow the user data rate to be increased by permitting MS to access more than one timeslot per TDMA frame. These new services are the High Speed Circuit Switched Data (HSCSD) and General Packet Radio Service (GPRS). Instead of limiting each user to only one specific time slot in the GSM TDMA standard, HSCSD allows individual data users to use consecutive time slots in order to obtain higher speed data access on the GSM network. HSCSD relaxes the error control coding algorithms originally specified in the GSM standard for data transmissions and increase the available application data rate to 14.4 kbps. HSCSD is able to provide a transmission rate up to 57.6 kbps to individual users by using up to four consecutive time slots. In contrast, GPRS uses packet-oriented connections on the radio interface whereby

a user is assigned one or a number of traffic channels only when a transfer of information is required, unlike HSCSD which dedicates circuit switched channels to specific users. HSCSD is ideal for real-time interactive web sessions however GPRS is well suited for non-real time internet usage including the retrieval of email, faxes, and asymmetric web browsing. When the eight time slots of a GSM radio channel are dedicated to GPRS, an individual user is able to reach high data rates up to 171.2 kbps (eight times slots multiplied by 21.4 kbps) [16], [17], and [19].

Another approach was introduced to increase the user data rate by employing a higher level modulation scheme under Enhanced Data Rates for GSM Evolution (EDGE).The driving force behind EDGE is to improve the data rates of GSM by means of enhancing the modulation methods. EDGE can switch between two different modulation techniques according to the channel condition. EDGE uses the existing Gaussian minimum shift keying (GMSK) modulation scheme in poor quality channels and eight-level phase shift keying (8-PSK) in good quality channels. This is done by the aid of link adaptation function that allows the MS and BS to evaluate the link quality and switch between the different types of modulation as necessary. Accordingly, the modulation scheme should be chosen according to the quality of the radio link to provide higher bit rates. EDGE provides data rates up to 384 kbps for a single dedicated user on a single GSM channel [9], [18], and [19].

These options provide significant improvements in Internet access speed over today's GSM technology and support the creation of new Internet-ready cell phones. However all of these options still have a limitation toward the multimedia and huge speeds that lead to 3G systems revolution.

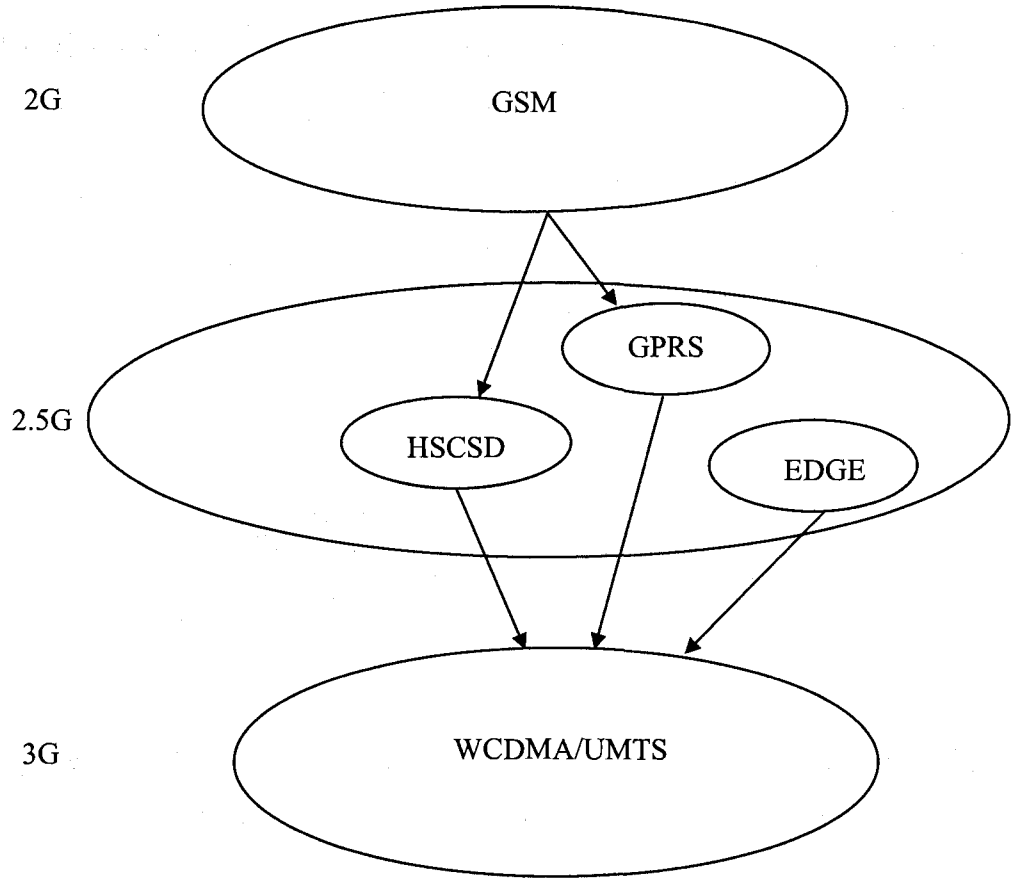

Figure 2-1: Various upgrade paths for 2G technologies

3G system is a future system that promises unparalleled wireless access in ways that have never been possible before. Companies developing 3G equipment predict that users one day will have the ability to receive live music, interactive web sessions, video calls, and conference calls with multiple parties, all from a small portable wireless device.

The eventual 3G evolution for GSM in Europe and most of the world have led to WCDMA, which is also called UMTS to support huge data rates up to 2 Mbps. Beside

the ability of WCDMA to serve huge number of users, its huge data rates are suitable for supporting multimedia communication. Fig. 2-1 illustrates the evolution of various 2G and 2.5G TDMA technologies into a unified WCDMA standard.

2.2. Background and Standardization of WCDMA

WCDMA is visionary air interface standard that has evolved since the end of the Twentieth-Century. The early version of WCDMA as a competitive open air-interface standard for the 3G wireless telecommunications was developed by the participation of European carriers, manufacturers, and government regulars collectively.

WCDMA was submitted by ETSI to ITU's IMT-2000 body in 1998 for considerations as a world standard. The idea behind WCDMA was to provide a high capacity upgrade path for GSM system and to assure background compatibility with the 2G GSM technology as well as all the 2.5G TMDA technologies. So the network structure of GSM data is retained by WCDMA with additional capacity and bandwidth provided by a new CDMA air interface. However a change out of the RF equipments at each BS is required for various 2G and 2.5G TDMA technologies like GSM, GPRS, and EDGE as well as the switching equipments. Around the turn of the century, several other competing WCDMA proposals were unified into a single WCDMA standard, and this resulting WCDMA standard is now called UMTS.

WCDMA is supporting huge data rates up to 2.048 Mbps per user, allowing high quality data, multimedia, streaming audio, streaming video and broadcast-type services to consumers. WCDMA designers assure that broadcasting, games, interactive video, and virtual private networking will be possible throughout the world using single mobile

handset. WCDMA requires a minimum spectrum of 5 MHz, which is an important distinction from the other 3G standards. With WCDMA, different data rates up to 2 Mbps will be carried simultaneously on a single WCDMA 5 MHz radio channel, and each channel will be able to support multiple calls simultaneously, depending on the radio channel conditions, and user velocity.

Due to of the high prices required for the deployment of new WCDMA radio system, the installation of WCDMA is likely be slow and gradual throughout the world. Thus the evolutionary path to the 3G requires a new generation of cell phones that support both the dual mode and tri mode and able to switch automatically between the 2G TDMA technology, EDGE or WCDMA service where it is available. It is expected by 2010 that WCDMA system will be fully installed around the world, eliminating the need for any backward compatibility with both the 2G and 2.5G TDMA technologies.

2.3. WCDMA System Architecture

Hereby, an overview of the UMTS system architecture is presented including an introduction to the logical network elements and interface. The same system architecture has been used in all main 2G systems and even some of the 1G systems, is utilized by the UMTS systems. From the standardization and specification point of view, both MS and UTRA network (UTRAN) consist of completely new protocols and interfaces that adapt with the new system design which is based on WCDMA radio technology. However, the definition of the CN is adopted from GSM. This mixture makes UMTS as major mobile system that accelerates and facilitates its introduction.

The UMTS system consists of a number of logical network elements, each of them with a defined functionality. The network elements are grouped in the UTRAN, the CN, and the MSs, which in 3GPP are called User Equipments (UE), as shown in Fig. 2-2 [9]. The UTRAN responsibility is mainly for handling all the radio-related functionalities. The CN is responsible for routing and switching calls and data connections to different destinations. The UE interfaces with the user and the radio interface. From the UMTS network architecture block diagram in Fig. 2-2, the UTRAN consists of a number of Radio Network Subsystems (RNS) that is connected to the CN through an open standardized interface called Iu interface. The RNS is composed of a Radio Network Controller (RNC) and a number of BSs, which are called Node Bs according to the 3GPP specifications. A Node B is connected to the RNC through standardized interface called Iub interface, to serve multiple cells. Each Node B acts as interpreter to convert the data flow between the Iub and Uu interfaces and to participate in the radio resource management (RRM). The RNC is responsible for controlling all the radio resources of all the Node Bs connected to it.

In the CN, both the Mobile Switching Centre (MSC) and the Serving GPRS Support Node (SGNS), serve the UE in its current location for circuit-switched (CS) and packet-switched (PS) services, respectively. Thus, the CN is architecturally a GSM phase 2.5G that is powered up to handle higher bit rates of the UMTS traffic.

The UE consists of two parts, the first part is the Mobile Equipment (ME) which is the user end point radio part used to access the radio communication channel requesting for speech or data service. The second part is the UMTS Subscriber Identity Module (USIM) which is a smart card that holds the subscriber identity and all subscription information.

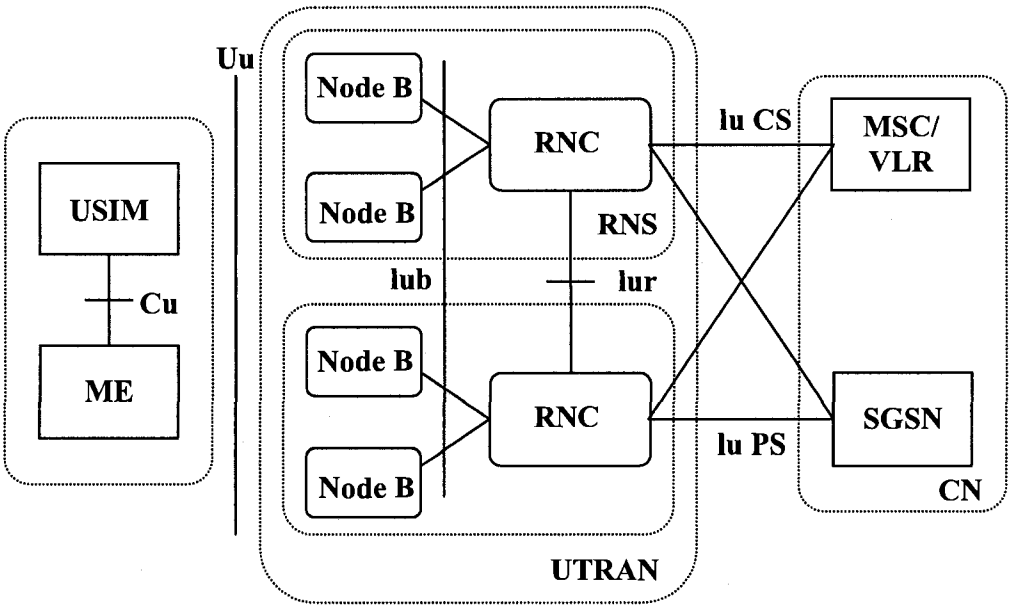

Figure 2-2: UMTS Network Architecture

However the Cu interface is the standardized interface between the ME and the USIM. Throughout the thesis the user terminal or equipment will be called MS, as well as the Node B will be called as BS.

2.4. WCDMA Air interface

WCDMA is an air interface used in the UMTS networks. However WCDMA is spread spectrum mobile air interface that utilizes DS-CDMA to provide better services and to support high capacity. The basic principle of CDMA systems is to spread the information data bits over a wide bandwidth by multiplying the data bits with Pseudo random bits of higher bit rate than the information data. The basics of CDMA are described in [1] and [10].

The frame structure of the WCDMA is shown in Fig. 2-3. The duration of a frame is 10ms, and contains 15 slots. Each of duration 0.667 ms and contains 2560 chips as this chip rate is 3.838 Mchips/s with carrier bandwidth of 5 MHz. The large bandwidth allows the support of different users' data rates services simultaneously at once. The transmitted signals at the same cell are separated by means of orthogonal codes known as channelisation codes that are extracted from an Orthogonal Variable Spreading Factor (OVSF) code tree [24]. The channelisation codes are used as variable multi-code connections with different SF to support very high variability of different bit rates. The SF represents the number of chips used to spread one data bit (i.e. different code length). Since these orthogonal codes have poor autocorrelation properties in the presence of fading channels, therefore, the transmitted signals again scrambled by Gold codes scrambling codes.

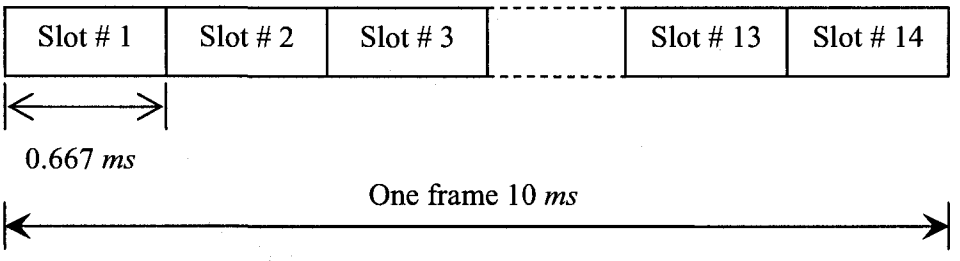

Figure 2-3: WCDMA frame structure

2.4.1 Channelization codes

Channelization codes are OVSF codes that preserve the orthogonality between different users. They are basically Walsh codes of different lengths that are able to preserve orthogonality between a user's different physical channels and even when they are

operating at different data rates. The OVSF codes are arranged in the form of a tree structure as shown in Fig. 2-4 for the purpose of code allocation. The following criterion should be applied for an addition code to be reserved: neither of the codes in the path from the target code to the root of the tree are already in use (i.e. for smaller SF), nor any of the codes in the branches above the target code (i.e. for higher SF). This restriction should be considered otherwise no orthogonality will be maintained and the code will not be orthogonal with every other code.

The codes are defined as $C_{ch,SF,k}$ where k is the code number and SF the spreading factor. In WCDMA the SF may vary from 4 to 256 chips in the uplink, however in the downlink it varies from 4 to 512 [8] and [20].

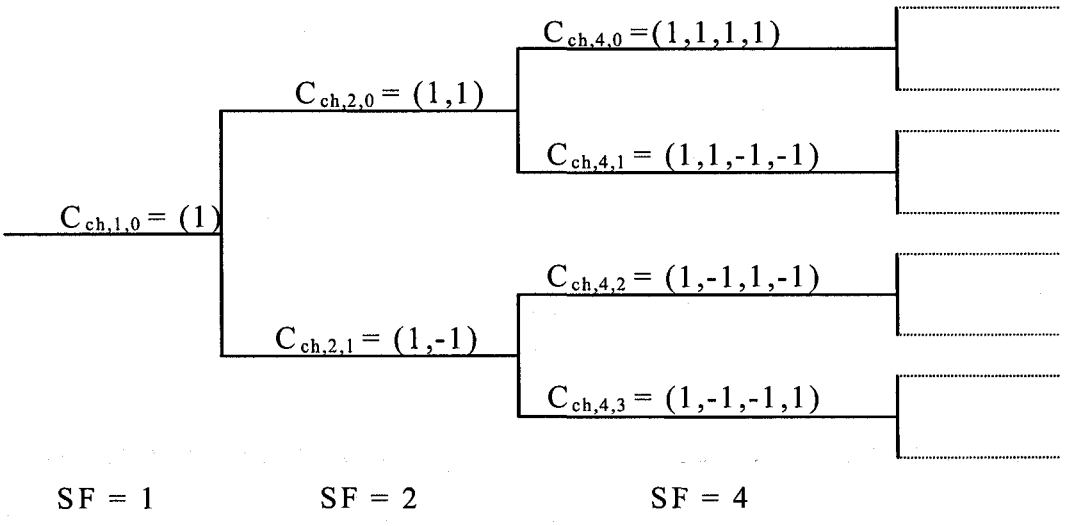

Figure 2-4: OVSF code tree

2.4.2 Scrambling codes

In the presence of Fading channels Walsh codes provide poor autocorrelation functions and non-zero cross-correlations functions. The nature of radio transmission with multi

path propagation renders Walsh codes unsuitable for multiple access codes. Since the channelization codes are Walsh codes of different lengths depending on the service provided, Walsh codes are scrambled by another codes having good autocorrelation and cross correlation properties known by scrambling codes.

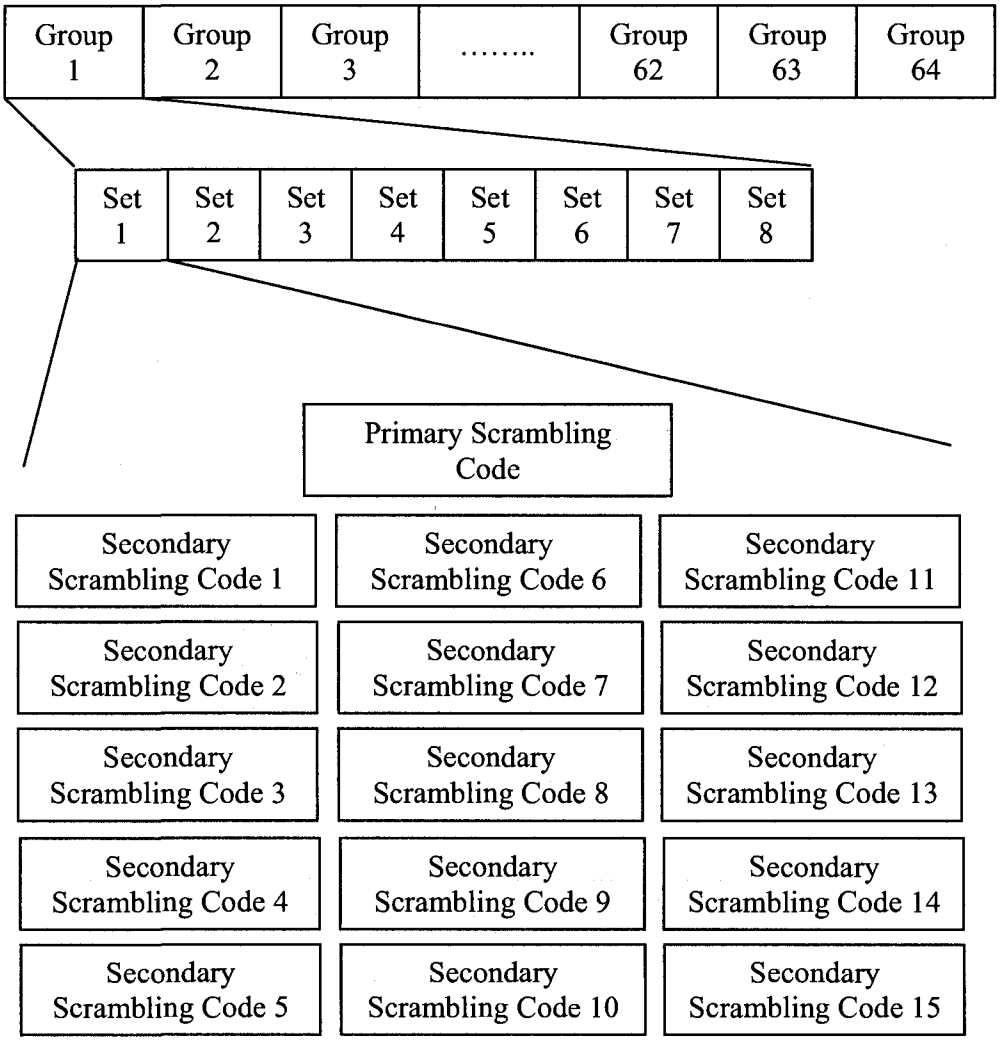

Figure 2-5: Scrambling code hierarchy [8]

The scrambling codes according to the UTRA FDD specification are 38400-chip segment of a 2^{18}-1 length Gold code truncated to one frame interval. The scrambling coded are complex valued of inphase and quadrature components. Primarily 8192 codes are used. For the 3.84 Mchips/s transmitted chip rate, the 38400 chip code lasts 10 ms (i.e. the whole frame duration).

The 8192 Scrambling codes are divided into 512 sets. Each set contains 16 codes composed of a primary scrambling code and 15 secondary scrambling codes. Eight sets grouped together are forming one group that contains 128 codes (8 primary scrambling codes and 8×15=120 secondary scrambling codes). Therefore in WCDMA there are 64 groups. One primary scrambling code and 15 secondary scrambling codes are assigned for one cell. Fig. 2-5 shows the scrambling code hierarchy of WCDMA.

A common rule of thumb is that OVSF channelization codes play an important rule in spreading users' data and to separate between different data flows belonging to the same user [25]. However Scrambling codes are used to separate data of mobiles belonging to the same cell in addition to its important participation in initial cell search algorithm as will be explained in details later [8].

2.5. Transport Channels and their mapping into Physical Channels

The physical layer always has a major impact on the equipment complexity as well as the system performance either from the mobile terminal side or the base station equipment side. The UTRA FDD physical layer specifications are contained in references [8], [9], [12], and [20–23].

Normally, the data generated at higher layers is carried over the air with transport channels, which are mapped to different physical channels. According to UTRA specification that the transport channels are services offered by physical layers to the higher layers [12], [26]. The physical layer is required to support variable bit rate transport channels in order to offer bandwidth-on-demand services. In UTRA, there are two basic types of transport channels called Dedicated Channels and Common Channels [12]. The main difference is that the Common Channel carries information to all MSs within a cell and are used by the MSs to access the network, whereas a Dedicated Channel is used by a MS for the duration of a call.

2.5.1 Dedicated Transport Channel

The only dedicated transport Channel is the dedicated channels for which the term DCH is used in the UTRA specifications. One DCH is allocated to one MS to carry all the information needed for a particular MS coming from higher layers, including data for the actual service. The DCH can be for both uplink and downlink. There are two types of dedicated physical channels assigned to carry the DCH [8]. The dedicated physical control channel (DPCCH) carries physical layer control information to/from a particular MS and the dedicated physical data channel (DPDCH) that transports the user traffic.

2.5.2 Common Transport Channel

The Common Transport Channels convey all information to/from all MSs within the same cell. The term CCH is used according to the UTRA specifications.

There are different kinds of CCH that are needed for the basic network operation.

- Broadcast Channel (BCH) - Downlink transport channel that is used to broadcast system and cell specific information over the entire cell.

- Forward Access Channel (FACH) - Downlink transport channel that carries small amount of information such as short packets of user data [8] [9].
- Paging Channel (PCH) – Downlink transport channel transmitted over the entire cell. PCH carries relevant data to the paging procedure associated when the network initiates communication with MS.
- Random Access Channel (RACH) – Uplink transport channel used by Ms requesting to set up connection to access the network resources.

Different transport channels are mapped into different physical channels to be transmitted over the air interface, though some of the transport channels are carried by identical physical channel.

- The common pilot channel known by CPICH is used to provide a common demodulation reference over the entire cell.
- The primary common control physical channel (P-CCPCH) carries BCH to provide general network information over the entire cell.
- The secondary common control physical channel (S-CCPCH) carries PCH and FACH for paging and packet data.
- The synchronization channel (SCH) that the MS uses for initial cell search and synchronization process.
- The Acquisition indication channel (AICH) that controls the use of common uplink channels.
- Page Indication Channel (PICH) that is associated with a PCH on an S-CCPCH to carry page indicators to MSs within a cell to examine the next S-CCPCH frame for paging.

- Physical Random Access Channel (PRACH) that carries RACH in the uplink by MS to request a service from a BS.

Further explanations in details for either transport or physical channel can be found in [8], and [9]. The detailed information on mapping the transport channels into the physical layer is explained in [12], [20], and [21]. Fig. 2-6 gives a brief on mapping the transport channels into physical channels.

However, for the rest of the thesis, only the UTRA FDD downlink channels which are involved in the initial cell search procedure by the MS need further explanation as will follow.

2.6. Signaling

Signaling is the data and information messages to be transmitted between the network and the terminals for the system operation. This section concentrates on the methods used for transmitting signaling messages generated above the physical layers needed for the synchronization process between the BS and the MS to assist the MS to synchronize to a BS of the lowest path loss. However, it should be clear that the SCH, CPICH, and P-CCPCH are the most important downlink channels that play important role in the cell search procedure. These physical channels are only used to facilitate cell search. In this section, the CPICH, P-CCPCH and SCH will be explained in detail.

2.6.1 Common Pilot Channel (CPICH)

It is a predefined bit sequence transmitted with constant bit rate with channelization code $C_{ch,256,0}$ (i.e. SF of 256), while its scrambling code is the cell's primary scrambling

code. The CPICH is continuously broadcast over the entire cell to provide a coherent reference to obtain SCH, P-CCPCH, AICH and PICH at eh MSs in a certain cell. That is because all of these mentioned channels do not carry their own pilot information.

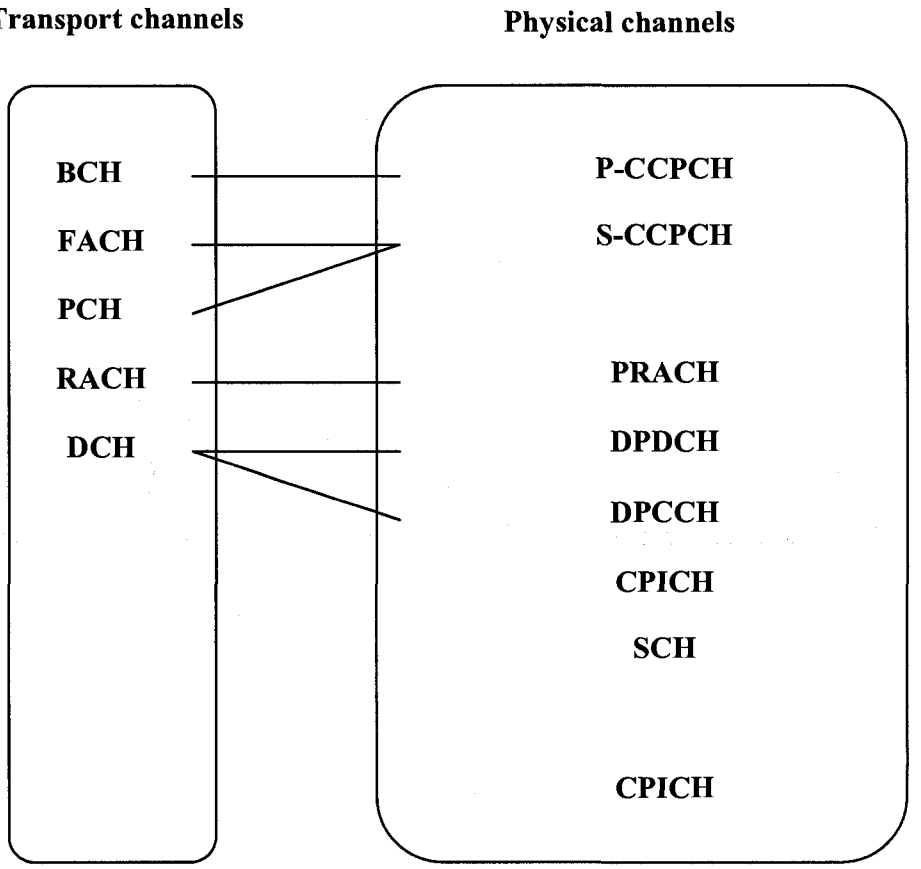

Figure 2-6: Transport channels into physical channels mapping [12]

2.6.2 Primary Common Control Physical Channel (PCCPCH)

P-CCPCH carries BCH which is transmitted continuously over the entire cell. P-CCPCH is spread by SF of 256 and scrambled by the cell's primary scrambling code. The P-CCPCH is transmitted with constant bit rate of 30 kbps. However the total bit rate is

reduced to 27 kbps as the P-CCPCH alternates with the SCH. Thus the P-CCPCH occupies 90% of the slot, while the first 10% of the slot is occupied by the SCH as shown in Fig. 2-7.

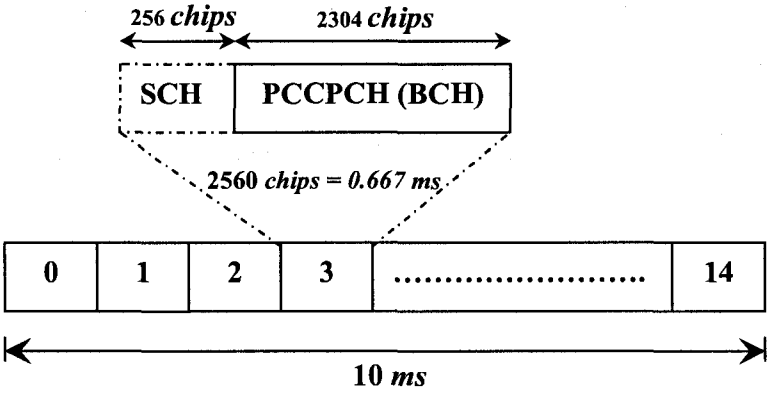

Figure 2-7: P-CCPCH frame structure

2.6.3 Synchronization Channel (SCH)

SCH is a basic function in any communication system. SCH is used by all the MSs in the network in the initial cell search process. As mentioned before, from Fig. 2-7 the SCH occupies the first 10% of these slots to be transmitted in the form of 256 chips with duration of $66.67\,\mu s$. The SCH is divided into two sub channels, the Primary and Secondary SCH that are transmitted over the 15-slots frame as in Fig. 2-8 [12].

The primary synchronization code (PSC) (shown as C_p in Fig. 2-8) is a system wide unique code sequence. The PSC is identical in every slot and for every BS to be transmitted repeatedly at the start of each slot for the whole frame. Basically, PSC is constructed as a so-called generalized hierarchical Golay sequence chosen to reduce the

complexity of the cell search procedure. In addition, it has good autocorrelation properties [20].

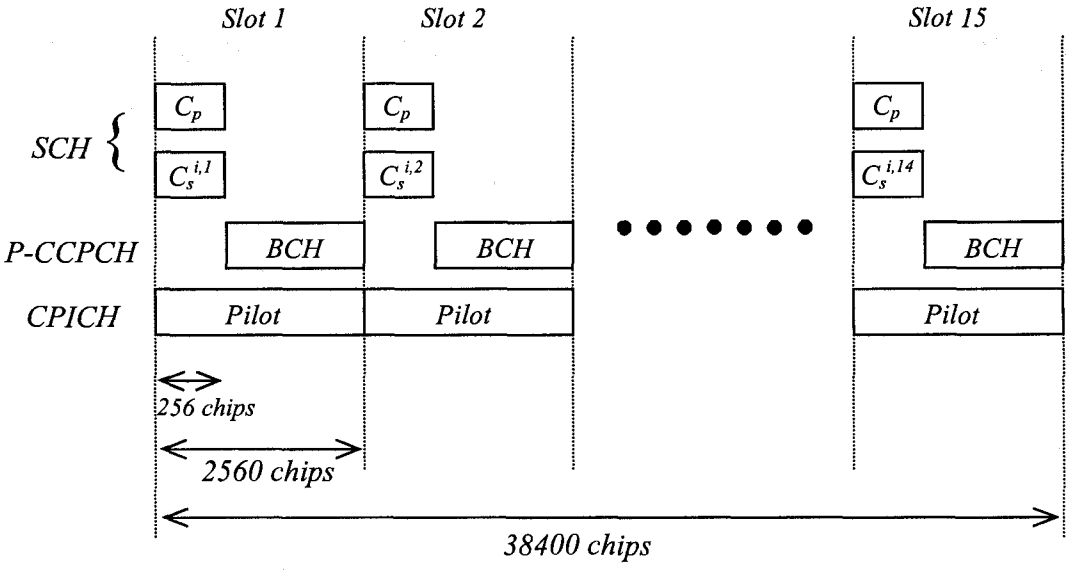

Figure 2-8: 10 *ms* SCH radio frame

The MS utilizes the PSC initially to detect the presence of a nearby BS and to identify the slot boundaries (i.e. start of each time slot).

The secondary SCH (shown as $C_s^{i,j}$, j=0, 1... 14 in Fig. 2-8) is transmitted simultaneously with the primary SCH at the beginning of each slot.

Unlike the PSC, the secondary synchronization code (SSC) varies from BS to BS and from slot to slot over the 15 slots of the whole frame. The 15 code symbols are sequentially transmitted once every frame. Each code symbol is chosen from 16 different Hadamard codes labeled from 1-16 of length 256 chips. The sequences of SSCs are used to encode the 64 different scrambling code groups such that the SSCs in a frame

constitute a predefined sequence that is associated with the scrambling code group used by the cell (see Fig. 2-5 of the scrambling code hierarchy). Each code group is represented by a Reed-Solomon (RS) word forming 64 RS words with unique cyclic-shifts to determine the frame boundaries and the scrambling code group. By the aid of the SSC, a MS is able to determine the scrambling code group out of the 64 code groups. The identified group has eight sets, and each set has a unique primary scrambling code that scrambling the pilot code. Each SSC corresponds to a code group and hence identification of the SSC sequence can be jointly performed with frame boundary synchronization. Once scrambling code group identified, the MS receiver cross-correlates the pilot code with all the eight possible primary scrambling codes of the eight sets in the group to determine the correct primary scrambling code. Since this code also scrambled the BCH data, this data can now be recovered. Both PSC and SSC are not subjected to multiplication by either channelization code or scrambling codes. By the mean of the SSC, the MS is able to detect the frame boundaries, in addition to defining the scrambling code group to which the primary scrambling code belongs to.

From the last section, it is clear that the cell search procedure is carried out in three stages: slot synchronization by the mean of the PSC, frame synchronization and scrambling code group identifications by the mean of SSC, and finally Scrambling code identification to detect the primary scrambling code to decode the BCH.

Next chapter will explain in details the cell search procedure and the state of art done in that field to enhance the synchronization time taken by MS to tune to the BS of the lowest path loss.

Chapter 3

Cell Search

3.1. Introduction

In the third generation networks, WCDMA and CDMA2000 are a wideband spread spectrum mobile air interface that utilizes the DS-CDMA method to achieve higher speeds and support more users. However in spread spectrum communication, synchronization process between the transmitter and receiver is a crucial problem as it impacts the system performance [1]. There is always a need to design efficient receiver structure and algorithms to reduce the synchronization time. If the classical serial search of synchronization techniques were applied in either CDMA2000 or WCDMA [1] [10], it would lead to unacceptable long synchronization time due to large number of scrambling code. Therefore GPS is introduced in CDMA2000 [8] as well as special synchronization channels in WCDMA to reduce the synchronization time [12].

In CDMA2000, the system relies on synchronized BSs using the same Scrambling code with different code shifts to enable the MS to acquire the scrambling code in relatively short time [4]. GPS is used as an external timing source to synchronize all the cell sites.

In contrast, WCDMA supports asynchronous BSs that assign different scrambling codes to the cell sites. In WCDMA the synchronization process is carried out in three stages called three stages cell search procedure: slot synchronization, frame synchronization and scrambling code-group identifications and, finally, primary scrambling-code identification. Each stage has its own error probability that depends on stage related and channel conditions parameters. These Parameters are defined and configured in a way that provides fast synchronization with a minimum processing load [5].

This chapter summarizes the efforts by research groups and the 3GPP working groups in order to design an efficient scheme and algorithm for each stage of the three stages of the cell search algorithm of WCDMA.

3.2. Three stages procedure cell search

The purpose of the three-stage cell search procedure has been considered for fast synchronization of downlink scrambling code of a cell served by a certain BS for achieving code and time synchronization with the BS's downlink scrambling code. Cell search is performed in three scenarios: initial cell search when a MS is powered on, idle cell search when MS goes from inactive to active mode acquiring service and target cell search during the normal operation to find possible handover candidate when the MS moves from cell to another during a call.

3.2.1 First Stage: Slot Synchronization

In synchronization process, the first stage of cell search procedure (slot synchronization) is the most critical stage since it deals with the largest amount of uncertainty in the cell search. In the first step of the three-step cell search, the MS is

trying to detect the slot boundaries using the PSC that is transmitted over the Primary SCH. The receiver at the MS searches for the slot timing by correlating the received signal with the Primary SCH code using a matched filter whose tab coefficient is matched to the 256-chips PSC. Generalized hierarchical Golay Sequence for PSC is used to reduce the complexity of the matched filter as well as its good autocorrelation properties [27]. The slot timing of the cell can be detected from the peak values of the matched filter. The slot synchronization may be determined from observation over one slot duration. Since the signal-to-noise ratio (SNR) of transmitted PSC is very low in addition to the fading channel effect, it is required to combine the correlation values from multiple slots to properly acquire the slot timing. This ensures that correct slot boundaries are identified.

3.2.2 Second Stage: Frame Synchronization and Code Group Identification

As mentioned in chapter 2, there are 16 secondary SCH sequences that are generated from Hadamard matrix labeled from 1-16. Unlike PSC, the SSC sequences vary from slot to slot. A frame (15 slots) of 15 secondary SCH symbols constitutes a codeword taken from a codebook representing the 64 scrambling code groups. These 64 codeword are (15, 3) RS words of 13 minimum distance constructed with unique cyclic shifts. The total number of codewords is 960 (64 codewords × 15 shifts). Both the PSC and the 16 sequences of the SSC are mutually orthogonal. Neither the PSC nor the SSC is scrambled by either channelisation code or scrambling code. During the second stage of three-stage cell search procedure, the frame synchronization and scrambling code group identification can be achieved using the SSC. The second step starts by correlating the received signal with all the 256-chips 16 Secondary SCH sequences using correlation bank. The decision is based on maximum likelihood detection after accumulating the

SSC correlation values over a frame. At the end, the candidate with the largest accumulated matrix is chosen to be passed to the third step for scrambling code identification. It is required to accumulate the correlation values from multiple slots to properly acquire the frame timing and the scrambling code group.

3.2.3 Third Stage: Scrambling Code Identification

During the third stage, the primary scrambling code of the group is identified by correlating the CPICH with the eight possible primary scrambling codes candidates within the code group identified from the second stage. Since the primary code also scrambled the BCH data, this data can now be recovered. After the primary scrambling code has been identified and the BCH transmitted on the P-CCPCH is detected, the cell search is finished.

3.3. Literature Review

The three-stage cell search procedure reduces the synchronization time of MS to tune to the BS of the lowest path loss. However, cell search is still complicated in the presence of signals that are intended for other MSs in the same cell as well as signals of other BS serving neighbor cells. That's why, cell search has been always point of research that attracts researchers and work groups around the world.

During the recent years, extensive research efforts focused on introducing efficient schemes and techniques for each stage of the three stages of the cell search algorithm in WCDMA in order to enhance the performance and the reduce the synchronization time. The driving force behind such growth in the number of research activity is the explosive growth in installation and deployment of UMTS systems all over the world. This section

summarizes the efforts done by research groups and the 3GPP working groups in order to introduce efficient methods and combining algorithms for each stage of the three stages of the cell search algorithm of WCDMA. An extensive and up-to-date literature review covering the most important aspects of synchronization process is then presented.

Wang and Ottosson in [28] introduced new combining technique for both the first and second stage of WCDMA cell search procedure. Both initial and target cell scenarios were studied in the proposed technique. Code and timing synchronization was achieved assuming low SNR and large frequency offset. Based on new statistical modeling of frequency error employed by Wang and Ottosson in [29] for WCDMA Synchronization, the frequency errors considered were 20 kHz and 0 Hz respectively, for initial cell search and target cell search.

In the system model, the signals of the SCH as well as the CPICH were generated from one BS to pass through Raleigh fading channel before adding noise effect. Assuming the delays of the multipaths varied slowly with time, so they were considered to be constant. Complex Gaussian process was used to model the inter-cell interference. However, the intra-cell interference was generated by summing up 16 different equal power signals.

It was the first time to suggest pipeline strategy with all the three stages running continuously such each stage fed the next stage by its output result. In the first stage of the three-stage cell search procedure, non-coherent combining technique was introduced reducing the effect of the large frequency errors. However, in the second stage coherent combining was introduced to acquire the frame boundaries and the downlink scrambling code group and it was compared to the results of the non-coherent combining at the same stage under same proposed channel condition. Based on the simulation results, Wang and

Ottosson concluded that using non-coherent combining in first stage and coherent combining in the second stage of cell search procedure would improve significantly the cell search performance and perform better synchronization time.

Mario et al in [30] extended the previously published results by Wang and Ottosson by investigating the new idea of oversampling technique of the received signal. The simulation showed that oversampling of the received signal had a significant performance impact on the cell search procedure and reduced the synchronization time. With no doubt, oversamling at the receiver increases the timing resolution and the robustness against errors. Since the slot synchronization (first stage) is the most crucial stage of the three-stage cell search procedure as it determines the timing resolution to the other 2 stages, oversampling of factor 4 (i.e. Tc / 4) was proposed for the first stage only with reduction in the sampling rate (normal chipping rate Tc=0.667ms/2650) for the second and third stages to reduce the computational complexity. The results indicated that the synchronization time was minimized in the presence of oversampling by a factor of 4. The graphs showed the superiority of oversampling of factor 4 over both of factor 1, 2 and 3. However oversampling of factor 2 was close to that of 4. it was suggested also passing multiple candidate from each stage instead of one candidate will reduce the synchronization time. However it will increase the design complexity and the utilization.

In [31] Estrada et al implemented in FPGA the three-stage cell search technique proposed in [28] taking into consideration memory structure design that can suit to 4 time oversampling as in [30]. This hardware implementation saved area and power that was critical issue in mobile terminal. The tested hardware implementation gave results that were very close to those obtained in [28].

In [32] the comparison between the Coherent, non-coherent and Differential combining was studied in the presence of Raleigh fading channel with frequency offset for asynchronous spread spectrum systems. From the computer simulation, it was shown that coherent combining had very poor performance in the presence of the channel distortion and the RF impairment and it could not be used in practice. However, Differential combining outperformed the non-coherent combining only under small frequency offset (Δf=0→200Hz).

Instead of applying the conventional non-coherent combining at the first stage of initial cell search, differential detection in [33] [34] was applied in the first stage of initial cell search with the utilization of inner-slot partial correlation since the frequency offset in two consecutive partial correlations was considered to be constant. In addition to slot synchronization provided by this scheme, the frequency offset could be estimated and antenna diversity used to facilitate the operation of the carrier synchronization. In the system model, the PSC was alternately transmitted using single antenna for each slot in the transmit diversity mode. In even numbered slots PSC transmitted on antenna 1, and in odd numbered slots PSC transmitted on antenna 2 as shown in Fig. 3-1. The generated signal experienced Raleigh fading channel. In the second stage of the cell search, coherent combining scheme was used as well as the three cell search stages were processed using the pipeline technique proposed in [28].The computer simulation verified the superiority of the proposed differential technique over the non-coherent technique at low SNR with the use of transmit antenna diversity.

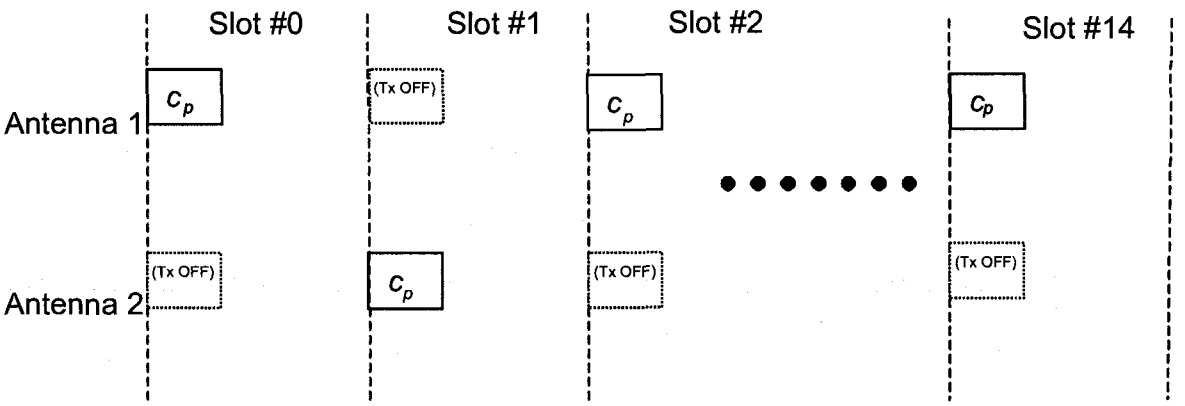

Figure 3-1: Two transmit antenna diversity

In [35] serial implementation of the cell search procedure was modeled by a Markov chain. From the model as in [1], the analytical expressions for mean synchronization time, detection, miss-detection, and false alarm probabilities for the different synchronization stages were derived under the assumption of Raleigh fading channel and frequency offset of 2 KHz. At the same time and under the same conditions, the mean synchronization time was calculated by the mean of computer simulation taking into account the fading channel effect and the 2 KHz frequency offset. Finally, the analytical results were compared with those obtained by simulation. In the computer simulation non-coherent combining was considered for the first and the second stage of the cell search proposing that non-coherent combining would increase the detection probability. In addition to combining would be over multiple slots in order to provide more reliability. The assumed simulation model consisted of SCH, CPICH, P-CCPCH and PICH of one BS. It was assumed that the generated signal of the target BS would experience interference from the neighbor cells that could be represented by Gaussian distribution. Comparing the analytical results with those obtained by computer simulation and at low SNR starting from -4dB, there was acceptable gap between both the analytical and the

simulation results of the mean synchronization time due to the effect of fading channel. The computer simulation occurred at Δf=2 KHz, however it was stated that the frequency offset had an impact on the mean synchronization time (i.e. the mean synchronization time increased approximately with the increase in the frequency offset).

Serial and parallel cell search techniques were proposed for the three stage cell search procedure. However, for the first time a hybrid configuration for the synchronization process was considered [36]. The first stage runs continuously and in parallel with the second and the third stage. However, the last two stages are serially running. That was behind the fact the third stage requires less number of slots than the second stage to provide any result, however its output depends on the second stage. That's in addition to the huge processing power consumed by those two stages. On the other hand, the first stage should run continuously searching for new cells by correlating the PSC received using a matched filter whose tab coefficient is matched to the 256-chips PSC. Consequently, it is important to minimize the complexity of the second and the third stages as of the positive effect on the battery life. Then formulae were derived for both mean and the worst case synchronization time. These formulae were verified through computer simulations that provided typical results in the range of 350ms at -18dB SNR.

For asynchronous cell site operation in DS-CDMA cellular mobile systems, Higuchi et al. proposed in [37] a fast cell search algorithm based on periodic masking of long spreading code that are transmitted periodically over the cell. To reduce the complexity of searching through all long scrambling codes used in the system, each cell transmits periodically a long code group identification code (GIC). Once the code group of the cell was detected, the scrambling code used by the cell can be easily identified. Simulation

results showed the significant outperformance in the synchronization time when the number of long spreading codes used was 512 and the number of GICs was 16. The research and development team at Ericsson proposed a modification for that idea [38]. Frame boundaries were detected in the second stage after identifying the code group in order to reduce the cell search time. This idea was accepted by the 3GPP specification to be applicable now a day in the second stage of the three-stage cell search procedure.

Ericsson in their working group draft proposed new idea by increasing the number of code groups in the second stage of the cell search [39]. They claim that increasing the number of code groups will reduce the number of scrambling codes in a code group. Thus the number of scrambling code correlators in the third stage will reduce. Their proposed scheme uses either 256, 128 or 64 code groups in the second stage of the cell search. They claim that the scheme using 256 code groups is the preferred scheme as it requires only two scrambling code correlators in the third stage of initial cell search. This will affect positively on the hardware complexity as well as on the decision reliability.

The three-stage synchronization process can operate either in serial or pipelined. In the serial approach, if the synchronization process failed at the end of any stage, the synchronization process returns to the beginning of the first stage and repeat the whole synchronization process. However in pipelined approach, the previous stage always produces new results to the following stage, and all stages are running in parallel as in Fig 3-2, so the last stage produces a new discovered code phase with each shift as will follow.

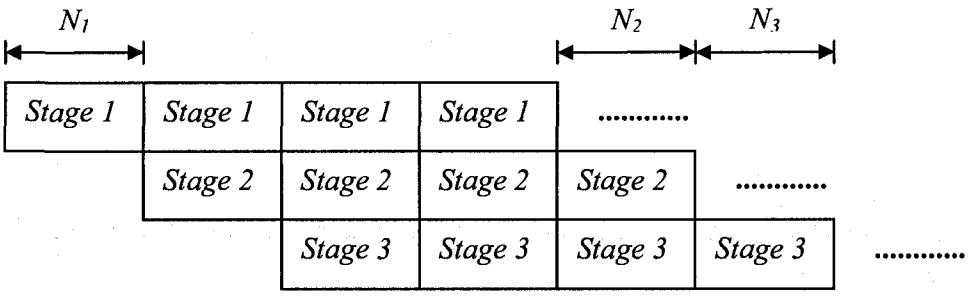

Figure 3-2: Three-stage cell search procedure using parallel pipeline technique [28]

However, the performance of the parallel cell search can be improved by adjusting the processing time in each step of the three-stage cell search procedure [40]. The second stage has been always taking longer processing time than those of the other two stages. This leads to excessive useless work for the first and the third stages of the cell search in addition to longer processing time. It is not proper to employ parallel three-stage cell search of equal stages processing time as this will contradict the idea of performance gain. For the second stage at least one frame should be received in order to identify the code group. However, 2 frames reveal much better performance. Therefore, for three-stage cell search of equal processing time [28], at least 90 slots are required for total cell search. Based on analytic derivations, Moon in [40] showed that the performance of the parallel cell search scheme can be improved by adjusting the processing time of step of the three-stage cell search depending on channel power allocation. From the simulation results, he concluded that either 14 slots, 30 slots and 2 slots or 13 slots, 30 slots and 3 slots can be used as the processing time of the first, second and third stages of the three-stage cell search respectively to provide better synchronization time. However, these

results were in the case of optimal Primary SCH loading factor (i.e. the power ratio of the Primary SCH to the total SCH) of 0.4 that was obtained from the computer simulations.

In the mentioned related work, all agreed on the superiority of pipeline technique in addition to the non-coherent combining in the first stage as well as coherent combining in the second stage. However, there has always been a conflict regarding the processing time of each stage of the three-stage cell search. In addition to, no one have discussed before the presence of more than one BS (Multi-target) in the vicinity of the MS.

Next chapter will investigate a host of WCDMA synchronization techniques used in cell search process. These techniques are considered for fast synchronization of scrambling code taking into consideration the presence of more than one BS in the vicinity of the MS, the effects of multi-path, frequency offset and Raleigh fading.

Chapter 4

Improved Cell Search Design

4.1. Introduction

This chapter investigates a host of new synchronization techniques for WCDMA used in cell search procedure. Mainly, this thesis chapter concentrates on the first stage of synchronization process (i.e. slot synchronization) of WCDMA. As the first stage (slot synchronization) is the most critical stage that provides timing resolution to the other 2 stages. The study is mainly based on computer simulations taking many practical system aspects into account like the presence of more than one BS (Multi-target) in the vicinity of the MS, and the effects of multipath, Raleigh fading, and carrier frequency offsets are considered. The new concept of parallel code verification circuits was introduced to the state of art pipelined techniques yielding results. These new synchronization techniques allow very efficient detection and improve the cell search in terms of synchronization time. The three stage cell search design and new proposed pipeline technique with verification circuits are explained in Sections 4.2, 4.3 and 4.4.

4.2. New Pipeline Technique

The proposed Pipelining technique is very efficient for WCDMA synchronization, where the synchronization results of each stage are continuously fed to the next stage every pipeline shift cycle (typically one frame but could be shorter) and the verification circuits are always in use. Fig. 4-1 shows an example of the operation of the new pipeline technique using two verification circuits. However the number of the verification circuits may vary according to the system design. For an efficient pipeline operation, the processing cost of the three synchronization stages of WCDMA is assumed to be equal (of length $m_1=m_2=m_3$ slots). The combined pipelining parallelism of verification circuits inherently reduces the time penalty due to missing correct code and false verification.

In Fig. 4-1 , the assumed verification time of the of the 2 parallel verification circuits is $m_1 \times m_4=2$ slots(if $m_1=1$ slot, $m_4=2$ slots which we defined as fast processing), all the false verification penalties (verification time wasted) reflect themselves as parallel and not in series waste of verification times. Assuming in Fig 4-1, that the first three verification trials failed, and the fourth succeeded, the total synchronization time in the parallel pipelined case would be 8 slots. This time is less than the serial search with no pipelining nor parallelism, which is given in this instance by 4 trials multiplied by the search time for each trial i.e. $4(3m_1 + m_1m_4) = 12m_1 + 4m_1m_4$ slots. Reason is simple, most verification losses due to code miss are absorbed (being run in parallel) by the processing times of stages 1, 2 and 3. Note that, the verification circuits are full in action all the time. Such combined use of parallelism and pipelining will reduce the mean synchronization time as will follow shortly. Throughout the thesis we assume the presence of 4 verification circuits (i.e. $m_1=1$ slot, $m_4=4$ slots known as fast processing

case). The four verification circuits provide reasonable results than those of two verifications circuits and less complexity than that of six verification circuits.

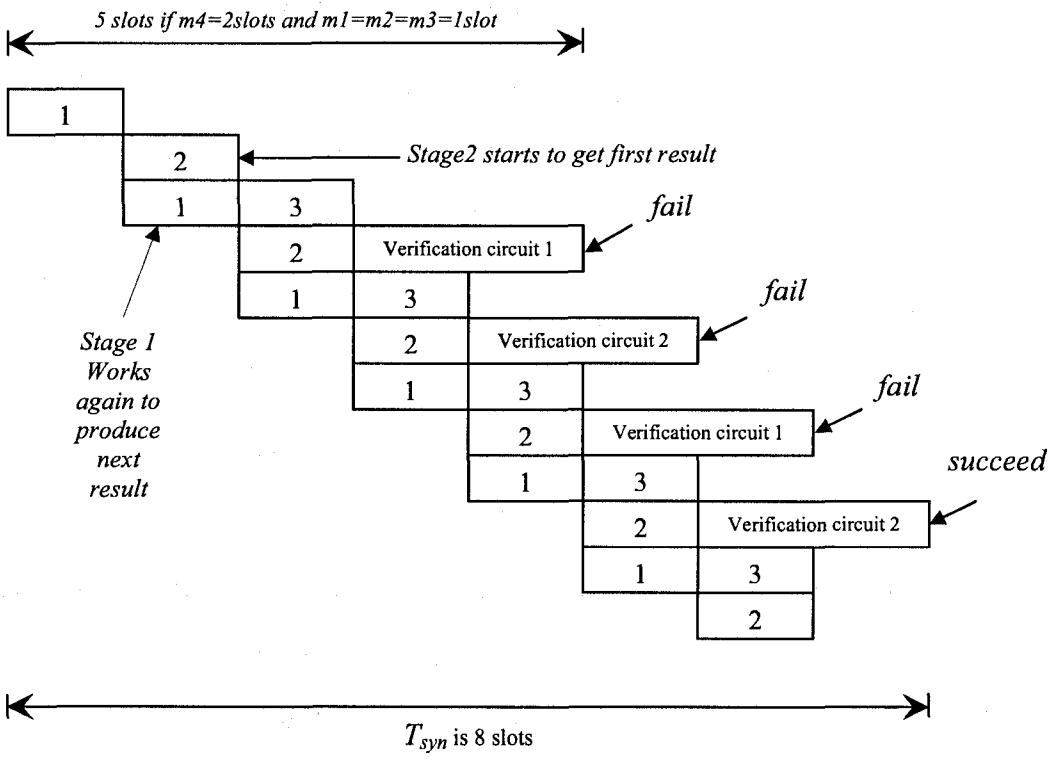

Figure 4-1: WCDMA parallel pipelined operation with 2 simultaneous verification circuits receiving in parallel

Beside fast processing case (m_1=*1* slot, m_4=*4* slots), slow processing case was also investigated, where m_1=*15* slots and m_4=*1*. This implies that code verification time is one frame = $m_1 \times m_4$ =*15* slots, each stage costs one frame of 15 slots to process, and the cheaper utilization of only one verification circuit (this case is not shown in Fig. 4-1).

This thesis concentrates on the first synchronization stage being the most crucial. Finding the slot boundary with high degree of confidence is essential to reducing the total synchronization time in WCDMA systems. In particular, two rules for combining the

matched filter results of each slot of the frame were investigated, assuming various amounts of frequency offsets, Raleigh fading and Additive White Gaussian Noise (AWGN) representing the data signals of all BSs. Four multipath signals for each of the four BSs were assumed in the vicinity of the applicable user, thus giving 16 possible multipaths that can be detected. Section 4.3 shows the exact signal transmitted from all BSs and the approximation where we replace all interference signals save the PSC signal by an equivalent AWGN.

For all subsequent peak detection rules (algorithms), a pipelined synchronization operation with sliding frame technique is assumed such that at the end of each slot we find the BS epoch (slot boundary) of the previous frame. For example, at the end of slot 16 (first slot of second frame) the pertinent synchronization results for the previous first frame (slots 1-15) is found. At the end of slot 17, the result for slots 2-16 is found and so on, and the frames are sliding slot by slot. Generating large number of frames to simulate the signal provided better confidence in results. Oversampling strategy was used to provide better results in calculating the slot boundary probability (first stage) of detection (P_{d1}) and the probability of false alarm (P_{fa1}) based on the numerous peak detection algorithms. However, only the first stage of the standard WCDMA synchronization was analyzed. The main result herein pertains only to the slot boundary detection of the 1st stage. However, once P_{d1} and P_{fa1} are found (as will be done shortly), we can still compute good bounds over the synchronization times as well.

In Fig 4-1, the parallel pipelined synchronization system is considered under steady state operation where all stages are engaged. After averaging over all possibilities code synchronization, the mean synchronization time can be computed as follows [43]:

$$T_{syn} = m_1(m_4 + 3) + m_1 \sum_{i=0}^{\infty} ia(1-a)^i = m_1(m_4 + 3) + \frac{m_1(1-a)}{a} slot - time. \quad (1)$$

This thesis shows that the fast processing case is possible for the first stage, using the sliding frame concept. However, for the second and third stages, of the WCDMA synchronization process, more hardware would be required if the processing time is $m_1=1$ slot, rather than the typical one frame processing time, i.e. $m_1=15$ slots (slow processing case).

In the above calculation of synchronization process time, independence of the results of the three synchronization process stages was assumed. This is the worst case assumption which is difficult to happen in practical life, and the two mean synchronization process times obtained in this case (for fast and slow processing) are thought of as upper bound on synchronization process time. Assuming the first stage performance is the limiting factor and so take $P_d = P_{d1} = P_{d2} = P_{d3}$.

In correlated situations, high values of interference may bring bad results from all three stages. More favorable results may lead to success of all three stages, and so on. In this case we may obtain two more synchronization process time results from (1) by substituting $a=P_{d1}$ and not P_{d1}^3, However these two extra results are thought of as lower bound on synchronization process time.

4.3. Signal and System Model

All received multipath samples of a given signal PSC, SSC, CPICH ...etc of same frame have the same random carrier phase, samples of one frame have the same Raleigh fading envelope, and received signal delay with respect to local MS time does not change.

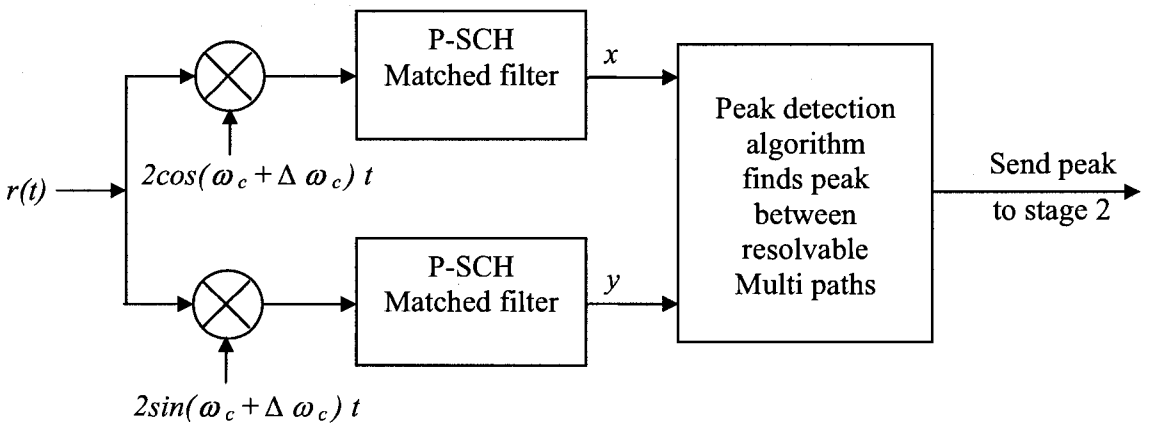

Figure 4-2: Carrier removal and despreading prior to application of peak detection algorithm

This is justified since the BS synchronization signals, PSC, SSC, and CPICH are all transmitted synchronous with each other and in streaming mode.

At the transmitter, Quadrature-PSK (QPSK) modulation technique is used, so the generated signal will be multiplied by the quadrature carriers $cos(\omega_c t)$ and $sin(\omega_c t)$ where ω_c is the angular carrier frequency of 2 GHz. However the generated signal while propagating will be subjected to propagation delay $\tau(t)$ according to the path ℓ taken (since the delays of multipaths vary slowly with time, they are considered to be constant, i.e. $\tau(t)=\tau$), fading channel represented by α the Raleigh fading factor which depends on the path of the signal taken and random phase error φ uniformly distributed on $[0,2\pi]$. Therefore, the received signal $r(t)$ at the MS receiver can be written as in (2), to represent all the users and control data signals received from different base stations.

$$r(t) = \sum_{b=1}^{NBS}\sum_{\ell=1}^{MP} \alpha_{b\ell} c_p(t-\tau_{b\ell})[\cos(\omega_c(t-\tau_{b\ell})+\varphi_{b\ell}) + \sin((\omega_c(t-\tau_{b\ell})+\varphi_{b\ell})] +$$
$$\sum_{b=1}^{NBS}\sum_{\ell=1}^{MP} \alpha_{b\ell} c_{sb}(t-\tau_{b\ell})[\cos(\omega_c(t-\tau_{b\ell})+\varphi_{b\ell}) + \sin((\omega_c(t-\tau_{b\ell})+\varphi_{b\ell})] +$$
$$\sum_{b=1}^{NBS}\sum_{\ell=1}^{MP} \alpha_{b\ell} P(t-\tau_{b\ell}) W_b(t-\tau_{b\ell}) S_{pb}(t-\tau_{b\ell})[\cos(\omega_c(t-\tau_{b\ell})+\varphi_{b\ell}) + \sin((\omega_c(t-\tau_{b\ell})+\varphi_{b\ell})] +$$
$$\sum_{b=1}^{NBS}\sum_{s=1}^{NU}\sum_{\ell=1}^{MP} \alpha_{b\ell} W_{sb}(t-\tau_{b\ell}) S_{is}(t-\tau_{b\ell}) d_{is}(t-\tau_{b\ell}) \cos(\omega_c(t-\tau_{b\ell})+\varphi_{b\ell}) +$$
$$\sum_{b=1}^{NBS}\sum_{s=1}^{NU}\sum_{\ell=1}^{MP} \alpha_{b\ell} W_{sb}(t-\tau_{b\ell}) S_{qs}(t-\tau_{b\ell}) d_{qs}(t-\tau_{b\ell}) \sin(\omega_c(t-\tau_{b\ell})+\varphi_{b\ell}) \quad (2)$$

where *NBS* is the number of base stations, *MP* is the number of multipaths, *NU* is the number of users, $C_p(t)$ is the *PSC*, $C_s(t)$ is the *SSC*, $P(t)$ is *CPICH*, $W(t)$ is the Walsh code, $S_i(t)+jS_q(t)$ is the complex scrambling code, $d(t)$ is the user and control data, τ is the delay ℓ^{th} path at time t, and $\Delta\omega_c$ is the frequency error (offset) between received carrier and local receiver carrier.

In (2), the first double summation represents the 256 chips PSC shown as C_p which is same in every slot. For every BS this code is transmitted repeatedly at the start of each slot of the frame to enable the MS receiver to identify the slot boundaries. The second double summation in represents the SSC of 15 code symbols transmitted in parallel with PSC to identify the code group and the frame boundaries. The third double summation represents the CPICH that is broadcasted over the entire cell to provide a common demodulation reference. The two triple summations represent the users' data that got spread with channelisation code followed by scrambling to differentiate between different users. From (2) it is clear that both PSC and SSC are not subjected to multiplication by either channelisation code or scrambling codes to reduce the complexity of the cell search.

For the first synchronization process stage, the received signal is correlated in the I & Q banks by the local matched filter carrier ($cos(\omega_c + \Delta\omega_c)\,t$ and $sin(\omega_c + \Delta\omega_c)\,t$), a subsequent LPF suppresses the double frequency terms, and the two matched filters each of length 256 chips representing the PSC code operate at the resulting signals yielding $x(t)$, and $y(t)$ signals as in Fig. 4-2. These outputs $x(t)$, and $y(t)$ signals are expressed in (3) and (4). Samples of the two matched filters are combined coherently or non-coherently in different ways yielding 5 scenarios. Coherent scenarios are assumed $x(t)$, $y(t)$, $x(t)+y(t)$, $x(t)-y(t)$ and the fifth non-coherent scenario $z(t) = \sqrt{x^2(t) + y^2(t)}$. After combining the signals either coherently or non-coherently, the combined signal is fed to peak detection algorithm to detect the peaks between the resolvable multipaths. Once the peak is detected, the slot boundary is identified and sent to the next stage. Since SIR of transmitted P-SCH code is very low, it is required to combine the correlation values from multiple slots to properly acquire the slot timing.

$$
\begin{aligned}
x(t) = & \sum_{b=1}^{NBS}\sum_{\ell=1}^{MP}\alpha_{b\ell}R_p(t-\tau_{b\ell})[\cos(\Delta\omega_c t + \omega_c\tau_{b\ell} - \varphi_{b\ell}) - \sin(\Delta\omega_c t + \omega_c\tau_{b\ell} - \varphi_{b\ell})] + \\
& \sum_{b=1}^{NBS}\sum_{\ell=1}^{MP}\alpha_{b\ell}R_{ps}(t-\tau_{b\ell})[\cos(\Delta\omega_c t + \omega_c\tau_{b\ell} - \varphi_{b\ell}) - \sin(\Delta\omega_c t + \omega_c\tau_{b\ell} - \varphi_{b\ell})] + \\
& \sum_{b=1}^{NBS}\sum_{\ell=1}^{MP}\alpha_{b\ell}R_{pp}(t-\tau_{b\ell})[\cos(\Delta\omega_c t + \omega_c\tau_{b\ell} - \varphi_{b\ell}) - \sin(\Delta\omega_c t + \omega_c\tau_{b\ell} - \varphi_{b\ell})] + \\
& \sum_{b=1}^{NBS}\sum_{s=1}^{NU}\sum_{\ell=1}^{MP}\alpha_{b\ell}R_{pwi}(t-\tau_{b\ell})\cos(\Delta\omega_c t + \omega_c\tau_{b\ell} - \varphi_{b\ell}) - \\
& \sum_{b=1}^{NBS}\sum_{s=1}^{NU}\sum_{\ell=1}^{MP}\alpha_{b\ell}R_{pwq}(t-\tau_{b\ell})\sin(\Delta\omega_c t + \omega_c\tau_{b\ell} - \varphi_{b\ell}) \qquad (3)
\end{aligned}
$$

$$y(t) = \sum_{b=1}^{NBS}\sum_{\ell=1}^{MP}\alpha_{b\ell}R_p(t-\tau_{b\ell})[\cos(\Delta\omega_c t+\omega_c\tau_{b\ell}-\varphi_{b\ell})+\sin(\Delta\omega_c t+\omega_c\tau_{b\ell}-\varphi_{b\ell})] +$$
$$\sum_{b=1}^{NBS}\sum_{\ell=1}^{MP}\alpha_{b\ell}R_{ps}(t-\tau_{b\ell})[\cos(\Delta\omega_c t+\omega_c\tau_{b\ell}-\varphi_{b\ell})+\sin(\Delta\omega_c t+\omega_c\tau_{b\ell}-\varphi_{b\ell})] +$$
$$\sum_{b=1}^{NBS}\sum_{\ell=1}^{MP}\alpha_{b\ell}R_{pp}(t-\tau_{b\ell})[\cos(\Delta\omega_c t+\omega_c\tau_{b\ell}-\varphi_{b\ell})+\sin(\Delta\omega_c t+\omega_c\tau_{b\ell}-\varphi_{b\ell})] +$$
$$\sum_{b=1}^{NBS}\sum_{s=1}^{NU}\sum_{\ell=1}^{MP}\alpha_{b\ell}R_{pwi}(t-\tau_{b\ell})\cos(\Delta\omega_c t+\omega_c\tau_{b\ell}-\varphi_{b\ell}) +$$
$$\sum_{b=1}^{NBS}\sum_{s=1}^{NU}\sum_{\ell=1}^{MP}\alpha_{b\ell}R_{pwq}(t-\tau_{b\ell})\sin(\Delta\omega_c t+\omega_c\tau_{b\ell}-\varphi_{b\ell}) \qquad (4)$$

The first double summation in (3) and (4) is the autocorrelation of the PSC represented by R_p. The second double summation represents the cross-correlation between the PSC and SSC shown as R_{ps}. The third double summation is the cross-correlation between the PSC and the CPICH represented as R_{pp}. However, the last 2 triple summations are the cross-correlation between the PSC and the users' scrambled data of the I and Q and are shown as R_{pwi} and R_{pwq} respectively.

Concentrating on the first stage of WCDMA synchronization process, (i.e. the slot synchronization process), (3) and (4) can be written as in (5), (6)

$$x'(t) = \sum_{b=1}^{NBS}\sum_{\ell=1}^{MP}\alpha_{b\ell}R_p(t-\tau_{b\ell})[\cos(\Delta\omega_c t+\omega_c\tau_{b\ell}-\varphi_{b\ell})-\sin(\Delta\omega_c t+\omega_c\tau_{b\ell}-\varphi_{b\ell})]+n(t) \qquad (5)$$

$$y'(t) = \sum_{b=1}^{NBS}\sum_{\ell=1}^{MP}\alpha_{b\ell}R_p(t-\tau_{b\ell})[\cos(\Delta\omega_c t+\omega_c\tau_{b\ell}-\varphi_{b\ell})+\sin(\Delta\omega_c t+\omega_c\tau_{b\ell}-\varphi_{b\ell})]+n(t) \qquad (6)$$

Where *n(t)* is an equivalent AWGN that models all the SSC, P-CPICH, and the users' data signals of different cells.

4.4. Slot Synchronization Rules

This section describes the different new techniques for WCDMA cell search and code synchronization process.

4.4.1 Rule 1, The Most likely sample Location

For each sliding frame, the sample locations within the slot corresponding to the 20 highest absolute values of each received signal samples of the slot are recorded. Further for Rule 1, we investigate 5 scenarios for possible samples to be processed, i.e. $x'(t), y'(t), x'(t) \pm y'(t)$ and $z(t) = \sqrt{x'^2(t) + y'^2(t)}$. The 15 sets of best maximum absolute 20 samples locations of each slot are then compared and the most occurring sample location of the processed signal over all slots is dumped as the possible BS received epoch, (called best location). Subtracting the matched filter code length (256 chips) from this, then yields the slot start, which is subsequently used by the next stage, i.e. SSC stage.

The signals are combined and processed. For simulation P_d is incremented by 1 whenever the detected multipath slot start location of one of the BS (the most likely) as obtained from the rule above coincides with one of the known multipaths, otherwise P_{fa} corresponding to false detection. Once P_d and $P_{fa} = 1 - P_d$ are found, the synchronization process time is computed as per (1).

4.4.2 Rule 2, Best of the Average of the Absolute

The output of the two matched filters $x'(t)$ and $y'(t)$ in (5), (6) are combined non-coherently forming $z(t) = \sqrt{x'^2(t) + y'^2(t)}$. The absolute values of *z(t)* samples at a certain location k of each sliding frame are averaged over the 15 slots of each sliding frame thus obtaining only 5120 running average samples of the original 76800 samples of

each sliding frame. The receiver subtracts 256 T_c from the sample location of the maximum of the 5120 samples to yield the most probable slot start to be sent to the second stage of the WCDMA standard.

During our simulation, the sample location of maximum (best candidate for slot start) of the 5120 samples is compared against the known locations of the 2×16 BSs multipath. If the location of the maximum value happened to coincide with one of the known BSs locations, P_d counter is incremented by 1 for each of the sliding frames. Once P_d and P_{fa} =1− P_d are found, T_{syn} is computed as per (1). Noticing that, this rule corresponds to a modified version of the classic matched filter detection as in [28]. However, this modified technique herein is threshold independent. This way, adjustment of this threshold and its variation with the number of like users, noise, and fading and its optimal choices is a delicate and complex issue that has been treated in the literature was avoided [41], [42].

4.5. Results

Various signals were generated at the receiver as per section 4.3 at different SIR and fading power (power of the Raleigh distributed random signal envelope). Each signal was processed as per the specified five peak detection scenarios in this thesis (i.e. *x(t), y(t), x(t)+y(t), ...*etc). Subsequent application of the peak detection Rule then yielded the probability of correct slot detection P_d as previously stated. All cases were simulated at a Doppler bandwidth of 10Hz and 100Hz. Raleigh faded signal envelope was simulated by generating two normal distributions, for fast processing case (m_1 =*1* slot, m_4=*4*) and slow

processing case (m_1 =15 slots, m_4=1) as mentioned before and for the worst case analysis ($a=P_d^3$) and for the best case correlated analysis ($a=P_d$).

All results were repeated at different carrier frequency errors (Δf of 0Hz, 100Hz, 4 KHz, and 20 KHz). Signals of 150 frames were simulated, which means 2236 sliding frames were averaged. The detection probabilities were obtained by simulation for the aforementioned peak detection rules, while the mean synchronization process time computed from (1).

For different carrier errors, the results are almost the same. This verifies that these two rules utilized in this thesis are robust to frequency offset and Doppler effect and can work even at large carrier errors. The reason is the assumed presence of more than one BS and the utilization of the new peak detection rules which are resilient to the carrier errors as well as Doppler effect.

For Rule 1, Figs 4-3.a, 4-4.a, 4-5.a, and 4-6.a represent the fast processing case at 10Hz Doppler effect and Δf of 0Hz, 100Hz, 4 KHz and 20 KHz respectively. Figs 4-3.b, 4-4.b, 4-5.b, and 4-6.b represent the fast processing case of 100Hz Doppler effect and Δf of 0Hz, 100Hz, 4 KHz and 20 KHz respectively.

Figs 4-3.c, 4-4.c, 4-5.c, and 4-6.c and Figs 4-3.d, 4-4.d, 4-5.d and 4-6.d represent the slow processing case of Rule 1 at 10Hz and 100Hz respectively and for the same mentioned carrier frequency offsets as in the fast processing case.

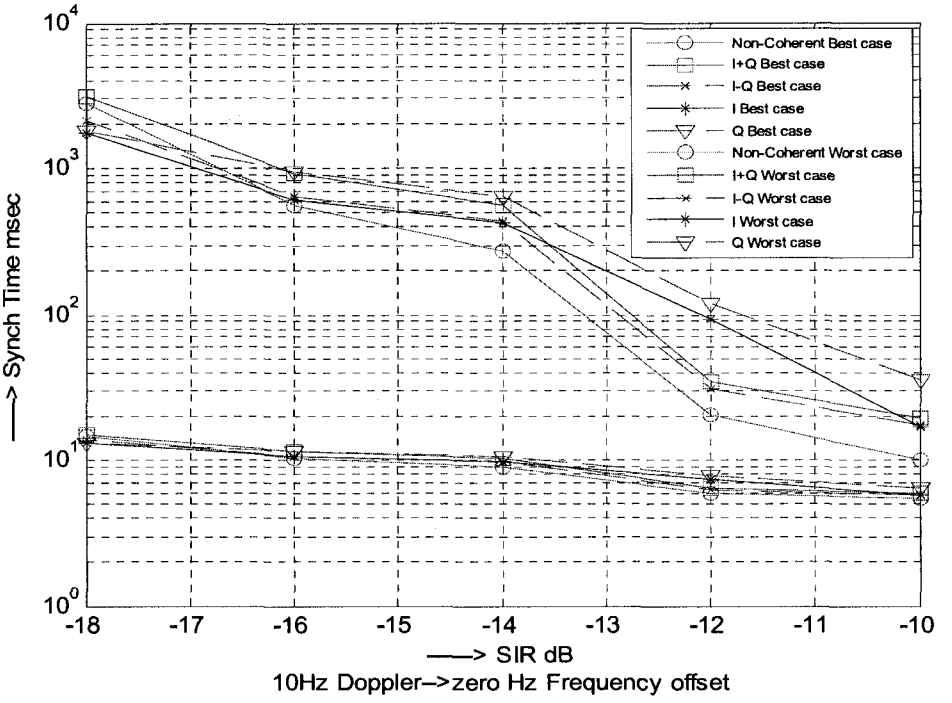

Figure 4-3.a: Rule 1 Fast Processing @ zero Hz frequency offset & 10Hz Doppler

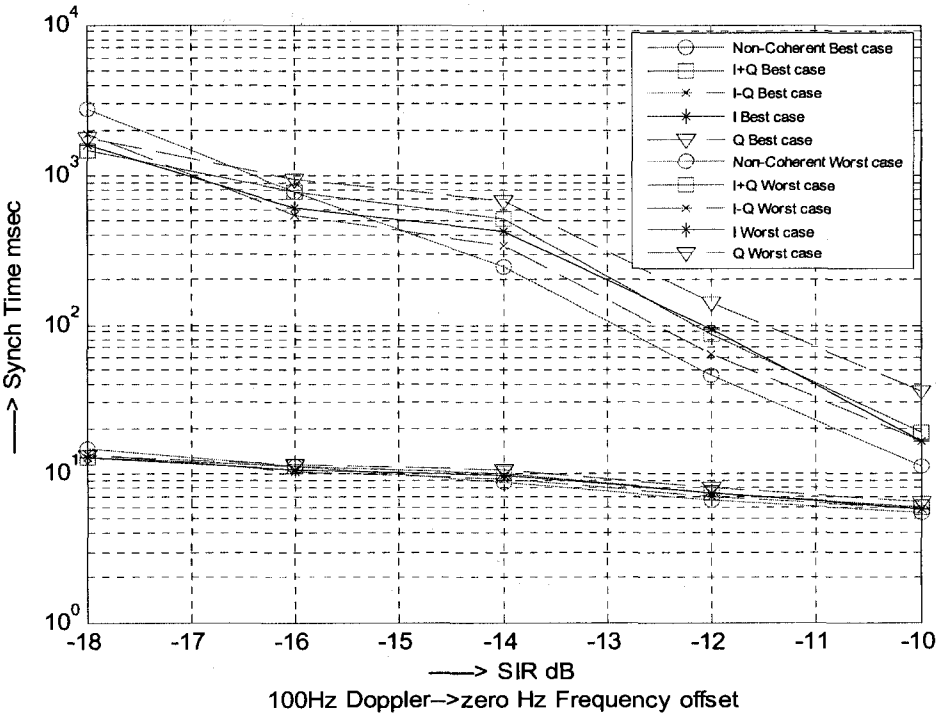

Figure 4-3.b: Rule 1 Fast Processing @ zero Hz frequency offset & 100Hz Doppler

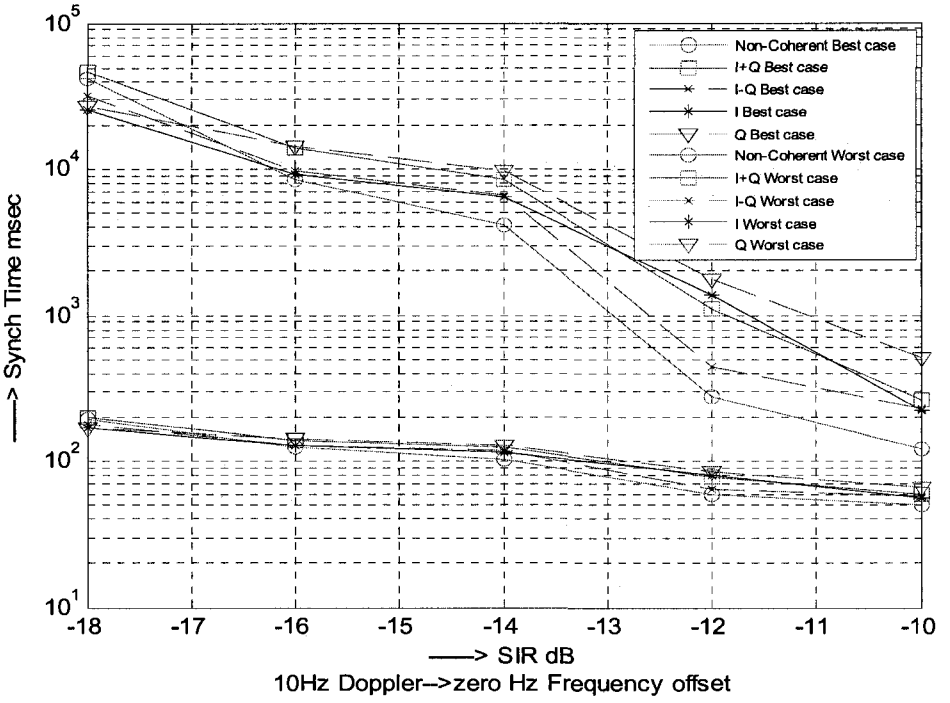

Figure 4-3.c: Rule 1 Slow Processing @ zero Hz frequency offset & 10Hz Doppler

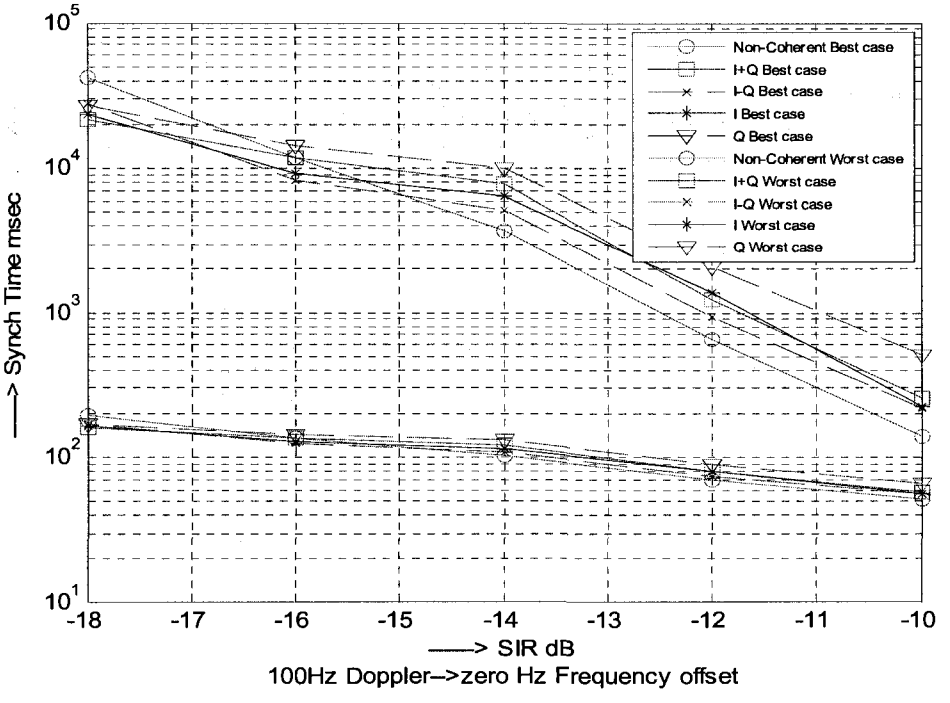

Figure 4-3.d: Rule 1 Slow Processing @ zero Hz frequency offset & 100Hz Doppler

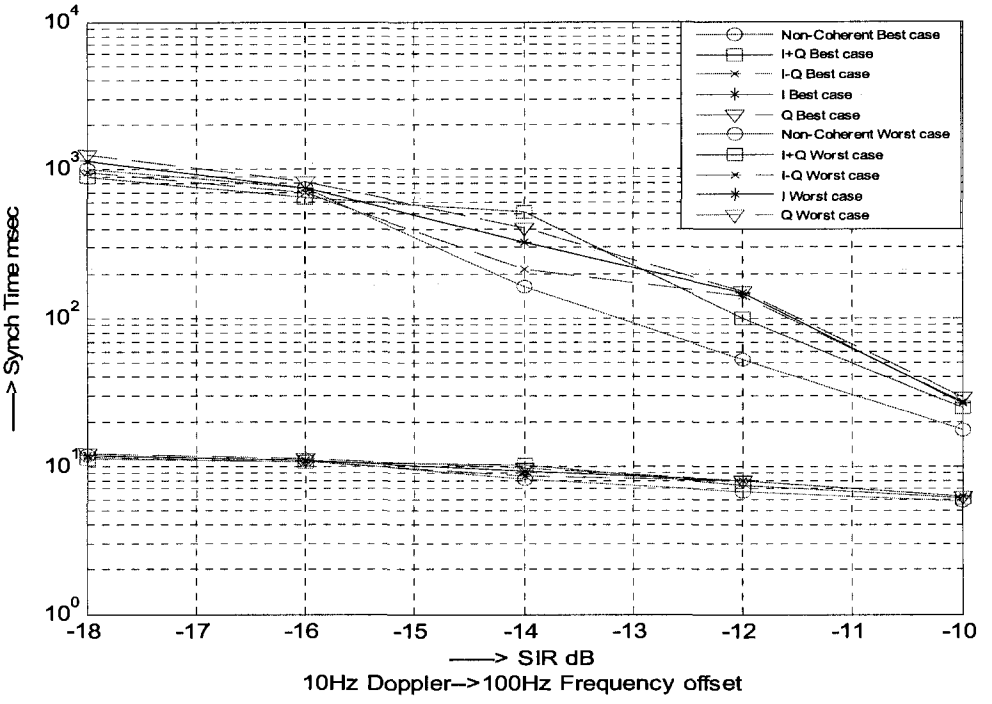

Figure 4-4.a: Rule 1 Fast Processing @ 100 Hz frequency offset & 10Hz Doppler

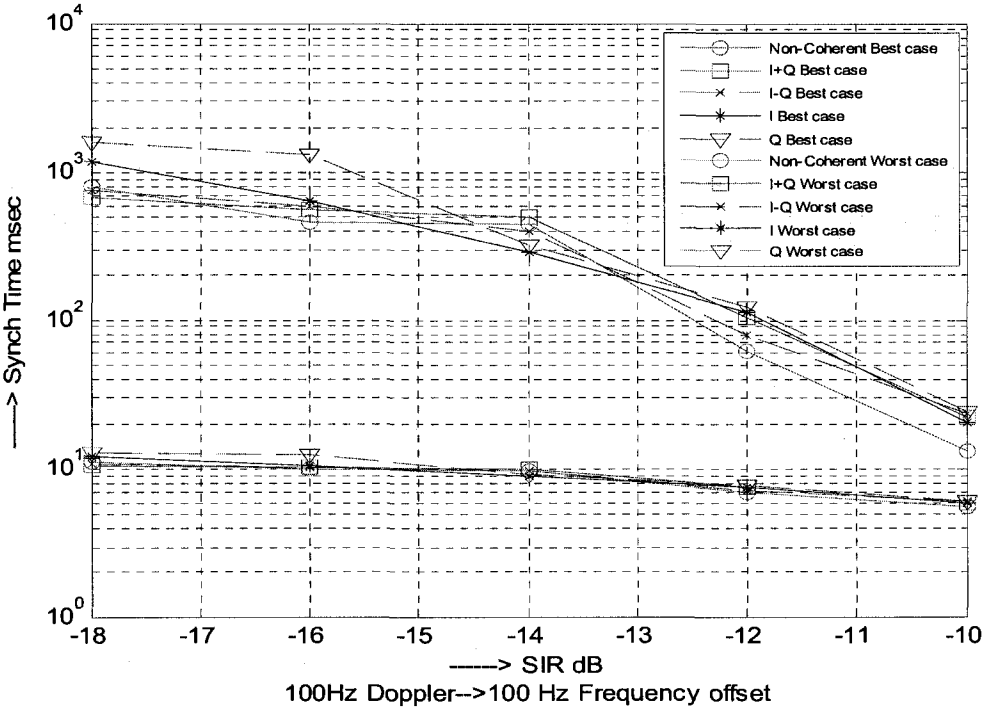

Figure 4-4.b: Rule 1 Fast Processing @ 100 Hz frequency offset & 100Hz Doppler

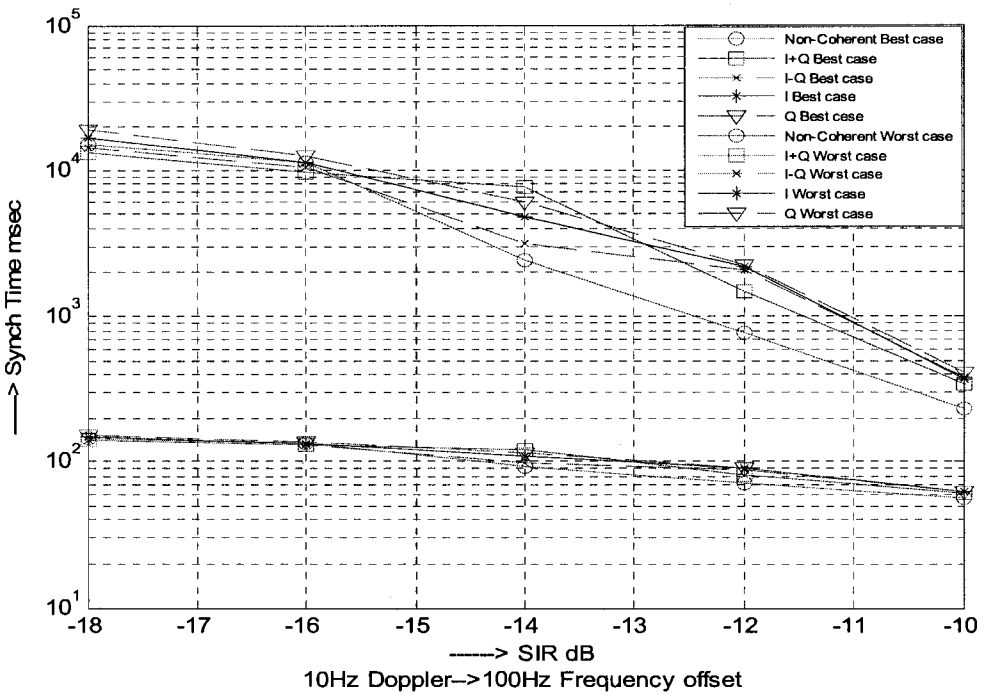

Figure 4-4.c: Rule 1 Slow Processing @ 100 Hz frequency offset & 10Hz Doppler

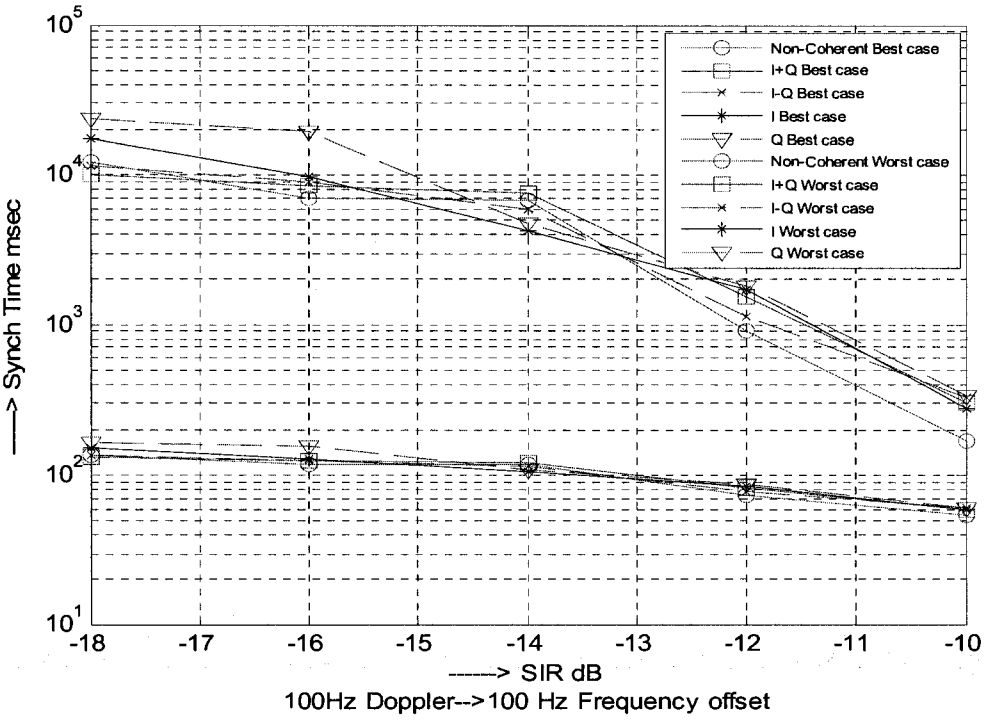

Figure 4-4.d: Rule 1 Slow Processing @ 100 Hz frequency offset & 100Hz Doppler

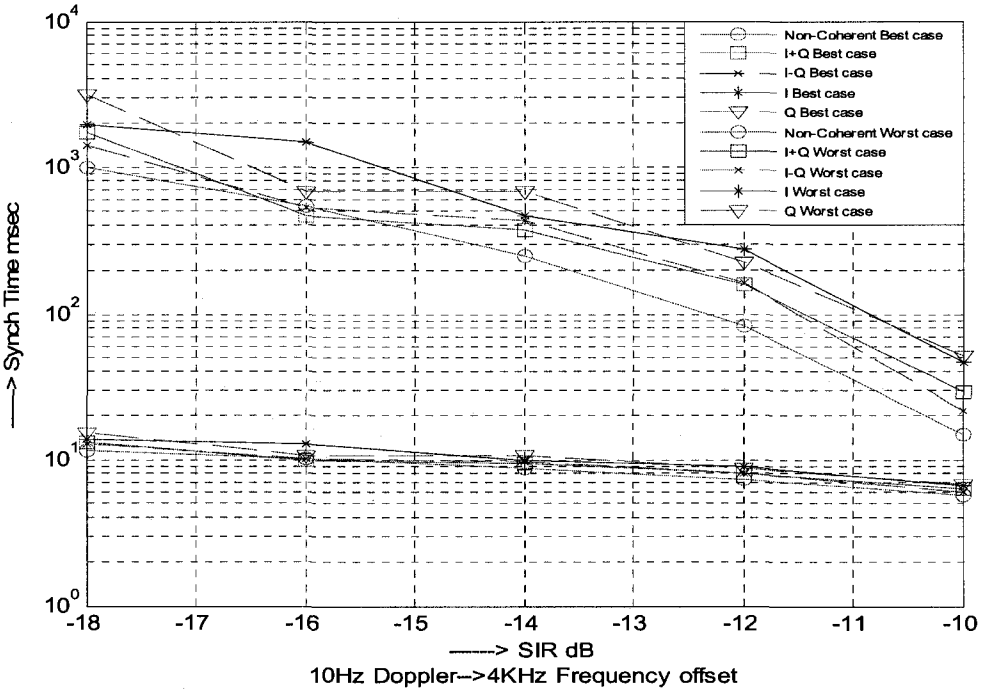

Figure 4-5.a: Rule 1 Fast Processing @ 4 KHz frequency offset & 10Hz Doppler

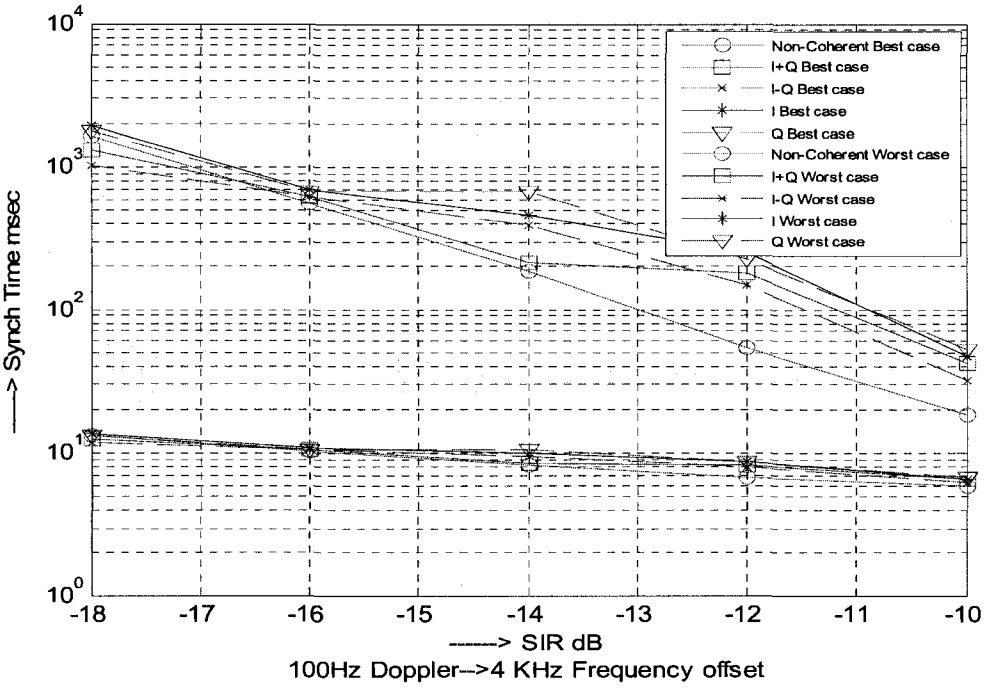

Figure 4-5.b: Rule 1 Fast Processing @ 4 KHz frequency offset & 100Hz Doppler

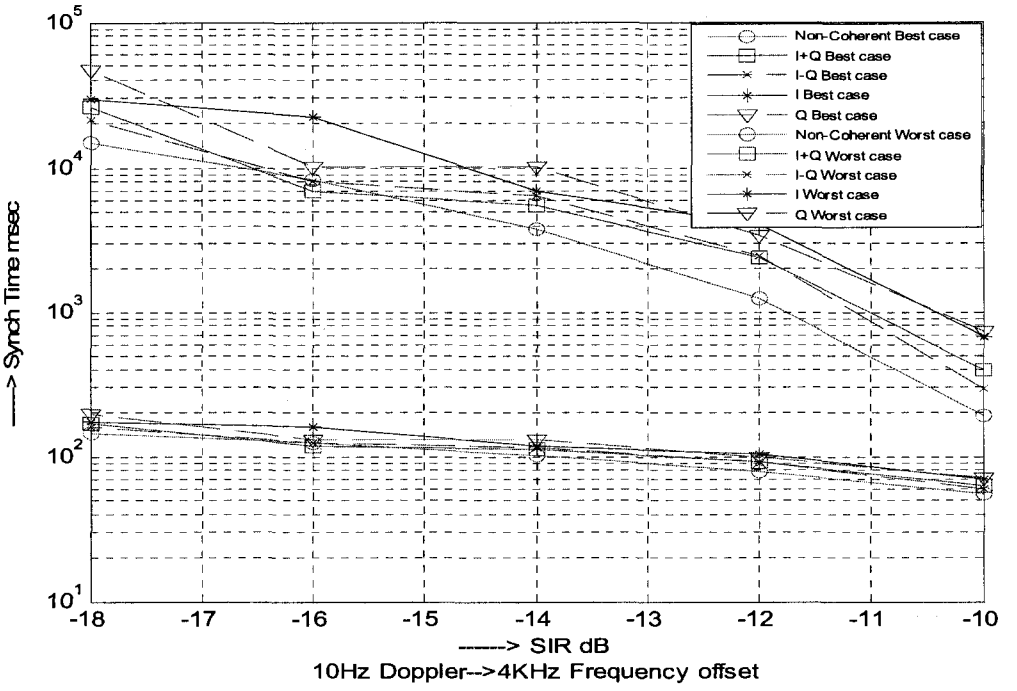

Figure 4-5.c: Rule 1 Slow Processing @ 4 KHz frequency offset & 10Hz Doppler

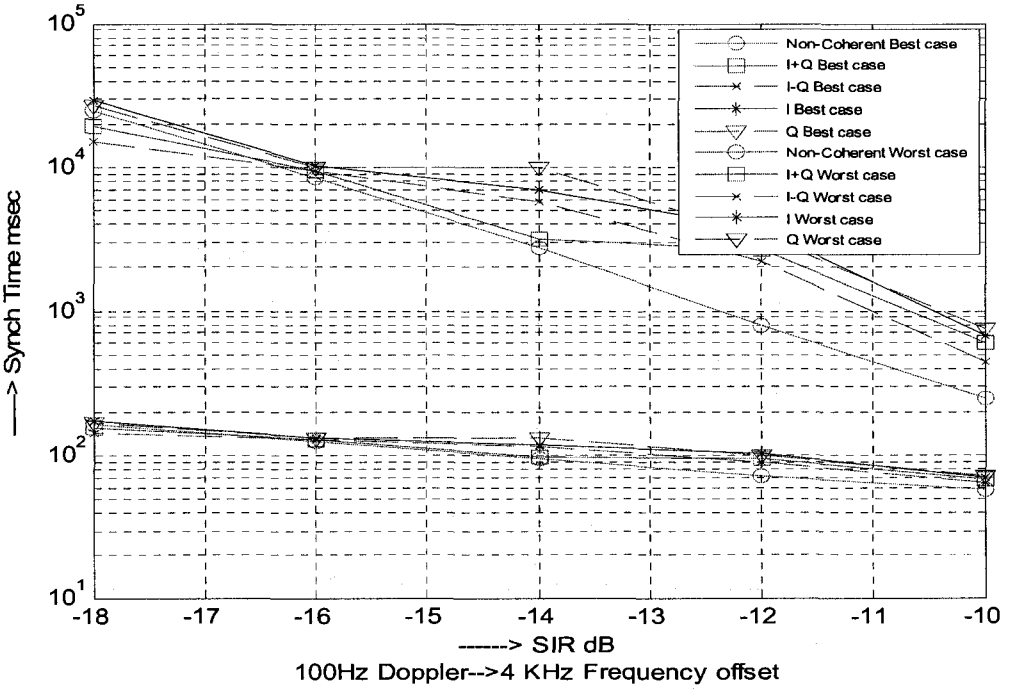

Figure 4-5.d: Rule 1 Slow Processing @ 4 KHz frequency offset & 100Hz Doppler

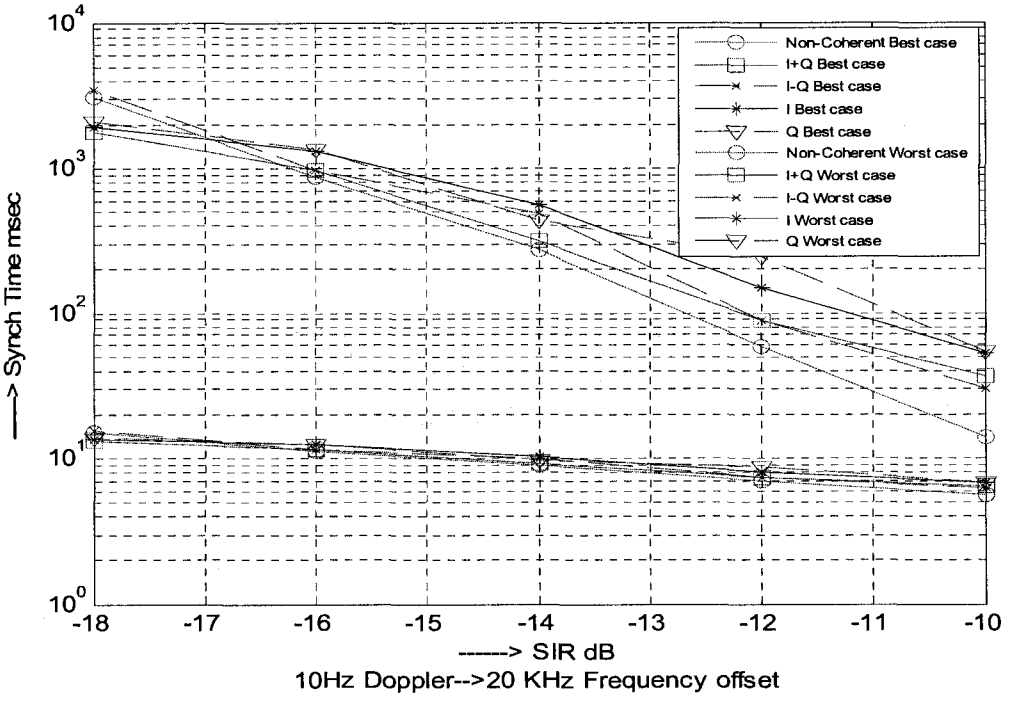

Figure 4-6.a: Rule 1 Fast Processing @ 20 KHz frequency offset & 10Hz Doppler

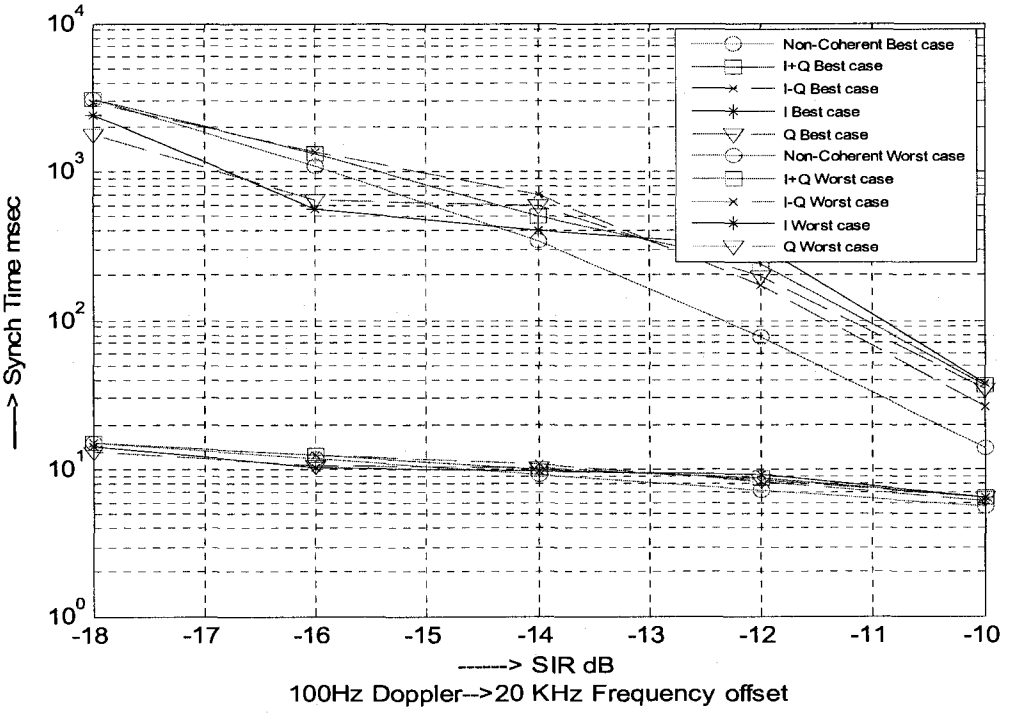

Figure 4-6.b: Rule 1 Fast Processing @ 20 KHz frequency offset & 100Hz Doppler

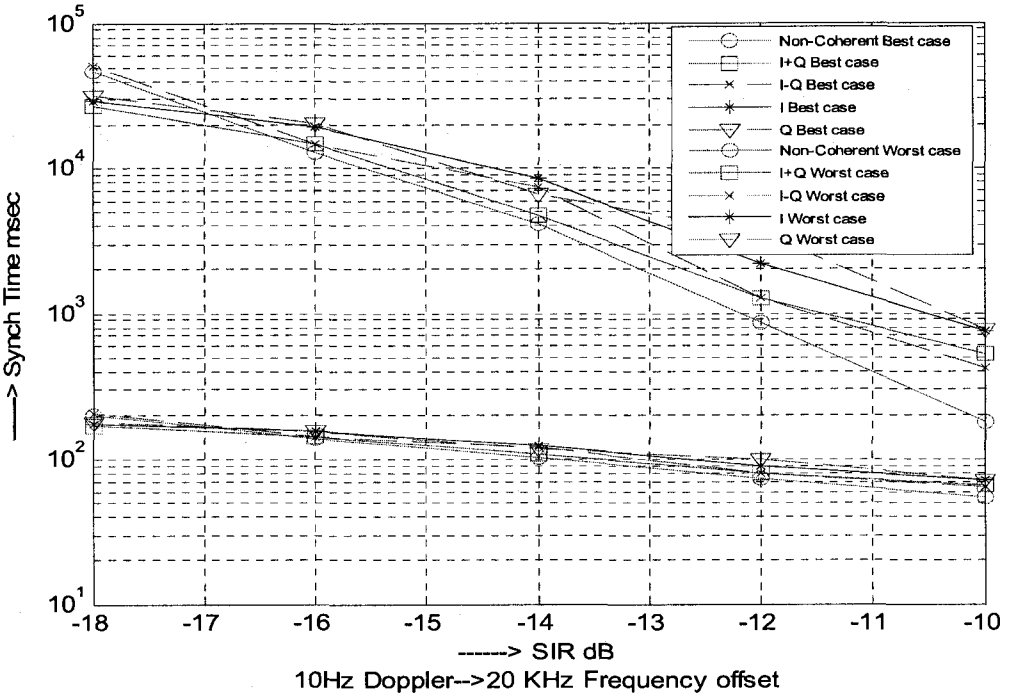

Figure 4-6.c: Rule 1 Slow Processing @ 20 KHz frequency offset & 10Hz Doppler

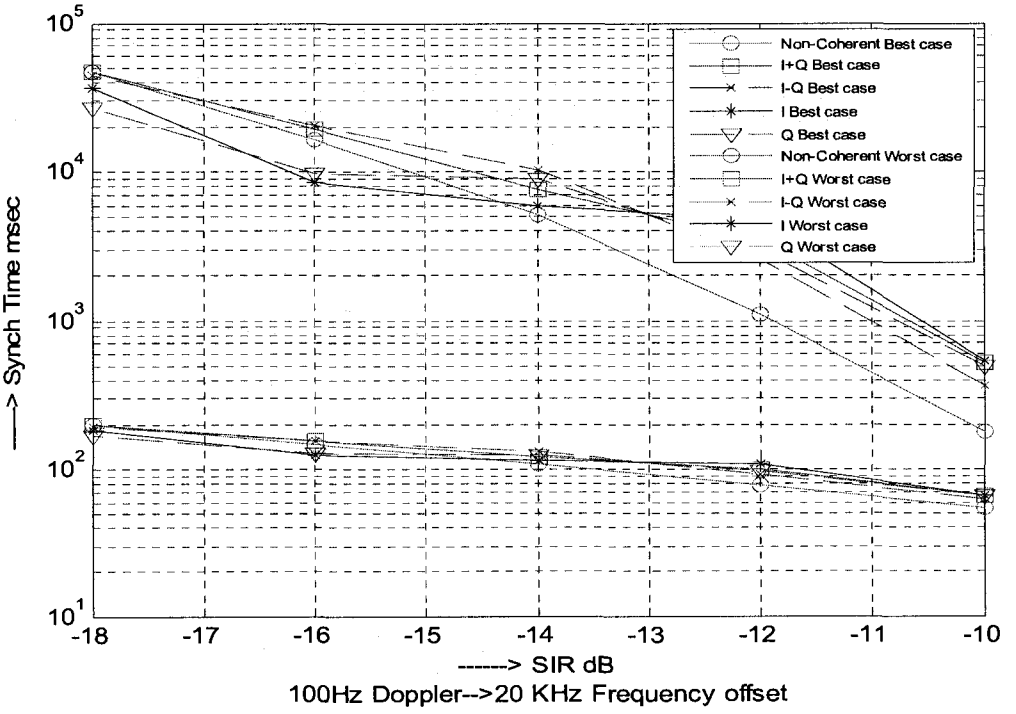

Figure 4-6.d: Rule 1 Slow Processing @ 20 KHz frequency offset & 100Hz Doppler

Although the simulation was repeated for different carrier frequency offsets (Δf=0Hz, 100Hz, 4 KHz and 20 KHz) and different Doppler effects (10Hz and 100Hz), the curves from Figs 4-3 to Figs 4-6 were almost identical for both the fast processing case and the slow processing case either the best case ($a=P_d$) or the worst case ($a=P_d^3$). This proves the robustness of Rule 1 against Doppler effect as well as the carrier frequency offset.

For fast processing case considering the best case ($a=P_d$), Figs (4-3.a&b), Figs (4-4.a&b), Figs (4-5.a&b) and Figs (4-6.a&b) at 10Hz and 100Hz Doppler effect respectively and different carrier frequency offsets as mentioned before provide very good results and show that the total synchronization process time is around 5ms at SIR of -10dB for the five different scenarios (i.e. $x`(t)$, $y`(t)$, $x`(t)+y`(t)$, ...etc). Gradually the synchronization process time increases for decreasing SIR. The synchronization process time will be approximately 15ms for the five different processing scenarios at -18dB. The five different processing scenarios provide almost the same synchronization process time considering the best case assumption. However for slow processing case considering the independency of the three stages of cell search procedure (i.e. worst case) as shown in Figs 4-3.c&d to Figs 4-6.c&d, the synchronization process time at -10dB is around 50ms. Gradually the synchronization process time increases to reach 150ms at -18dB for the five different processing scenarios (i.e. the curves are shifted up by 10% difference in synchronization process time than those of best case of fast processing case).

The worst case always gives poor results at very low SIR considering either fast or slow processing case. The upper bound of Figs 4-3.a&b to Figs 4-6.a&b represent the worst case ($a=P_d^3$) of the fast processing at 10Hz and 100Hz Doppler effect respectively and at the different aforementioned carrier frequency offsets. The synchronization process

time for the processing scenario $z(t)$ is approximately around 15ms outperforming the other four processing scenarios ($x'(t)$, $y'(t)$, $x'(t) \pm y'(t)$) by 10ms at -10dB. However at -14dB, the total synchronization process time at different carrier frequency offsets and different Doppler effects is approximately around 350ms for the $z(t)$ scenario and 500ms for the other 4 scenarios ($x'(t)$, $y'(t)$, $x'(t) \pm y'(t)$). At SIR less than -14dB, the five different scenarios start to overlap giving almost the same performance such that the total synchronization process time is around 800ms for the five processing scenarios at -16dB. The gap between the worst case and the best case is small at -10dB and increases gradually by decreasing SIR till -14 dB. Starting from -14dB the performance gap drastically increases to reach the maximum at -18 dB. That's because of the effect of the small values of the probability of detection of the first stage of cell search on the synchronization process time at very low SIR plus the independency assumption (i.e. $a=P_d^3$) of the three stages of the cell search procedure. The effect of the independence of the probability of detection of the three stages (i.e. $a=P_d^3$) is clear at very low SIR (-14dB → -18dB). Always the scenario $z(t)$ provides the best synchronization process time between the five different scenarios ($x'(t)$, $y'(t)$, *and* $x'(t) \pm y'(t)$) till -14dB for all the worst cases followed by $x'(t) \pm y'(t)$. However $x'(t)$ *and* $y'(t)$ provide the lowest values for synchronization process time because combining the correlation values is very important to properly acquire the slot boundaries. But starting from -14dB all the five scenarios give almost the same synchronization process time for the worst case assumption. The total synchronization process time at SIR of -18dB for the worst case of fast processing is around 2sec for Δf of 0Hz and 20 KHz and around 1sec for Δf of 100Hz and 4 KHz including all stages of the WCDMA synchronization process standard

for the worst case assumption (independent). The results of the slow and fast processing case came within 10%.

The synchronization process time at different frequency offset and Doppler effect is almost the same. At SIR= -10dB and Δf=4 KHz, Fig 4-5.a shows that the synchronization process time $T_{syn} \cong$ 30msec including all stages of the WCDMA synchronization process standard for the independent worst case assumption ($a=P_d{}^3$). This is compared to T_{syn} of 300msec in [35] at approximately the same environment. Different curves of Rule 1 at different frequency offsets and different Doppler effects show that Rule 1 is immune to carrier frequency error as well as Doppler effects.

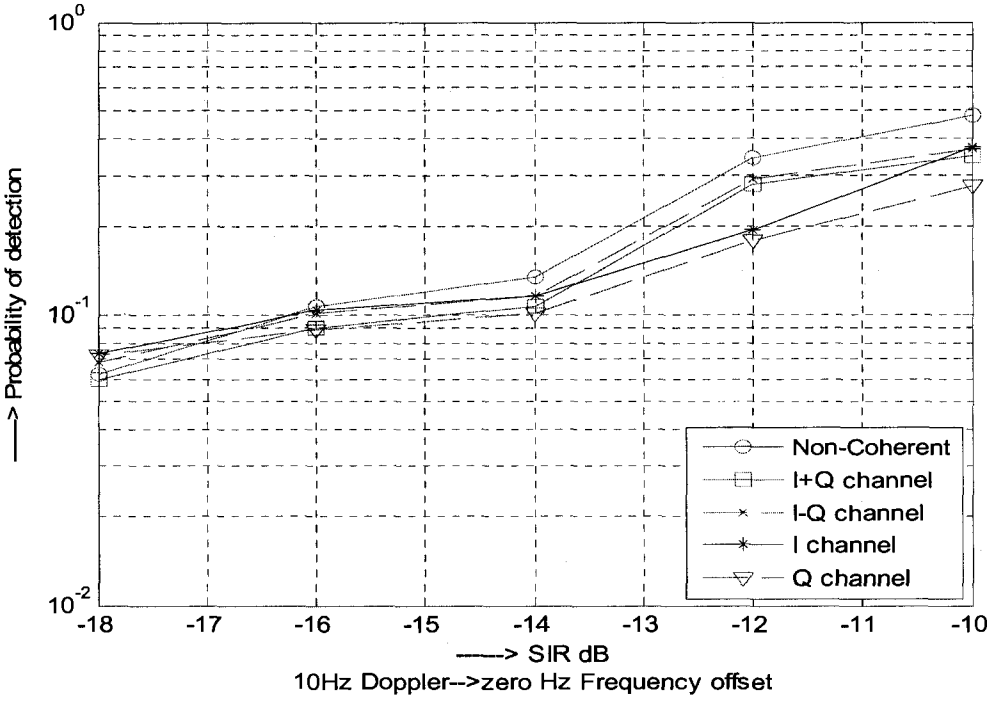

Figure 4-7.a: Rule 1 P_d @ zero Hz frequency offset & 10Hz Doppler

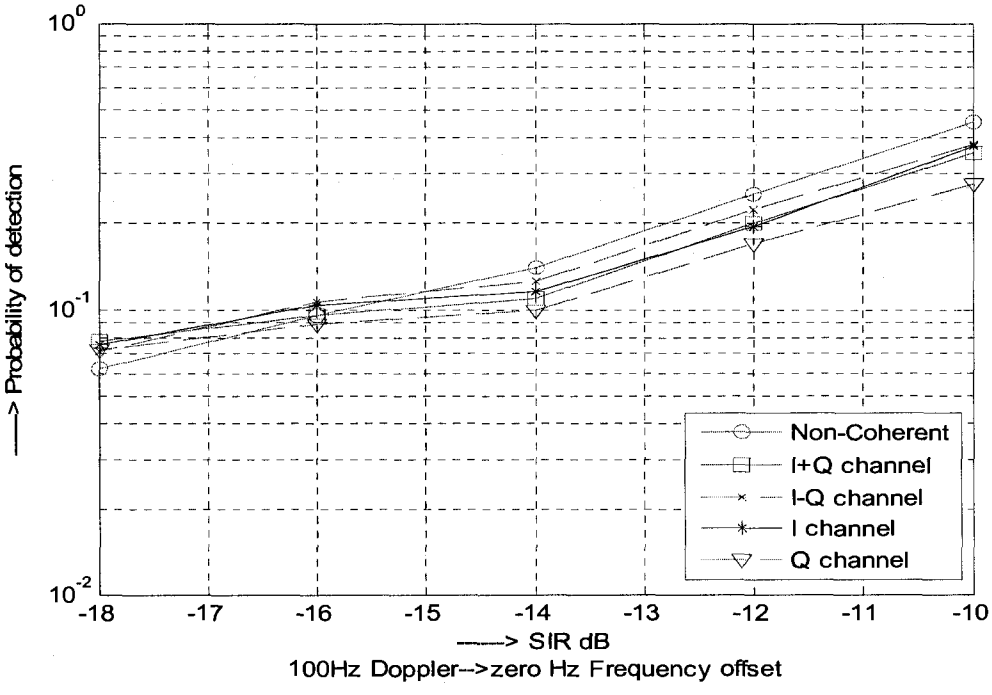

Figure 4-7.b: Rule 1 P_d @ zero Hz frequency offset & 100Hz Doppler

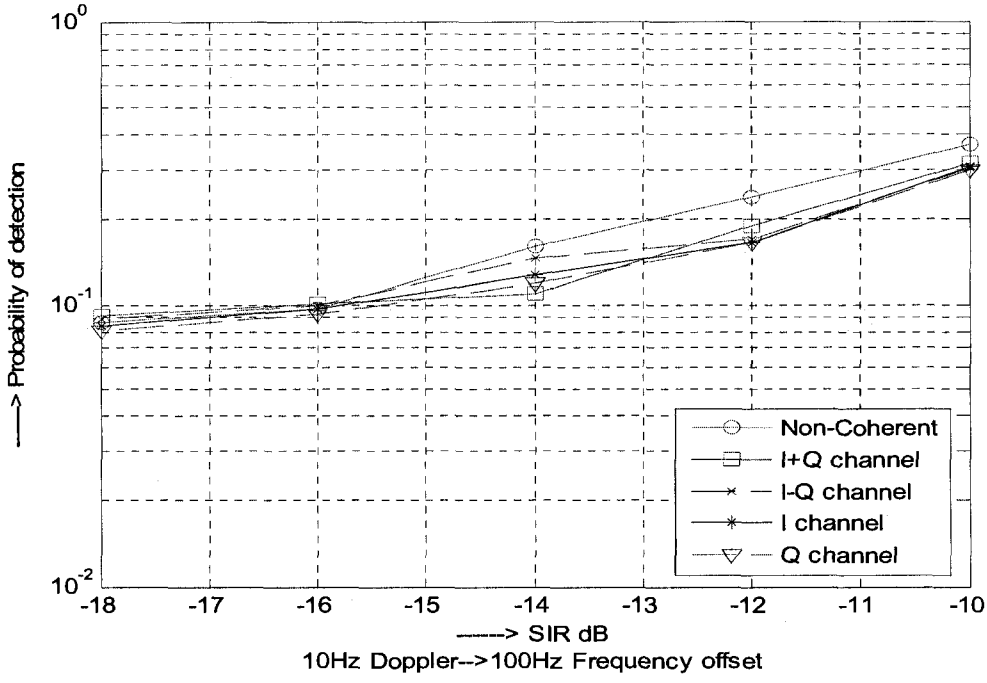

Figure 4-8.a: Rule 1 P_d @ 100 Hz frequency offset & 10Hz Doppler

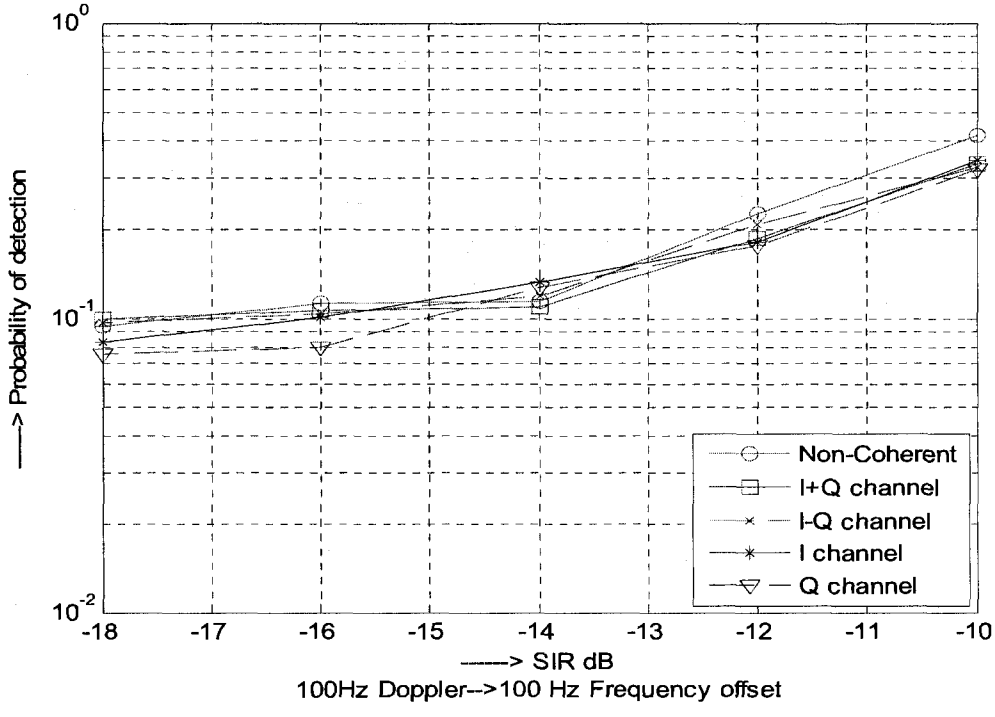

Figure 4-8.b: Rule 1 P_d @ 100 Hz frequency offset & 100Hz Doppler

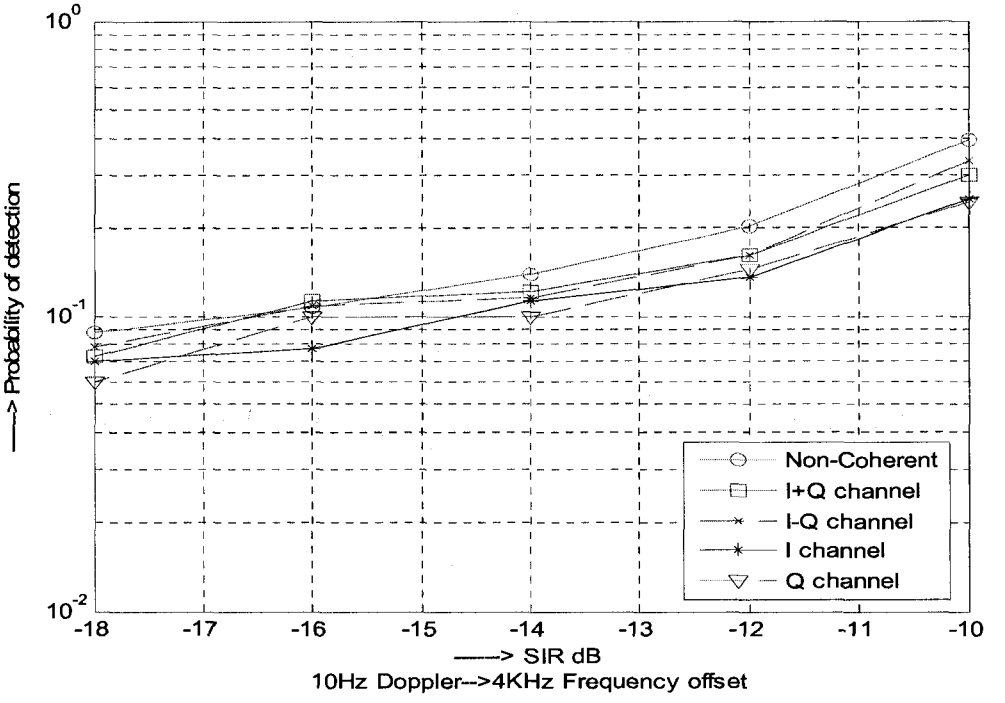

Figure 4-9.a: Rule 1 P_d @ 4 KHz frequency offset & 10Hz Doppler

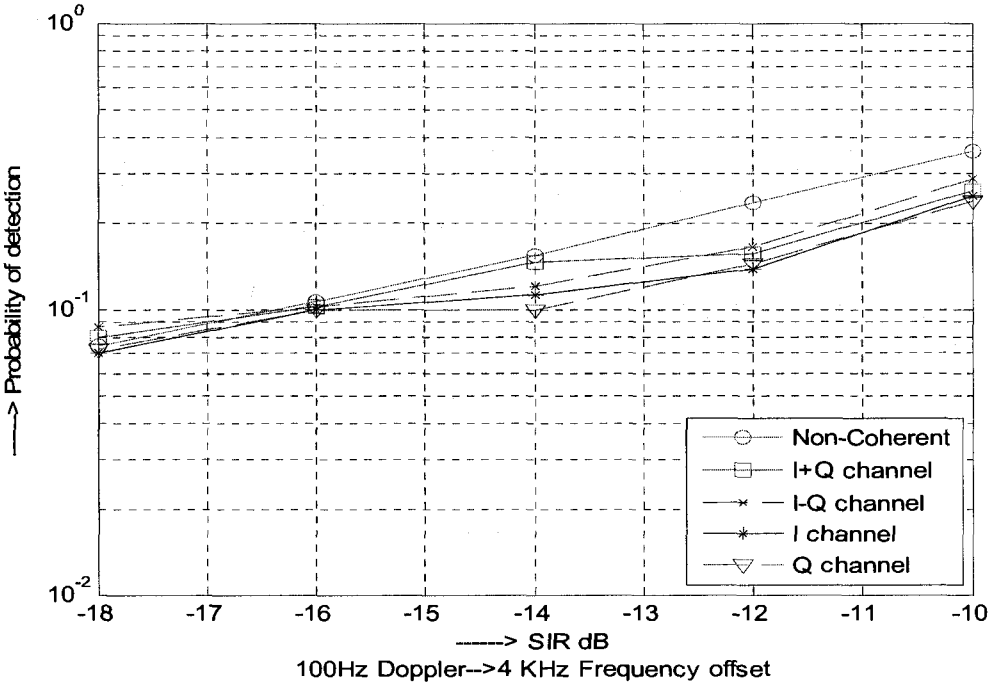

Figure 4-9.b: Rule 1 P_d @ 4 KHz frequency offset & 100Hz Doppler

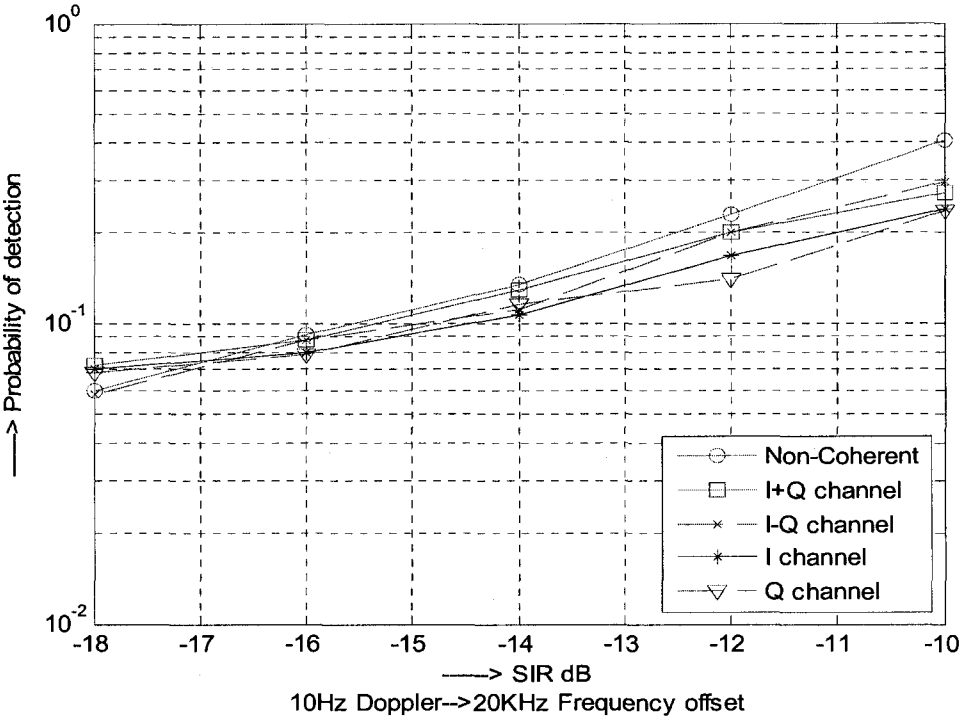

Figure 4-10.a: Rule 1 P_d @ 20 KHz frequency offset & 10Hz Doppler

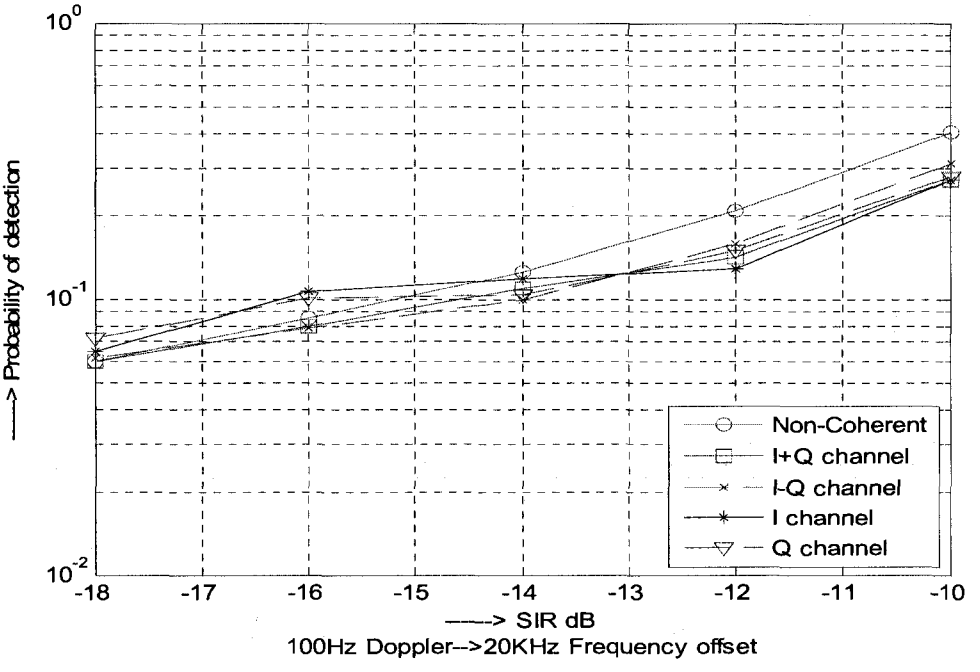

Figure 4-10.b: Rule 1 P_d @ 20 KHz frequency offset & 100Hz Doppler

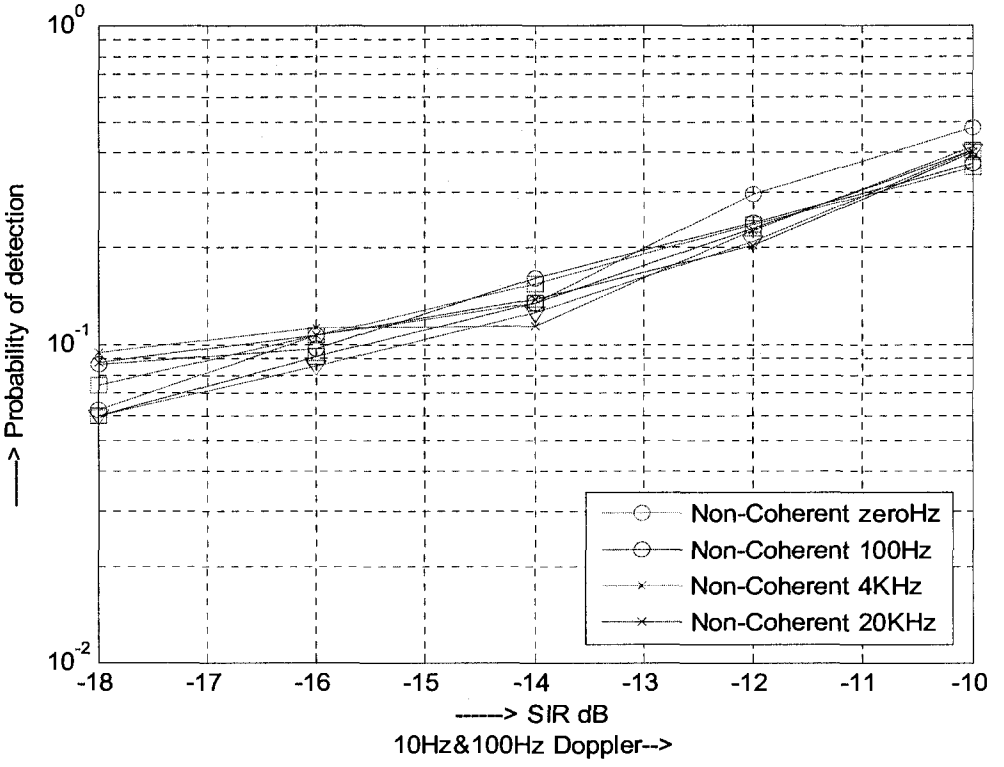

Figure 4-11: Rule 1 P_d for all Doppler effects and all Δf

Figs 4-7.a, 4-8.a, 4-9.a and Fig 4-10.a represent the probability of detection of the first stage of the three-stage cell search procedure at 10Hz Doppler for Δf of 0Hz, 100Hz, 4 KHz and 20 KHz respectively. Figs 4-7.b, 4-8.b, 4-9.b and Fig 4-10.b represent the probability of detection of the first stage of the three-stage cell search procedure at 100Hz Doppler for Δf of 0Hz, 100Hz, 4 KHz and 20 KHz respectively. Acceptable probability of detection was obtained for different Doppler effect and different carrier frequency offsets at SIR of -10dB. However the probability of detection gradually decreases for decreasing SIR. The aforementioned overlap of synchronization process time is so clear in Figs 4-7 to Figs 4-10 due to the overlapping of the probability of detection starting from -14dB to give almost the same probability of detection and thus, the same

synchronization process time. However the probability of detection of the processing scenario *z(t)* provides slightly better values till -14dB other than those of *x`(t), y`(t)* and *x`(t)±y`(t)*. At -18dB the five different scenarios (*x`(t), y`(t)...etc*) almost have the same probability of detection, thus the same synchronization process time. Fig 4-11 shows P_d for the five scenarios (.e. *x`(t), y`(t), x`(t)+y`(t),* ...etc) at 10 Hz and 100Hz Doppler effect and in the presence of Δf 0f 0Hz, 100Hz, 4 KHz and 20 KHz. From this Fig, different scenarios at different Doppler effects and different carrier frequency offsets are almost the same and are overlapping. The average probability of detection for Rule 1 is approximately 0.4, 0.2, 0.15, 0.1 and 0.07 at -10dB, -12dB, -14dB, -16dB and -18dB respectively. From this Fig, we can conclude that Rule 1 is Robust to Doppler effect and carrier Frequency error.

Figs 4-12.a, 4-13.a, 4-14.a, and 4-15.a represent the probability of detection of Rule 2 at 10 Hz Doppler effect and at Δf of 0Hz, 100Hz, 4 KHz and 20 KHz respectively. Figs 4-12.b, 4-13.b, 4-14.b, and 4-15.b represent the probability of detection of Rule 2 at 100 Hz Doppler effect and at Δf of 0Hz, 100Hz, 4 KHz and 20 KHz respectively.

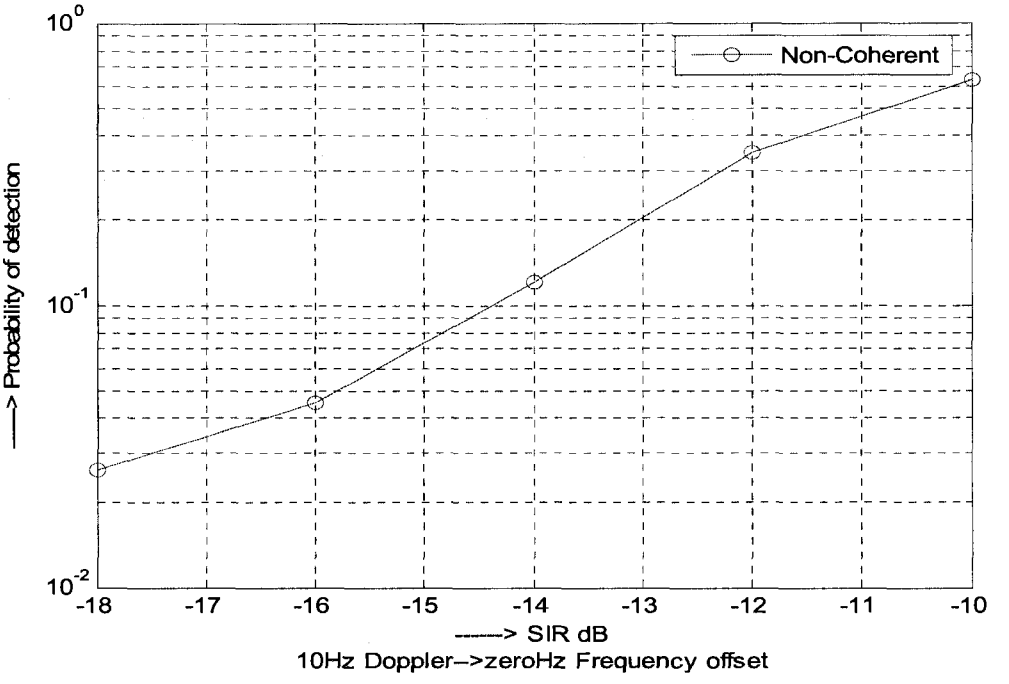

Figure 4-12.a: Rule 2 P_d @ zero Hz frequency offset & 10Hz Doppler

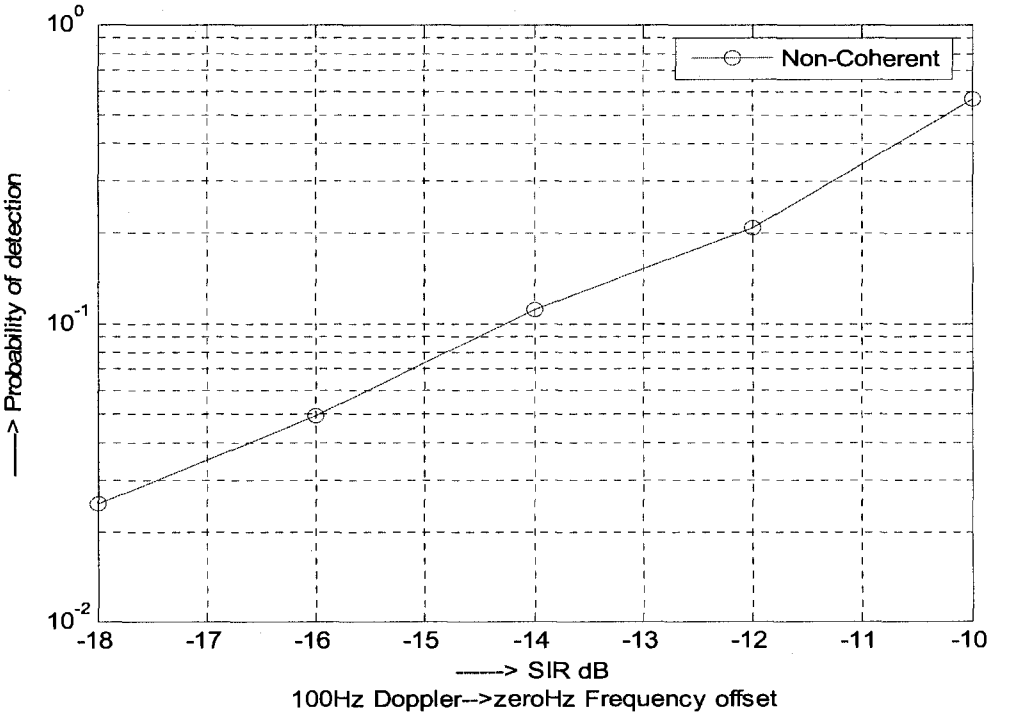

Figure 4-12.b: Rule 2 P_d @ zero Hz frequency offset & 100Hz Doppler

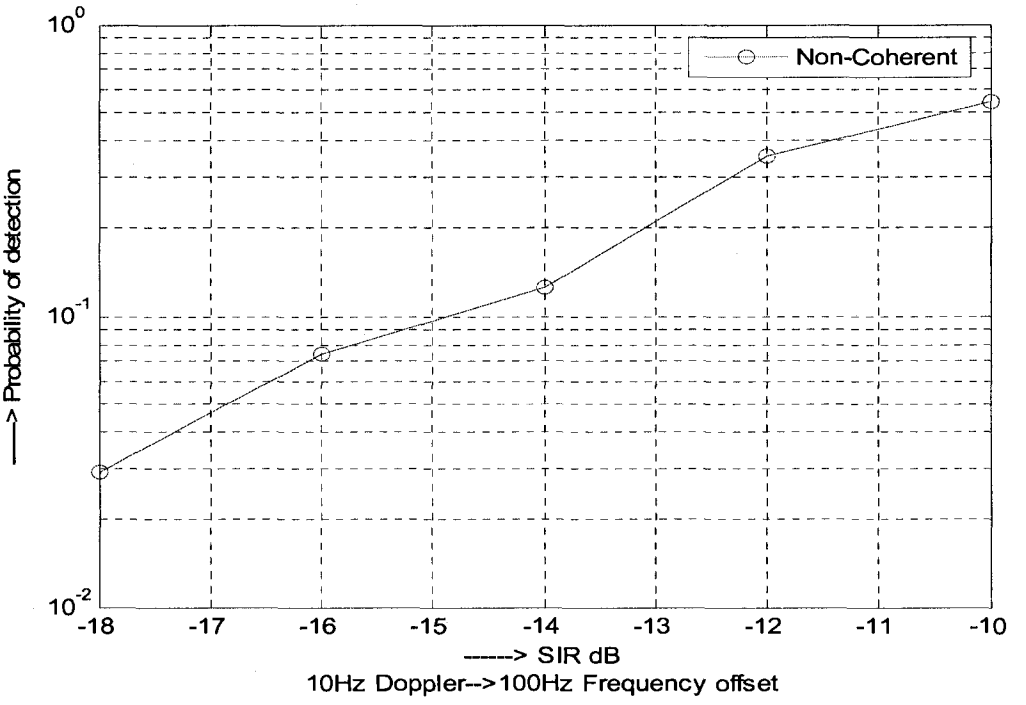

Figure 4-13.a: Rule 2 P_d @ 100 Hz frequency offset & 10Hz Doppler

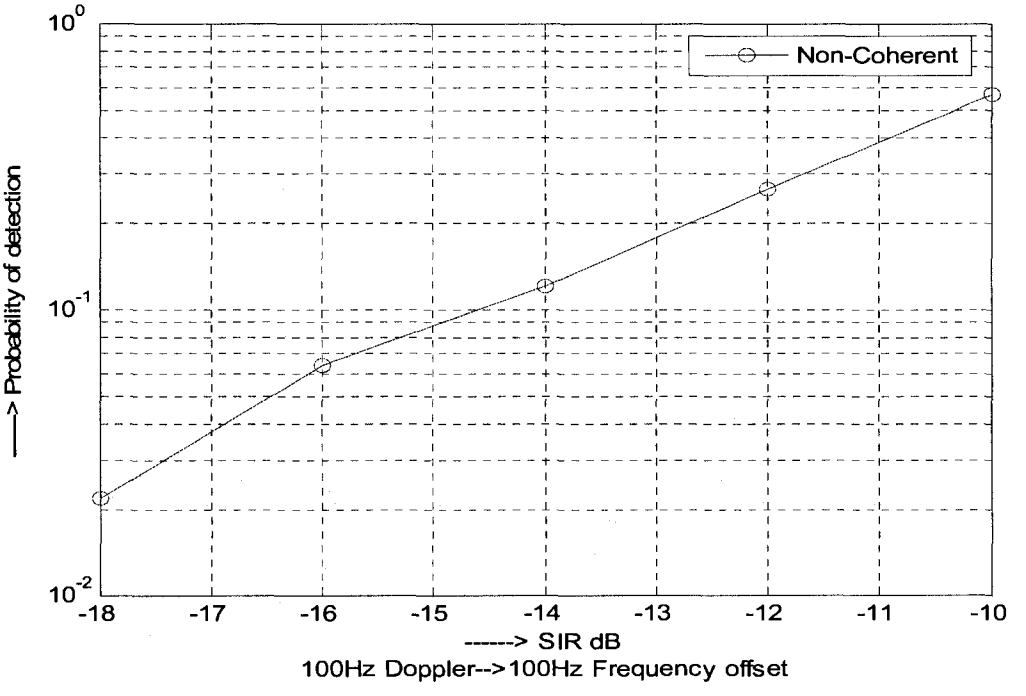

Figure 4-13.b: Rule 2 P_d @ 100 Hz frequency offset & 100Hz Doppler

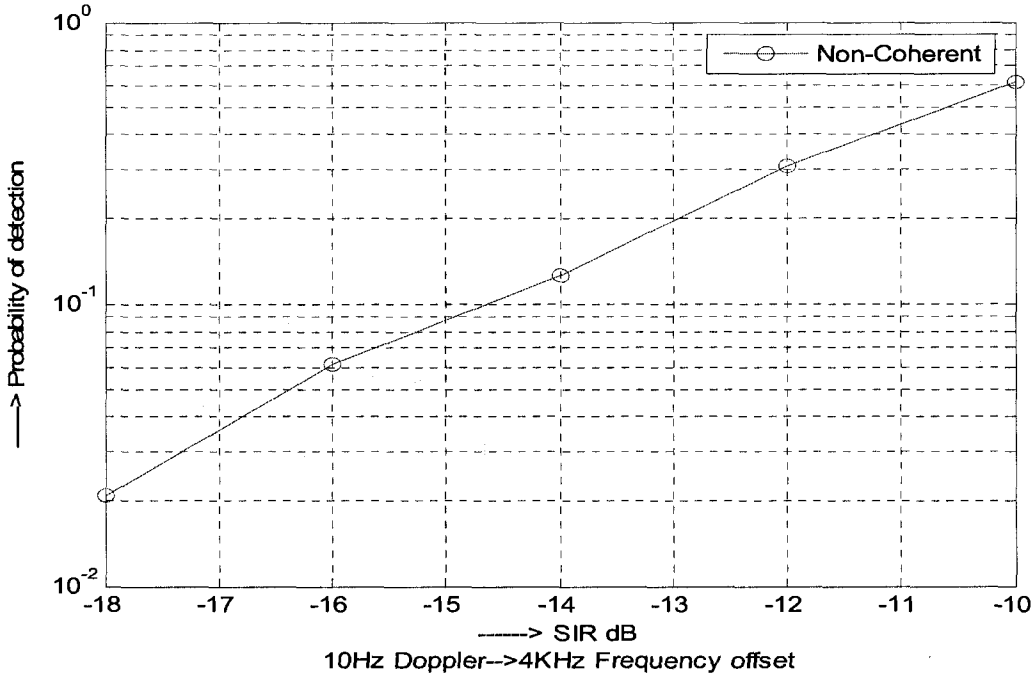

Figure 4-14.a: Rule 2 P_d @ 4 KHz frequency offset & 10Hz Doppler

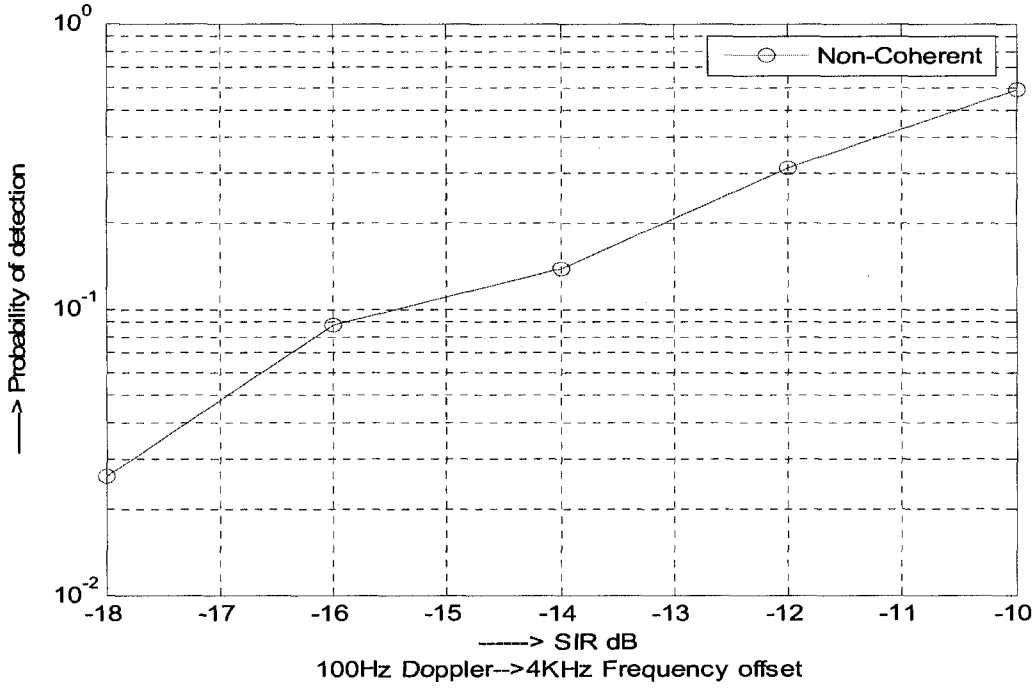

Figure 4-14.b: Rule 2 P_d @ 4 KHz frequency offset & 100Hz Doppler

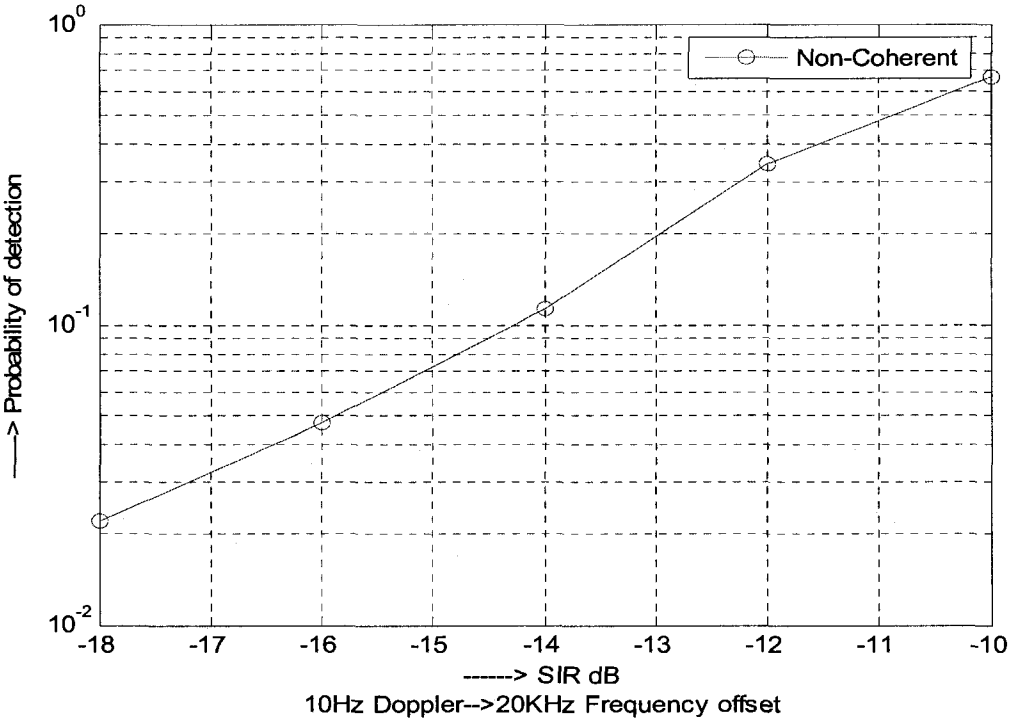

Figure 4-15.a: Rule 2 P_d @ 20 KHz frequency offset & 10Hz Doppler

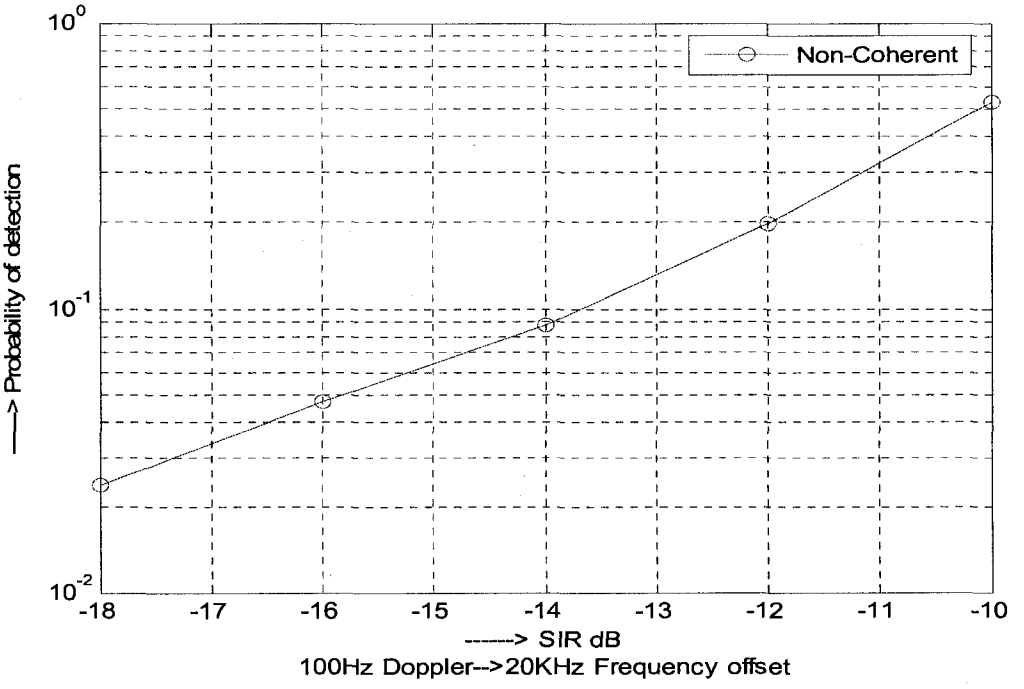

Figure 4-15.b: Rule 2 P_d @ 20 KHz frequency offset & 100Hz Doppler

For the same Doppler effect all the curves at different carrier frequency offsets have the same tendency. However at Different Doppler effect the Figures have almost the same curves but are not exactly identical as in Rule 1. For example at the same Doppler effect (10Hz) as shown in Figs 4-12.a to 4-15.a, P_d at different carrier frequency offsets (0Hz, 100Hz, 4 KHz and 20 KHz) is more than 0.6 at SIR of -10dB. This high value of probability of detection will result in very small synchronization process time for all cases either fast processing or slow processing and for Best and worst case too. Unlike Rule 1, the curves drastically decrease such that P_d decreases by a factor of 0.5 per -2dB decrease in the SIR. Thus, for different carrier frequency offsets at 10Hz Doppler effect, P_d is around 0.6, 0.3, 0.15, 0.07 and 0.03 at -10dB, -12dB, -14dB, -16dB and -18dB respectively.

At 100Hz Doppler effect and for different carrier frequency offsets as shown in Figs 4-12.b to 4-15.b. The curves had almost the same values like each other. However the curves at 10Hz Doppler effect provide slightly better performance than those at 100Hz. P_d at -10dB at 100Hz Doppler for different carrier frequency offsets is around 0.55 slightly less than that of 10Hz Doppler effect. Like 10Hz Doppler, the curves drastically decrease such that P_d decreases by a factor of 0.5 per -2dB decrease in the SIR. Thus, for different carrier frequency offsets at 10Hz Doppler effect, p_d is approximately 0.55, 0.25, 0.12, 0.06 and .025 at -10dB, -12dB, -14dB, -16dB and -18dB respectively. Fig 4-16 shows the comparison between the effect of the 10Hz Doppler and 100Hz Doppler on the probability of detection and the system performance. Rule 2 is unlike Rule 1 which is completely robust to Doppler effect. From the Fig, it is clear that the probabilities of detection at 10 Hz Doppler of different carrier frequency offsets are slightly higher than

those at 100 Hz between SIR of -12dB till SIR of -16dB. However at SIR of -10dB and at -18 dB, there is not much performance difference for different Doppler effects. This can be justified since the rapid variation in the Fading channel is better for the system performance, in addition to considering the very low SIR that has a very big impact on the system performance. However due to this slight difference, it is possible to consider the probabilities of detection of different curves are almost in the same range and provide almost the same synchronization process time for different cases. Finally, we conclude that Rule 2 is also robust to carrier frequency offset due to the effect of non-coherent combining of the two I and Q branches of the signal. In addition to the averaging of the samples over the entire frame reduces the Doppler effect compared to [28].

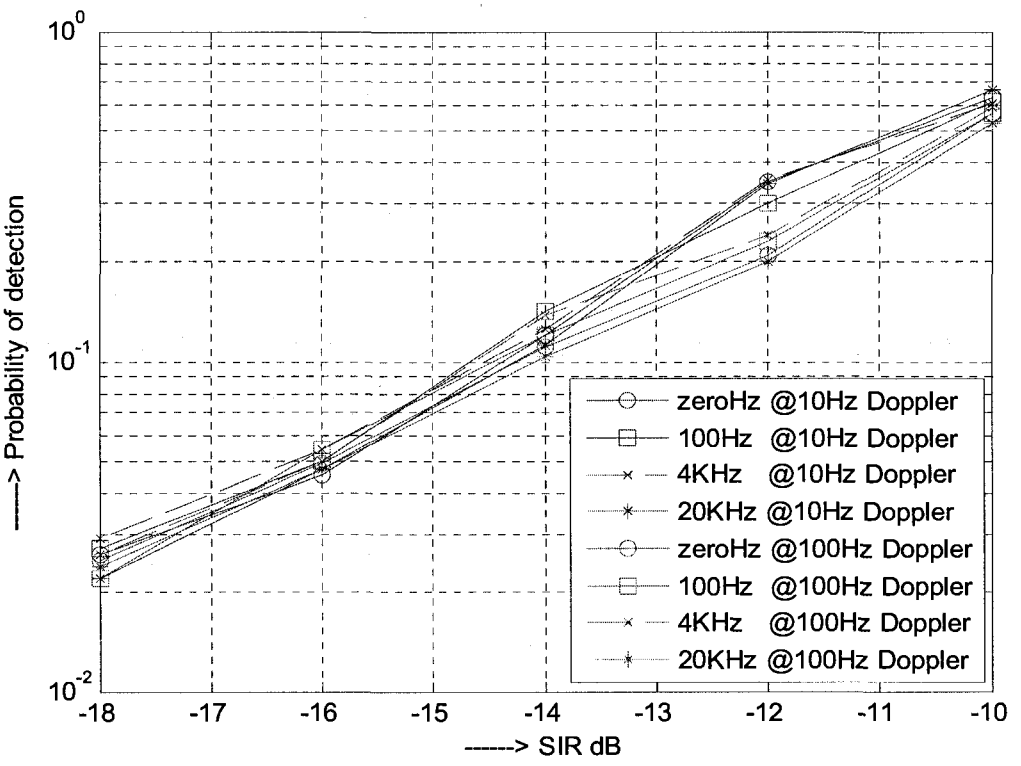

Figure 4-16: Rule 2 P_d for all Doppler effects and all Δf

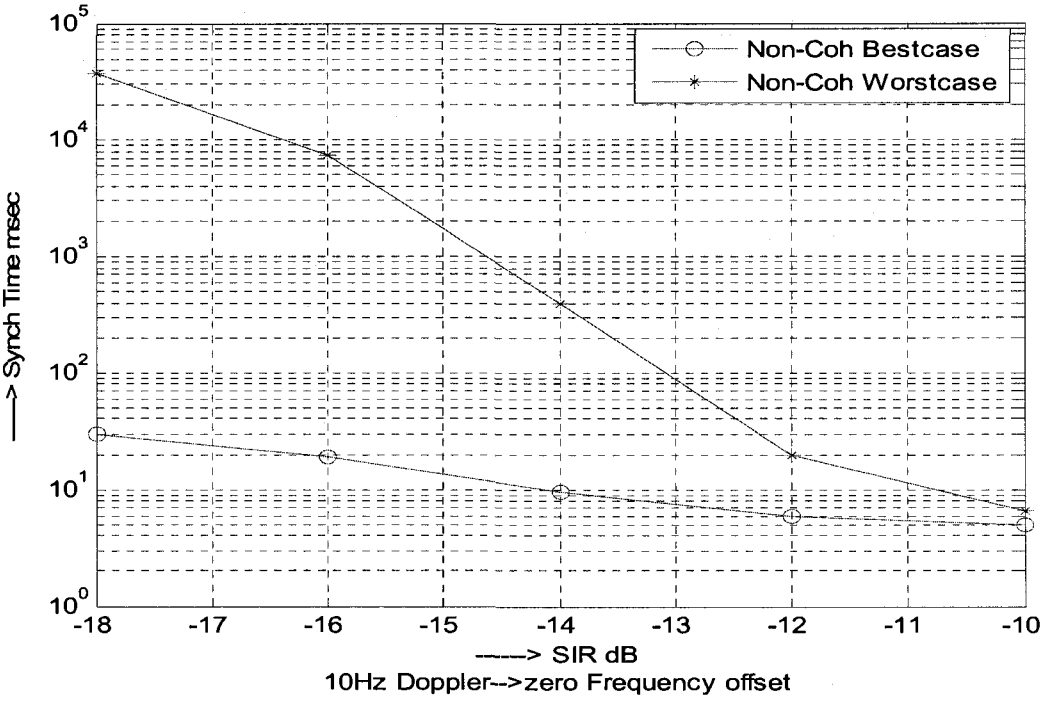

Figure 4-17.a: Rule 2 Fast Processing @ zero Hz frequency offset & 10Hz Doppler

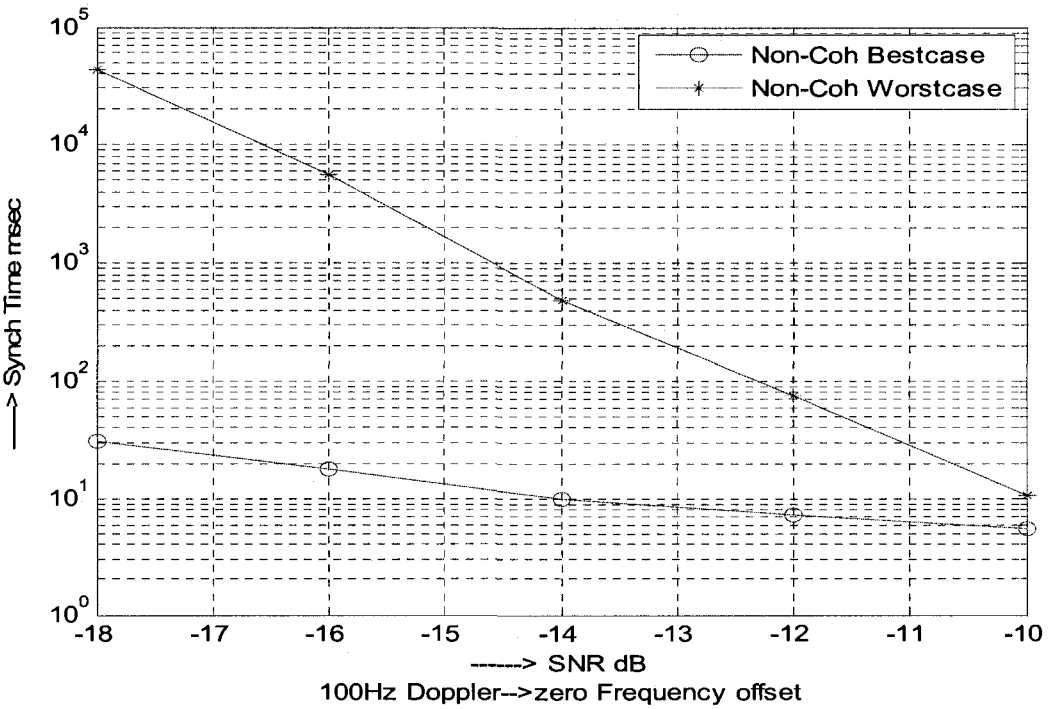

Figure 4-17.b: Rule 2 Fast Processing @ zero Hz frequency offset & 100Hz Doppler

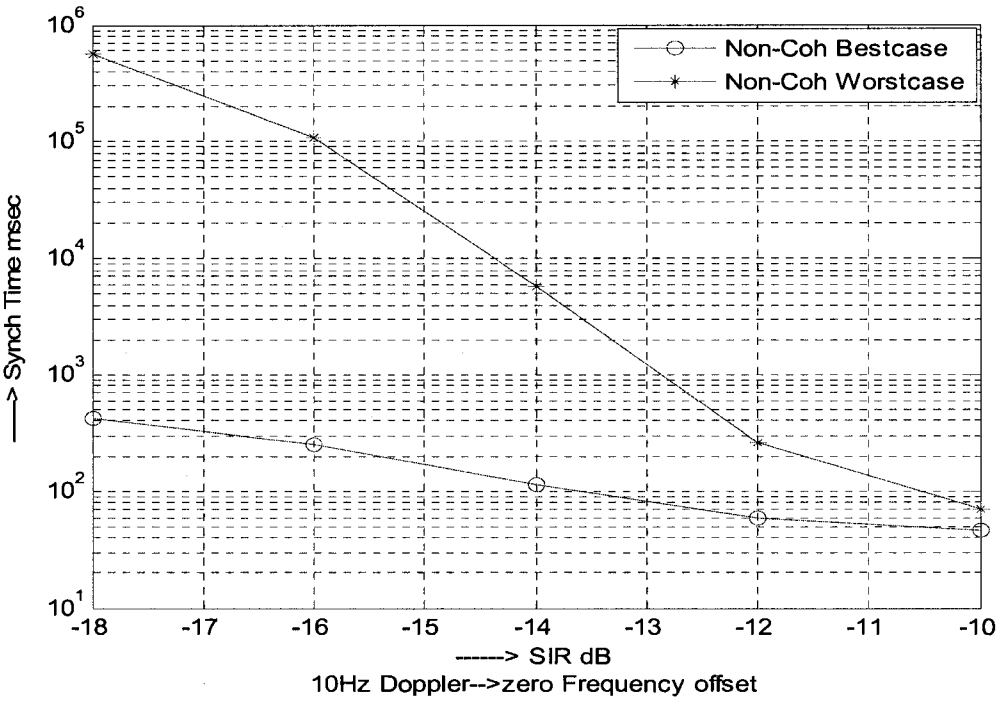

Figure 4-17.c: Rule 2 Slow Processing @ zero Hz frequency offset & 10Hz Doppler

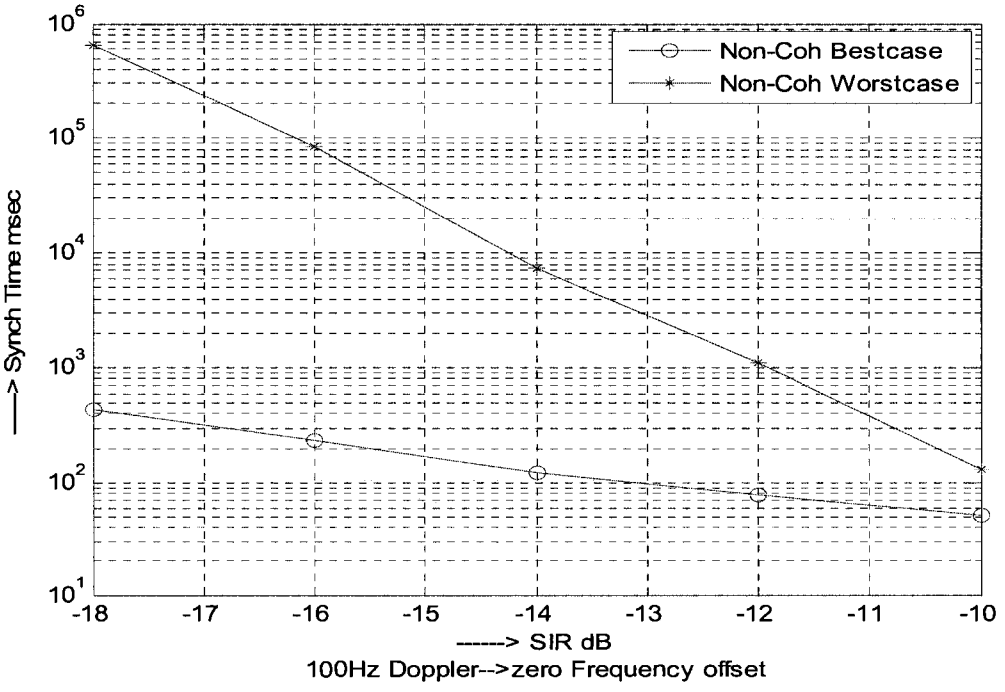

Figure 4-17.d: Rule 2 Slow Processing @ zero Hz frequency offset & 100Hz Doppler

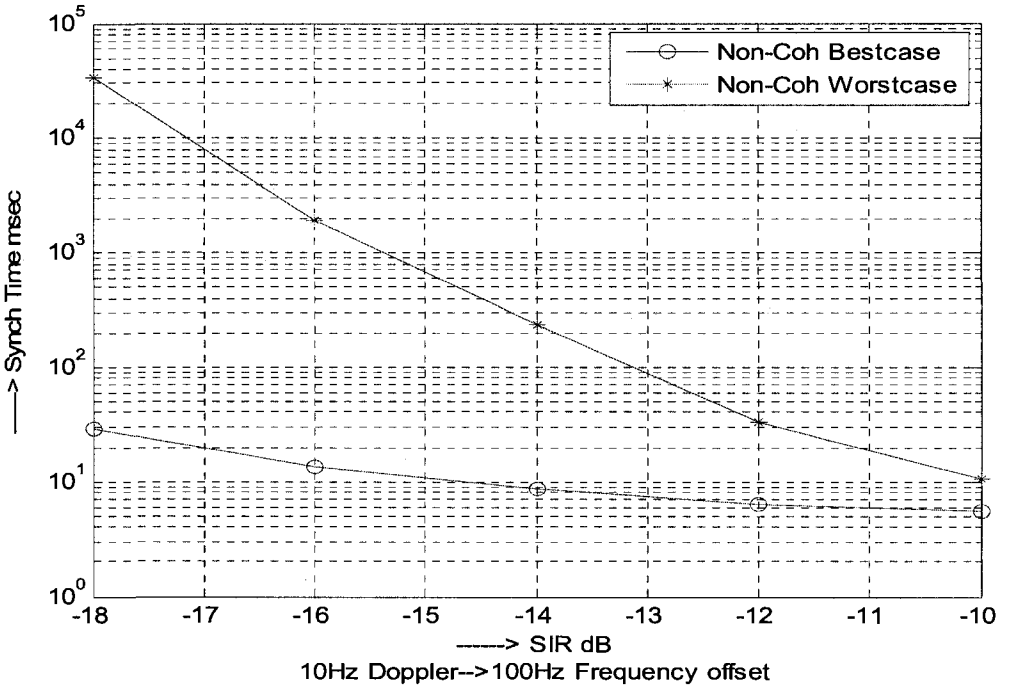

Figure 4-18.a: Rule 2 Fast Processing @ 100 Hz frequency offset & 10Hz Doppler

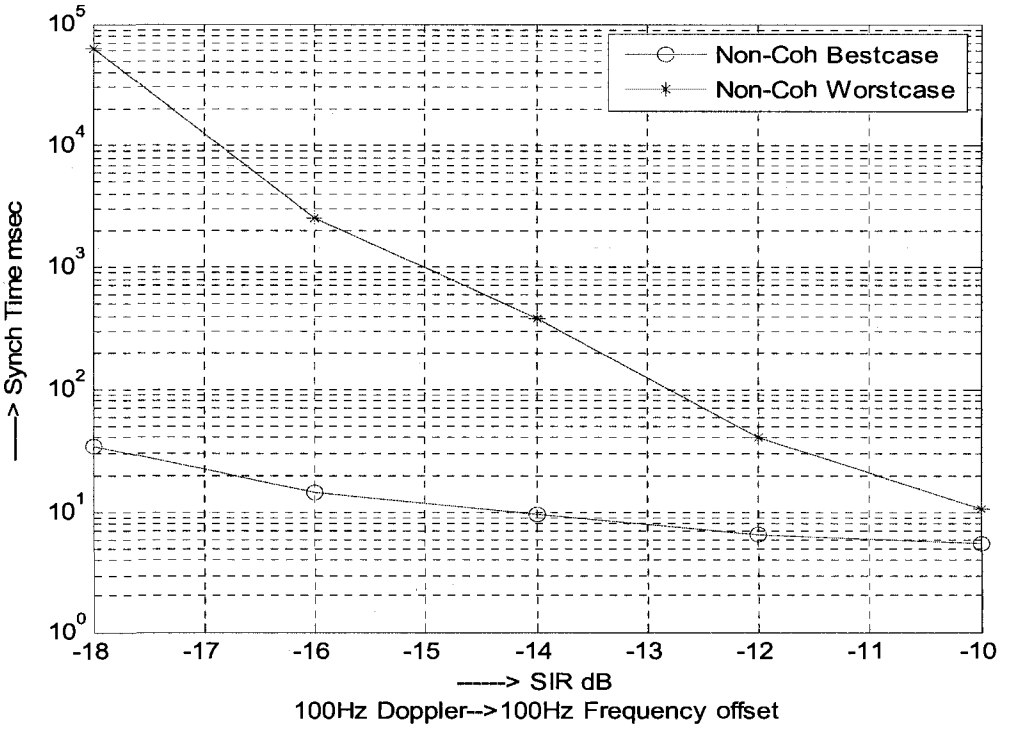

Figure 4-18.b: Rule 2 Fast Processing @ 100 Hz frequency offset & 100Hz Doppler

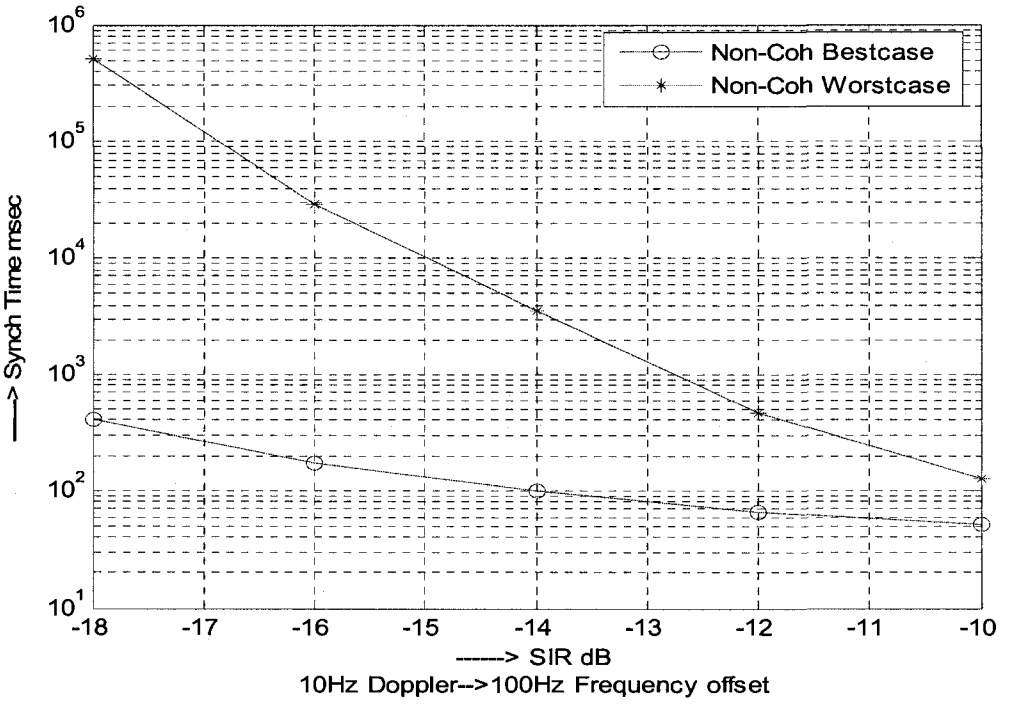

Figure 4-18.c: Rule 2 Slow Processing @ 100 Hz frequency offset & 10Hz Doppler

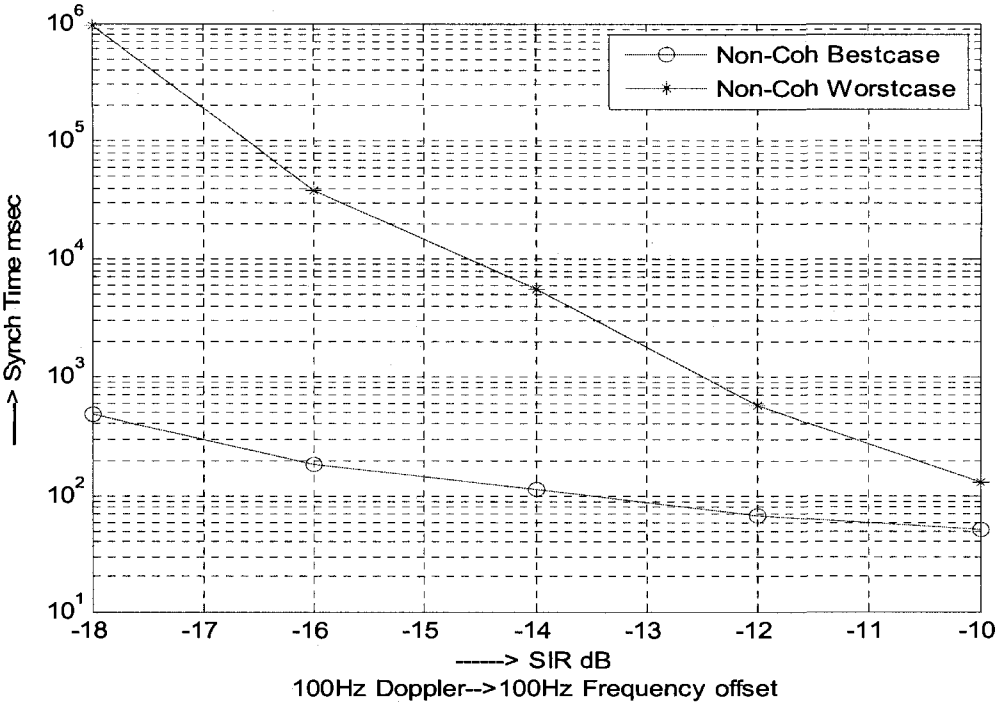

Figure 4-18.d: Rule 2 Slow Processing @ 100 Hz frequency offset & 100Hz Doppler

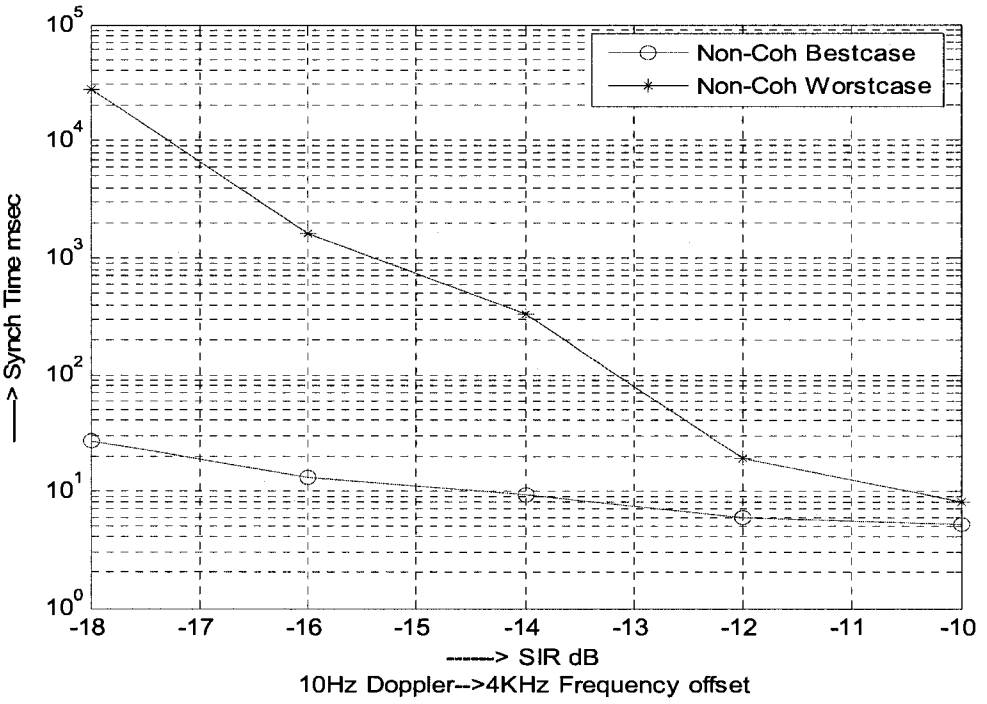

Figure 4-19.a: Rule 2 Fast Processing @ 4 KHz frequency offset & 10Hz Doppler

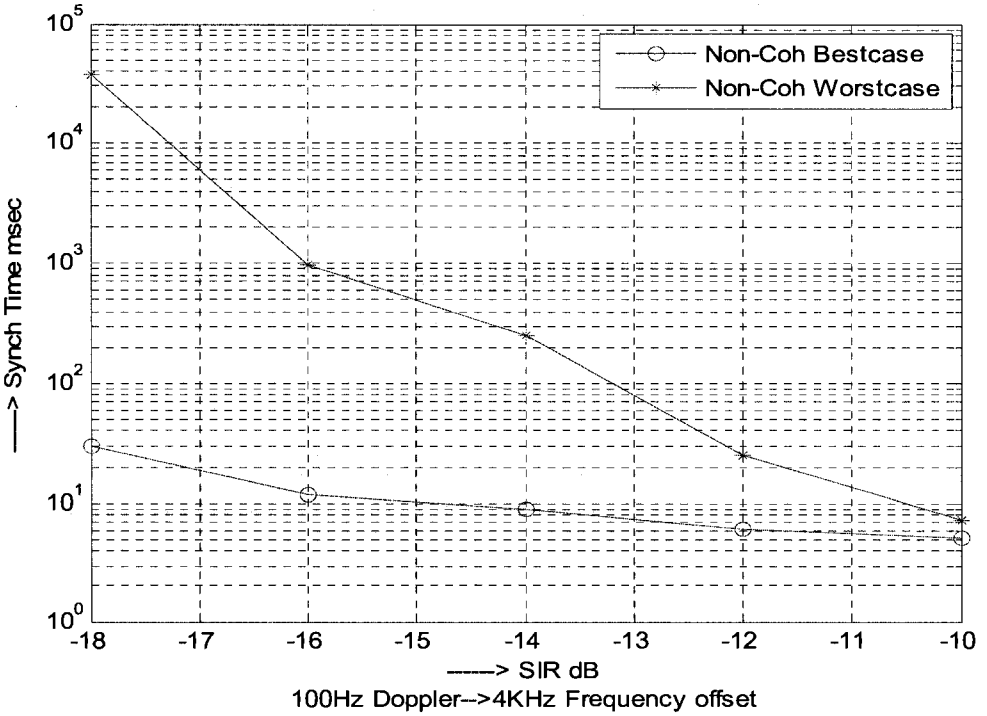

Figure 4-19.b: Rule 2 Fast Processing @ 4 KHz frequency offset & 100Hz Doppler

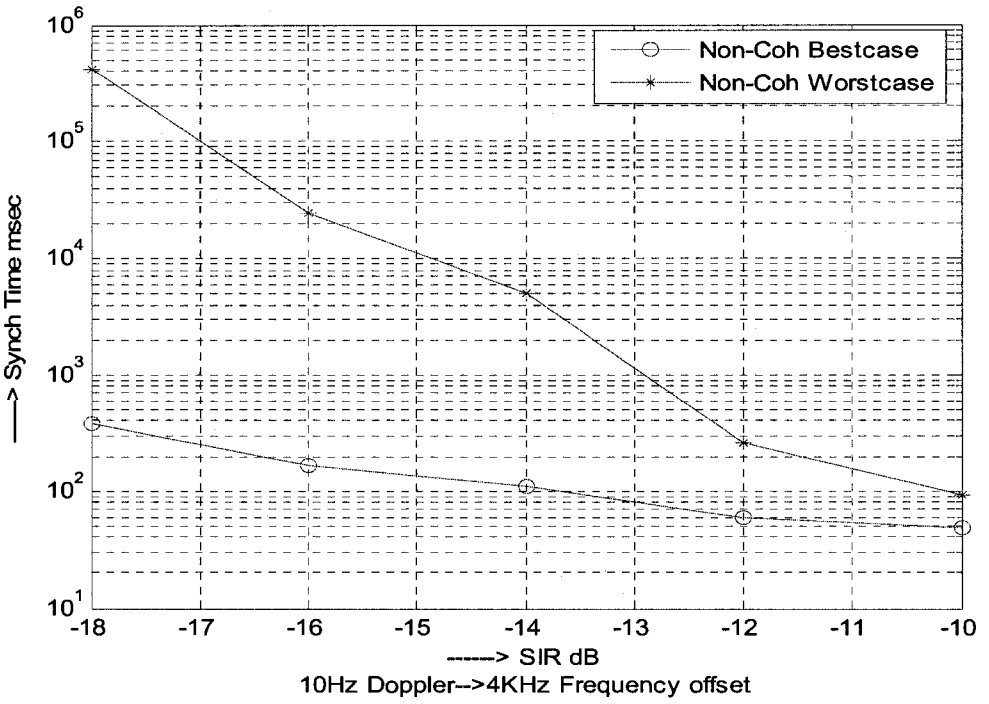

Figure 4-19.c: Rule 2 Slow Processing @ 4 KHz frequency offset & 10Hz Doppler

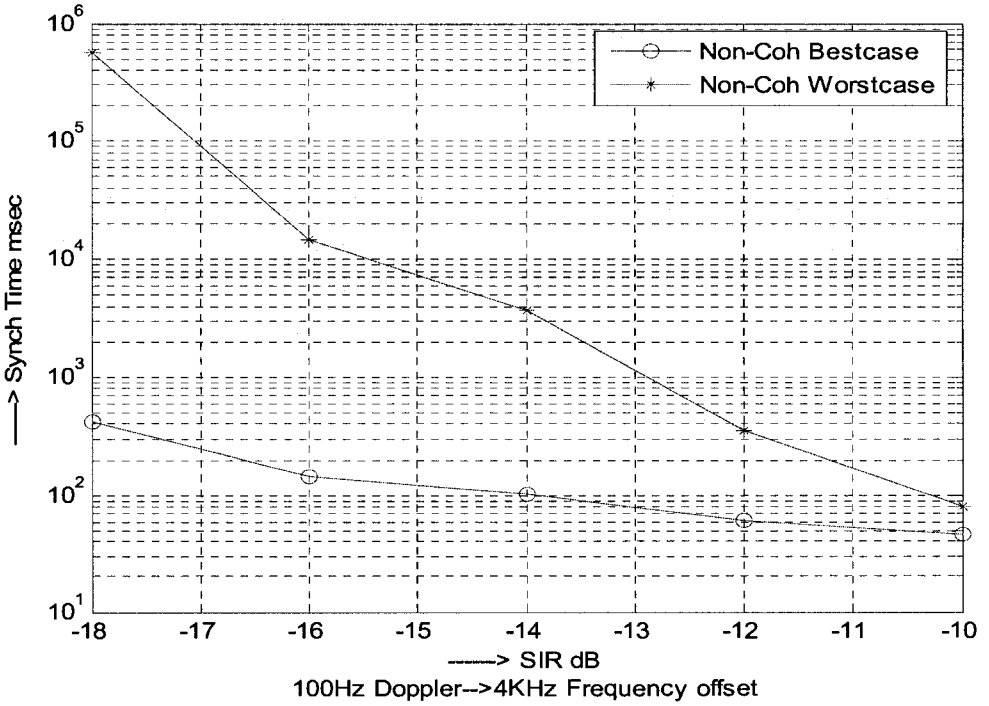

Figure 4-19.d: Rule 2 Slow Processing @ 4 KHz frequency offset & 100Hz Doppler

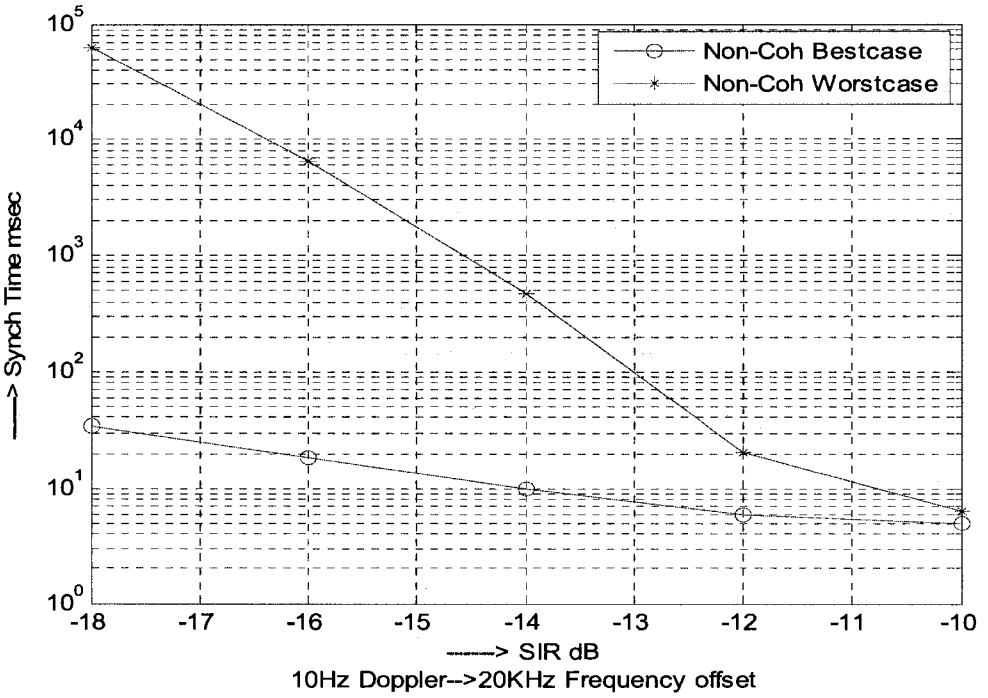

Figure 4-20.a: Rule 2 Fast Processing @ 20 KHz frequency offset & 10Hz Doppler

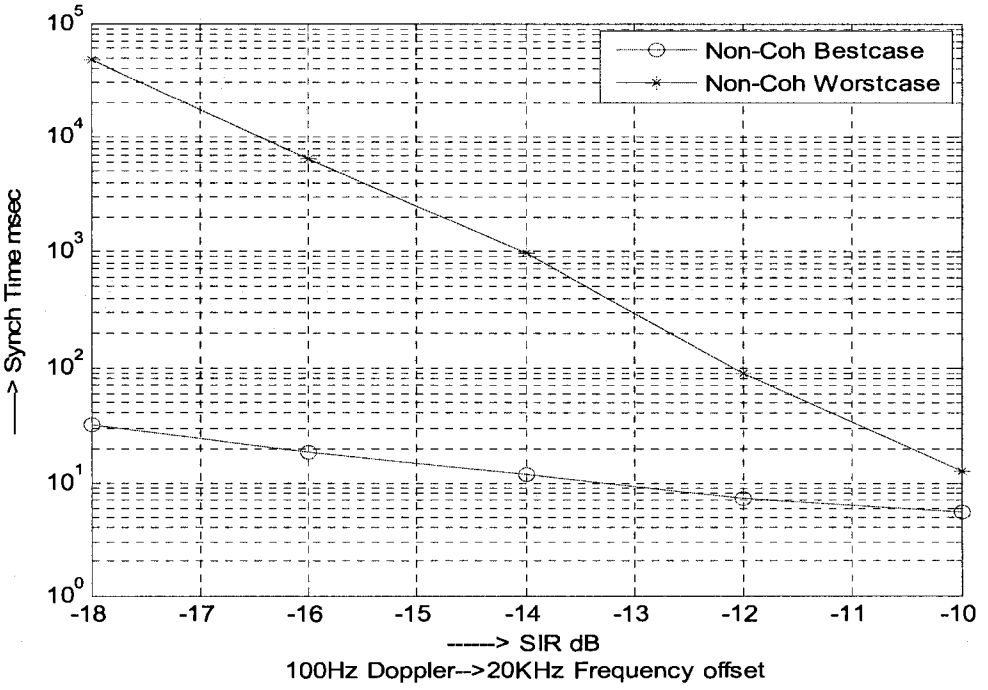

Figure 4-20.b: Rule 2 Fast Processing @ 20 KHz frequency offset & 100Hz Doppler

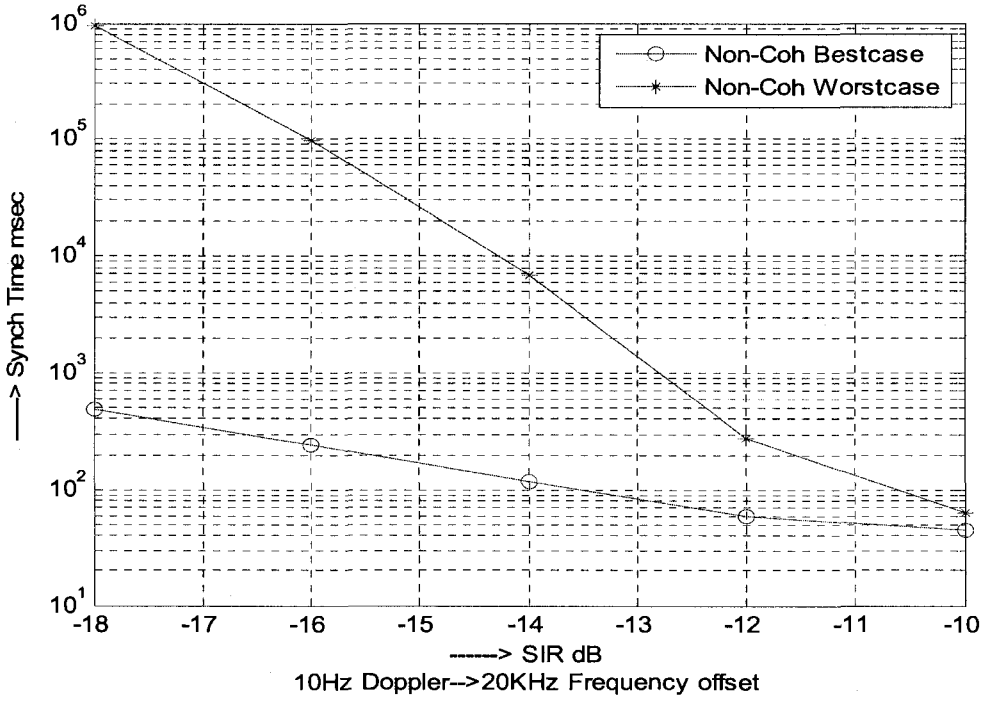

Figure 4-20.c: Rule 2 Slow Processing @ 20 KHz frequency offset & 10Hz Doppler

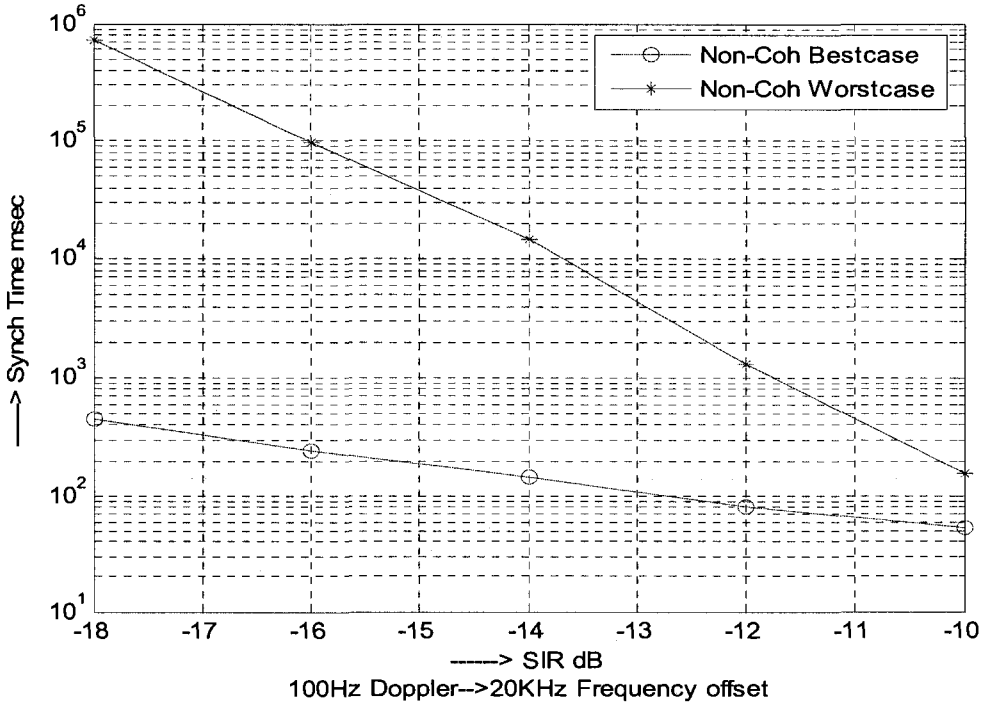

Figure 4-20.d: Rule 2 Slow Processing @ 20 KHz frequency offset & 100Hz Doppler

As in Rule 1, Figs 4-17.a, 4-18.a, 4-19.a and 4-20.a represent the Fast processing case at 10Hz Doppler considering carrier frequency offsets of 0Hz, 100Hz, 4 KHz and 20 KHz respectively. However Figs 4-17.b, 4-18.b, 4-19.b and 4-20.b represent the same fast processing case for 100Hz Doppler. Figs 4-17.c, 4-18.c, 4-19.c and 4-20.c and 4-17.d, 4-18.d, 4-19.d and 4-20.d represent the slow processing case at 10Hz and 100Hz Doppler effect respectively and for the same aforementioned carrier frequency offsets.

From the graphs of Rule 2, it is so clear that Rule 2 is as Rule 1 with regard to robustness to frequency offset since both use non-coherent combining. In addition to its acceptable robustness to Doppler effect due to the averaging over the whole frame as mentioned before. For Rule 2, reasonable values for probability of detection were obtained which affected positively the synchronization process time. At SIR of -10dB, synchronization process time is around 5 ms and 10ms for the best and worst case of the fast processing case respectively at different Doppler effects and different mentioned frequency offsets. These values are comparable to the results of [34] even without using the antenna diversity combining techniques of the said reference.

At -12dB the synchronization process time is approximately 7ms and 100ms considering best and worst case of fast processing case respectively. At -14dB the synchronization process time for the best case of the fast processing case is around 10ms, however it is 1sec for the worst case. The synchronization process time is approximately 30 ms at -18dB considering the best case. However unacceptable results are obtained starting from -14dB considering the worst case of fast processing. The slow processing figures of Rule 2 show that slow processing case provide good values considering the best case. However the worst case of slow processing provide poor results starting from -

14dB. This can be justified since our simulations were at very low SIR (from -10dB to -18dB) in addition to the worst case assumption ($a=P_d^3$) that considers the independency of the probability of detection for the three different stages of the cell search procedure. This assumption is hard to be found in practice. However, we used the worst case assumption to find the upper bound of synchronization process time for our new techniques used in cell search algorithm. For both rules, fast outperforms slow processing case by approximately 10%. However complex hardware design will be required.

Best (correlated) and worst (independent) cases synchronization process time are shown in the results of both rules, where one notices the marked difference between the independent and dependent assumptions. These worst case results especially for slow processing are in contrast with the very good synchronization process time values in [28], [34]. Even after using pipelining, multi target BS and parallel Multi code verification circuits. This may be attributed to the fact that the results are based on simulations, worst case independent assumption, consider 3 stages, consider verification times and assumes stages 2 and 3 have same synchronization process performance as the first stage (worst case stage as it deals with the largest amount of uncertainty in the cell search).

Chapter 5

Conclusions and Future Work

In this chapter, the conclusions drawn from computer simulations are summarized. Finally, future investigations are proposed.

5.1. Conclusions

Two different non-coherent slot synchronization techniques for the first stage of WCDMA synchronization process were presented. The presence of more than one BS, few multipath signals, utilization of more than one verification circuit, and pipelining have all helped to reduce the mean synchronization time. Good results were obtained for fast processing cases and when the various stages are correlated. The same was observed for very low SIR values. Because of time limitations, detection probabilities of all three stages were assumed to be the same, leading to a worst case assumption. The proposed pipeline technique with many verification circuits reduces the penalty due to missing correct code and false alarm.

5.2. Future Work

The results obtained in this thesis have provided a quite realistic picture of the first synchronization stage of WCDMA codes. However there are some open areas to continue

investigations for enhancing the synchronization time in the second and the third stages which may impact the overall cell search. Dependant assumption for the probability of detection of the three stages of the cell search algorithm should be considered in future work rather than the independent assumption of the three synchronization stages. In addition to implementing the aforementioned techniques in hardware (FPGA), such that a subsequent comparison with the simulation results should be made.

Appendix

This appendix contains parts of the MATLAB codes used in the simulation of Rule 1 and Rule 2. The results of the simulation are then used to draw the synchronization time and the probability of detection of each rule at different SIR.

A.1. Data Generation

This code is used to generate data according to the proposed sliding frame technique. The generated data is at 100Hz Doppler effect and Δf of 100Hz.

```
%%%%%%%%%%%%%%%%%%%%%%%%%%%%%%%%%%%%%%%%%%%%%%%%
clear all;
clc;
snr=1;      % SNR
NBS=4;      % number of BSs
NP=10;      % number of paths is 5 but due to over sampling, is 10
t=10e-3/(76800);            %oversampling rate is 2
Ts=0:t:((5376000)-1)*t;     %we have 70 frames,ie 1050 slots
%Ts=0:t:38399*t;                     %sampling intervals
Wc=2*pi*2e9; ferror=100; dWc=2*pi*ferror;     % freq & freq error
a = -1; b = 1;                      %values for U-distribution
```

```
TAW = [ 4100 4101 4105 4106 4110 4111 4116 4117 4119 4120;
        1500 1501 1510 1511 1515 1516 1520 1512 1522 1523;
       3700 3701 3704 3705 3707 3708 3710 37011 3713 3714;
       2050 2051 2053 2054 2057 2058 2060 2061 2066 2067];


I(1:5376000)=0;    % inphase
Q(1:5376000)=0;  % Quadrature
counter=0;
% The generated data at 100Hz Doppler (i.e. the channel changes each frame of interval
% 10 ms)
while(counter<70)
%Generating the PHI(phase error):
PHI = (2*pi)*(a + (b-a) * rand(NBS,NP));
%Generating the Alpha (Raleigh coffecient):
for i = 1:NBS
   for w = 1:NP
      x = randn();
      y = randn();
      alpha(i,w) = sqrt((x^2)*(y^2));
   end
end
for (w=1:NBS)
   for (k=1:NP)
```

```
for(i=1:1:76800)

I(counter*76800+i)=I(counter*76800+i)+((snr*alpha(w,k)*my_lastmod_auto_corr(count
er*76800+i,TAW(w,k)))*(cos(dWc*Ts(counter*76800+i)+Wc*TAW(w,k)*t-PHI(w,k))-
sin(dWc*Ts(counter*76800+i)+Wc*TAW(w,k)*t-PHI(w,k))));

Q(counter*76800+i)=Q(counter*76800+i)+((snr*alpha(w,k)*my_lastmod_auto_corr(cou
nter*76800+i,TAW(w,k)))*(cos(dWc*Ts(counter*76800+i)+Wc*TAW(w,k)*t-
PHI(w,k))+sin(dWc*Ts(counter*76800+i)+Wc*TAW(w,k)*t-PHI(w,k))));
    end
  end
end
counter=counter+1;
clear alpha;
clear PHI;
end % end of while loop
save('data1f100hz.mat')
%%%%%%%%%%%%%%%%%%%%%%%%%%%%%%%%%%%%%%%%%%%%%%%%%%%%%%%%%%%%%%%%
```

A.2. Rule 1

The following code is used to simulate the generated data according to the proposed method in Rule 1.

```
%%%%%%%%%%%%%%%%%%%%%%%%%%%%%%%%%%%%%%%%%%%%%%%%%%%%%%%%
clear all;
DN=0; DA=0; DS=0; DI=0; DQ=0;
clc;
v=10;    %variance of noise
load('data10f4khz.mat')  %to load the generated data by file data1%data2
I_noise=sqrt(v)*randn(1,5376000);
Q_noise=sqrt(v)*randn(1,5376000);
I=I+I_noise;
Q=Q+Q_noise;
frame_length=76800;  slot_length=5120;  slot_number=0;
N=sqrt(I.^2+Q.^2);
A=I+Q;
S=I-Q;
while(slot_number<1035)
  first_sample=slot_number*slot_length+1;
  last_sample =slot_number*slot_length+frame_length;

  % the data part for calcualting the PD
  dataframe_I=I(first_sample:last_sample);
  dataframe_Q=Q(first_sample:last_sample);
  dataframe_N=N(first_sample:last_sample);
  dataframe_A=A(first_sample:last_sample);
```

```
dataframe_S=S(first_sample:last_sample);
   % implementing the scheme over the data frames
% try_Best_Ran function returns the location of the most occuring
% sample over the frame
[N_ind]=try_Best_Ran(dataframe_N);
[A_ind]=try_Best_Ran(dataframe_A);
[S_ind]=try_Best_Ran(dataframe_S);
[I_ind]=try_Best_Ran(dataframe_I);
[Q_ind]=try_Best_Ran(dataframe_Q);
% to compare the most occuring sample with the different genrated
% multipaths
y_N=max_index(N_ind,TAW,NBS,NP);
y_A=max_index(A_ind,TAW,NBS,NP);
y_S=max_index(S_ind,TAW,NBS,NP);
y_I=max_index(I_ind,TAW,NBS,NP);
y_Q=max_index(Q_ind,TAW,NBS,NP);
if(detection(y_N,TAW,NBS,NP)==1)
   DN=DN+1;
end
if(detection(y_A,TAW,NBS,NP)==1)
   DA=DA+1;
end
if(detection(y_S,TAW,NBS,NP)==1)
```

```
    DS=DS+1;
  end
  if(detection(y_I,TAW,NBS,NP)==1)
    DI=DI+1;
  end
  if(detection(y_Q,TAW,NBS,NP)==1)
    DQ=DQ+1;
  end
  slot_number=slot_number+1
end  %this end is of the while loop
```

A.3. Rule 2

The following code is used to simulate the generated data according to the proposed method in Rule 2.

```
%%%%%%%%%%%%%%%%%%%%%%%%%%%%%%%%%%%%%%%%%%%%%%%%%%
clear all;
DN=0; DA=0; DS=0; DI=0; DQ=0;
v=9;    %variance of noise  (9 15 24 38 60)
load('data10f200hz.mat')  %to load the generated data by file data1%data2
I_noise=sqrt(v)*randn(1,5376000);
Q_noise=sqrt(v)*randn(1,5376000);
I=I+I_noise;
Q=Q+Q_noise;
```

```
frame_length=76800;  slot_length=5120;  slot_number=0;
N=sqrt(I.^2+Q.^2);
while(slot_number<1035)
   first_sample=slot_number*slot_length+1;
   last_sample =slot_number*slot_length+frame_length;
   % the data part for calcualting the PD
   dataframe_N=N(first_sample:last_sample);
   % implementing the scheme over the data frames
   % function average takes one frame and returns average represented in one slot
   new_dataframe_N=average(dataframe_N);
   % to detect the index of the highest peak
   [c_N,y_N]=max(new_dataframe_N);
   if(detection(y_N,TAW,NBS,NP)==1)
      DN=DN+1;
   end
   slot_number=slot_number+1;
end  %this end is of the while loop
d(1)=DN/1000;
```

Reference

[1] Rodger E. Ziemer, Roger L. Peterson and David E. Borth, "Introduction to Spread Spectrum Communications", Prentice Hall, Inc, 1995.

[2] Simon Haykin, "Communication Systems", John Wiley& Sons, 2001

[3] GSM standards etsi.com (retrieved in April 2008)

[4] Theodore S. Rappaport, " Wireless Communications", Prentice Hall, Inc, 2002.

[5] Time Division Multiple Access: http://en.wikipedia.org/wiki/Time_division_multiple_access (retrieved in April 2008)

[6] IS-95: http://en.wikipedia.org.wiki/IS-95 (retrieved in April 2008)

[7] www.imt-2000.org (retrieved in April 2008)

[8] Raymond Steele, Chine-Chun Lee and Peter Gould, "GSM, CDMAOne and 3G systems", John Wiley & Sons, Ltd, 2001

[9] Harri Holam and Anitta Toshkala, "WCDMA for UMTS, Radio access for third generation mobile communications", John Wiley & Sons, Ltd, 2001, 2004

[10] Don Torrieri, "Principles of Spread Spectrum Communication Systems", Springer, 2005

[11] www.3gpp.org (retrieved in April 2008)

[12] 3GPP Technical Specification 25.211, Physical Channels and Mapping of Transport Channels onto Physical Channels (FDD).

[13] www.3gpp2.org (retrieved in April 2008)

[14] http://ieeexplore.ieee.org/iel5/6/18918/00873918.pdf?arnumber=873918 (retrieved

in April 2008)

[15] WCDMA (UMTS) Deployment Handbook, Planning and Optimization Aspects, John Wiley& Sons, LTD, ISBN: 9780470033265

[16] http://en.wikipedia.org/wiki/High-Speed_Circuit-Switched_DataHSCSD (retrieved in April 2008)

[17] www.vocal.com/white_paper/GPRS_wp1pdf.pdf (retrieved in April 2008)

[18] www.ericsson.com/solutions/tems/library/tech_papers/tech_related/edge_wp_technical.pdf (retrieved in April 2008)

[19] www.3gamericas.org/pdfs/gsm_to_umts-siemens.pdf (retrieved in April 2008)

[20] 3GPP Technical Specification 25.213, Spreading and Modulation (FDD)

[21] 3GPP Technical Specification 25.214, Physical Layer Procedures (FDD)

[22] 3GPP Technical Specification 25.215, Physical Layer – Measurements (FDD)

[23] 3GPP Technical Specification 25.302, Services Provided by the Physical Layer

[24] Adachi, M. Sawahashi, K. Okawa, "Tree-structured generation of orthogonal spreading codes with different lengths for forward link of DS-CDMA mobile radio", IEE Electronic Letters, Vol.33 No. 1, pp. 27–28, January 1997.

[25] Saloua Ammari, Armelle Wautier, "Interference factor evaluation for CDMA system capacity analysis" VTC 2001 spring. IEEE VTS 53rd pp1573-1577 vol.3

[26] 3GPP TS 25.302: "Services Provided by the Physical Layer".

[27] Siemens and Texas Instruments, "Generalised Hierachical Golay Sequence for PSC with low complexity correlation using pruned efficient Golay correlators", TSG-RAN Working Group1 Meeting 5, TSGR1-554/99.

[28] Y. Wang and T. Ottosson, "Cell search in WCDMA," IEEE J. Select Areas

communication, vol. 18, pp. 1470-1482, Aug.2000.

[29] Y. Wang and T. Ottosson, "Initial frequency acquisition in WCDMA," IEEE VTC, Amesterdam, pp. 1013-1017 Sep. 1999.

[30] Mario Kiessling, Syed Majtaba, "Performance Enhancement to the UMTS Initial Cell Search Algorithm" ICC 2002, New York, USA, pp. 590-594

[31] A. Estrada, M. Lunardon, L. Marcato "Initial Synchronization Procedure for UMTS-FDD Mode in FPGA" MIEL 2002, Nis, Yugoslavia, pp. 663-666.

[32] Lee and Shin, "Differentially Coherent Combining for Slot Synchronization in Inter-Cell Asynchronous DS/SS systems" Proc. On PIMRC 2000, pp. 1405-1409, Sep.2000

[33] June Moon and Ying-Hwan Lee, "Cell Search Robust To Initial Frequency Offset In WCDMA Systems", IEEE PIMRC 2002, pp. 2039-2043.

[34] June Moon and Ying-Hwan Lee, "Rapid Slot Synchronization in the Presence of Large Frequency Offset and Doppler Spread in WCDMA Systems", IEEE Trans on wireless comm. Vol. 4, NO 4, July 2005, pp. 2039-2043.

[35] A. Zoch and Gerhard P. Fettweis, "Cell Search Performance Analysis for W-CDMA" Communications, 2002. ICC 2002. IEEE International Conference on volume 2, 28 April-2May 2002 Pages: 940-944 vol.2.

[36] Stamatis Kourtis, "Investigation of the mobile terminal optimum operation point in UMTS-FDD initial cell search procedure", Personal, Indoor and Mobile Radio Communications, 2000. PIMRC 2000. The 11th IEEE International Symposium on Volume 1, Issue, 2000 Page(s):348 - 352 vol.1

[37] K. Higuchi, M. Sawahashi, and F. Adachi, "Fast cell search algorithm in inter-cell

asynchronous DS-CDMA mobile radio," IEICE Trans commun., vol.E81-B, no.7, pp.1527-1523, July 1998.

[38] Nystrom, K. Jamal, Y.-P. E. Wang, and R. Esmailzadeh, "Comparison of cell search methods for asynchronous wideband CDMA cellular system", in Proc. IEEE, Int. Conf. Universal Personal Commun., Florence, Italy, Oct. 1998.

[39] Ericsson, "New downlink scrambling code grouping scheme for UTRA/FDD", TSG-RAN Working Group1 Meeting 6, TSGR1#6(99)884".

[40] Moon Kyou Song, "Performance Comparison of Stepwise Serial and Parallel Cell Search in WCDMA" IEICE TRANS COMMUN., VOL. E88-B, NO.6 June 2005.

[41] Aissaoui A., Hammoudi Z. and Farrouki A. "Adaptive PN code acquisition using automatic censoring for DS-CDMA communication". IEEE Waveform Diversity and Design Conference 2007. International, June 2007 Page(s):169 – 173

[42] S. Sriram, and S. Hosur, "An Analysis of the 3-Stage Search Process in W-CDMA," VTC 2000 spring. IEEE VTS 53rd pp 2673-2679 vol.3

[43] A.Hassan, Y.Chakfeh, A.k.Elhakeem, "Pipelined, Multi-target, Peaks Combining Techniques for WCDMA Signal Acquisition in fading channels" IEEE International Conference on Wireless and Mobile Computing, WiMob 2008, Avignon France.